



# **Communications Technology**

**T 7.6**

## **Antenna Technology**

**by Dr. J.M. Kloza**

**K. Breidenbach**

4th edition

Version: 03BB02PME14W10

**568 702**



## Notes

### EMI

The sensitive electronics of the equipment described in this manual can be affected in experiments by ESD (electrostatic discharge). Therefore, electrostatic charging should be avoided especially through the use of in appropriate lab facilities. Discharging by grounding is also recommendable.

### Topic limitation

This manual might contain additional experiments with devices which are not included in the scope of delivery. In this case only those experiments can be performed for which LD delivered the required material. Thus customers are not entitled to claim for compensation such as free-of-charge deliveries of supplementary apparatus. Additional experiments deviating from the procedures described herein are possible if carried out by qualified personnel taking into consideration prevailing security standards.

### Results of measurement examples

All measurement results were obtained with the indicated test setups. The experiments can still produce results that differ from the sample solutions. Reasons for this are, among others:

- Setting of the measuring points
- Components and measuring tolerances
- Fluctuations in the supply voltages etc..

### Third party information

Enclosed literature of third-party devices and software should be read before performing the experiments.

**Further claims from this experiment manual do not exist!!**

<b>Notes</b> .....	<b>2</b>
EMI .....	2
Topic limitation .....	2
Results of measurement examples .....	2
Third party information .....	2
<b>Equipment overview</b> .....	<b>8</b>
<b>Symbols and abbreviations</b> .....	<b>9</b>
<b>1. Antenna measurement station</b> .....	<b>10</b>
Antenna rotation platform .....	10
Safety .....	11
Definitions.....	11
Horizontal and vertical diagrams .....	11
Far field condition .....	11
Front to back ratio .....	12
Directivity .....	12
Gain .....	12
Material.....	13
Experiment setup .....	14
Experiment procedure .....	15
Results .....	15
Formulas in directional diagrams .....	16
Free fit for directional diagrams .....	16
Formula pool.....	16
<b>Dipole antennas</b> .....	<b>21</b>
Fundamentals.....	21
Material.....	24
Experiment set-up .....	24
Experiment procedure .....	24
1. Horizontal diagrams of the $\lambda/2$ -dipole .....	24
2. Horizontal diagrams of the $\lambda$ -dipole .....	25
3. Horizontal diagrams of the $3\lambda/2$ -dipole .....	25
4. Horizontal diagrams of the $2\lambda$ -dipole .....	25
5. Horizontal diagrams of the $4\lambda$ -dipole .....	25
6. Attenuation of cross-polarized waves .....	26
7. Vertical diagrams of the $\lambda/2$ -dipole .....	26
Results .....	27
1. Horizontal diagrams of the $\lambda/2$ -dipole .....	27
2. Horizontal diagrams of the $\lambda$ -dipole .....	28
3. Horizontal diagrams of the $3/2\lambda$ -dipole .....	29
4. Horizontal diagrams of the $2\lambda$ -dipole .....	29
5. Horizontal diagrams of the $4\lambda$ -dipole .....	30
6. Attenuation of cross-polarized waves (PLF) .....	30
7. Vertical diagrams of the $\lambda/2$ -dipole .....	30

<b>Yagi antennas</b> .....	<b>31</b>
Fundamentals.....	31
Material.....	34
Experiment set-up .....	34
Experiment procedure .....	34
1. Horizontal diagrams of the Yagi-R antenna.....	34
2. Horizontal diagrams of the Yagi-D antenna.....	35
3. Horizontal diagrams of the Yagi-DR antenna .....	35
4. Horizontal diagrams of the Yagi-4DR antenna .....	35
Variant.....	36
Results .....	37
1. Horizontal diagrams of the Yagi-R antenna.....	37
2. Horizontal diagrams of the Yagi-D antenna.....	38
3. Horizontal diagrams of the Yagi-DR antenna .....	39
4. Horizontal diagrams of the Yagi-4DR antenna .....	40
<b>Aperture antennas</b> .....	<b>42</b>
Fundamentals.....	42
Open waveguides and horns.....	42
Material.....	45
Experiment set up .....	45
Experiment procedure .....	46
1. Horizontal diagrams of the large horn antenna.....	46
2. Polarization loss of the large horn antenna .....	46
3. Vertical diagrams of the large horn antenna.....	47
4. Vertical diagrams of the small horn antenna .....	47
5. Horizontal diagrams of the small horn antenna .....	47
6. Horizontal diagrams of waveguide antennas.....	47
Variants .....	48
Polarization effects on the transmission channel.....	48
Vertical diagrams of open waveguides .....	48
Results .....	49
1. Horizontal diagrams of the large horn antenna.....	49
2. Polarization loss of the large horn antenna (PLF) .....	49
3. Vertical diagrams of the large horn antenna.....	50
4. Vertical diagrams of the small horn antenna .....	50
5. Horizontal diagrams of the small horn antenna .....	51
6. Horizontal diagrams of waveguide antennas.....	52
Variants .....	53
Polarization effects on the transmission path .....	53
<b>Reflector antennas</b> .....	<b>54</b>
Fundamentals.....	54
Parameters of the dish antenna .....	55
Questions .....	58
Material.....	58

Experiment set-up .....	59
Experiment procedure .....	59
1. Horizontal diagrams of the parabolic reflector with $\lambda/2$ -dipole .....	59
2. Horizontal diagrams of the parabolic reflector with Yagi-R .....	60
3. Horizontal diagrams of the parabolic reflector with Yagi-D .....	60
4. Horizontal diagrams of the parabolic reflector with Yagi-DR .....	61
5. Horizontal diagrams of the parabolic reflector with Yagi-4DR .....	61
Variant .....	61
The use of different radiators .....	61
Answers .....	62
Results .....	63
1. Horizontal diagrams of the parabolic dish antenna with $\lambda/2$ -dipole .....	63
2. Horizontal diagrams of the parabolic dish antenna with Yagi-R .....	64
3. Horizontal diagrams of the parabolic dish antenna with Yagi-D .....	65
4. Horizontal diagrams of the parabolic dish antenna with Yagi-DR .....	66
5. Horizontal diagrams of the parabolic dish antenna with Yagi-4DR .....	67
Hints .....	68
<b>Helix antennas .....</b>	<b>69</b>
Fundamentals .....	69
Polarization of antennas and waves .....	69
Helix antenna .....	71
Material .....	73
Experiment set-up .....	73
Experiment procedure .....	74
1. Directional diagram of helical antennas with same SOP .....	74
2. Directional diagram of helical antennas with orthogonal SOP .....	75
3. The influence of reflections for antennas with orthogonal SOP .....	75
4. Influence of reflections for antennas with the same SOP .....	76
Variants .....	76
Polarizer between two helical antennas with orthogonal SOP .....	76
Measuring the SOP of a nearly circular polarized wave .....	76
Results .....	77
1. Directional diagram of helical antennas with same SOP .....	77
2. Directional diagram of helical antennas with orthogonal SOP .....	77
3. The influence of reflections for antennas with orthogonal SOP .....	78
4. Influence of reflections for antennas with the same SOP .....	79
Variants .....	80
Polarizer between two helical antennas with orthogonal SOP .....	80
Measuring the SOP of a nearly circular polarized wave .....	81
<b>Array antennas .....</b>	<b>82</b>
Fundamentals .....	82
Linear arrays .....	83
Planar arrays .....	85
Microstrip technology .....	85

Microstrip antennas .....	86
Questions .....	88
Material.....	89
Additionally required.....	89
Experiment set-up .....	90
Experiment procedure .....	91
1. Horizontal diagrams of the slot antenna, $N = 7$ .....	91
2. Horizontal diagrams with reduced number of slots, $N = 5$ .....	91
3. Horizontal diagrams with reduced number of slots, $N = 3$ .....	91
4. Vertical diagrams with reduced number of slots, $N = 3$ .....	92
5. Vertical diagrams of the slot antenna, $N = 7$ .....	92
6. The formation of grating lobes .....	92
7. Beam squinting and scanning by means of phase control .....	92
8. Horizontal diagrams of the microstrip antenna .....	93
9. Vertical diagrams of the microstrip antenna .....	93
Answers.....	94
Results .....	96
1. Horizontal diagrams of the slot antenna, $N = 7$ .....	96
2. Horizontal diagrams with reduced number of slots, $N = 5$ .....	97
3. Horizontal diagrams with reduced number of slots, $N = 3$ .....	98
4. Vertical diagrams with reduced number of slots, $N = 3$ .....	98
5. Directional diagrams of the vertical slot antenna, $N = 7$ .....	99
6. The formation of grating lobes .....	101
7. Beam squinting and scanning by means of phase control .....	101
8. Horizontal diagrams of the microstrip antenna .....	101
9. Vertical diagrams of the microstrip antenna .....	102
<b>Gain and matching.....</b>	<b>103</b>
Fundamentals.....	103
Single slots .....	103
The three-antenna method .....	106
Material.....	108
Experiment procedure .....	109
1. Horizontal diagrams of single slots .....	109
2. Matching slot antennas.....	110
3. The three antenna method .....	112
Results .....	114
1.1 Horizontal diagrams of the single slot, type A.....	114
1.2 Horizontal diagrams of the single slot, type B.....	114
1.3 Horizontal diagrams of the single slot, type C .....	114
1.4 Horizontal diagrams of the single slot, type D .....	115
1.5 Joint display of all single slots.....	115
2. Matching slot antennas.....	116
3. The three antenna method .....	117



<b>Service .....</b>	<b>118</b>
1. Is RF power being generated? .....	118
2. Is the PIN modulator operating?.....	118
3. Check the cross-polarization .....	118

## Equipment overview

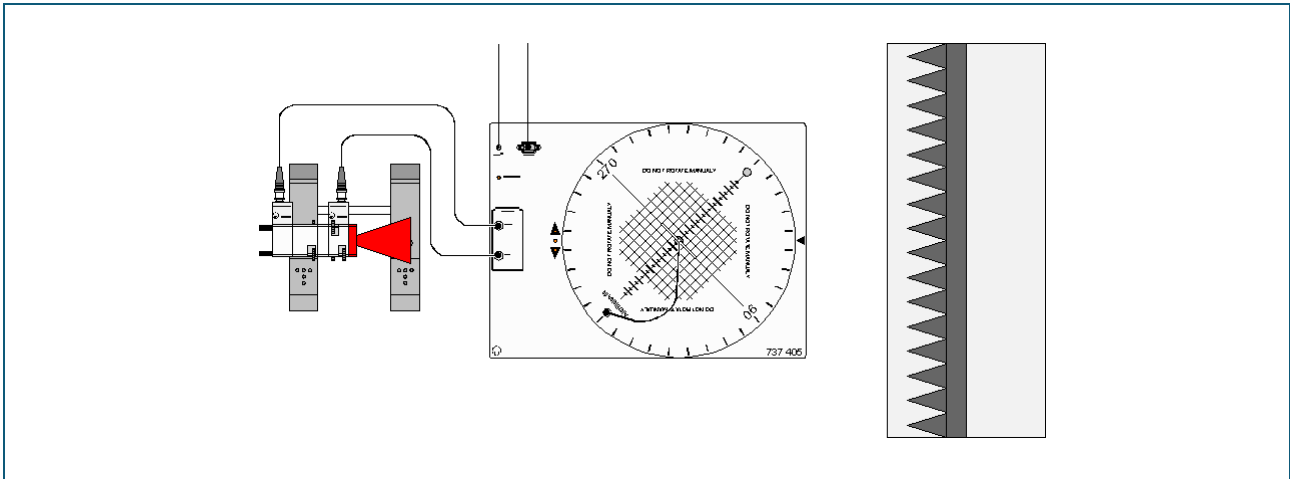
		Dipole antennas	Yagi antennas	Aperture antennas	Reflector antennas	Helix antennas	Array antennas	Gain and matching
737 01	Gunn oscillator	1	1	1	1	1	1	1
737 03	Coax detector	--	--	1	--	1	1	1
737 033	Coax transition	--	--	--	--	1	--	1
737 035	Transition waveguide / coax	--	--	1	--	1	1	1
737 05	PIN modulator	1	1	1	1	1	1	1
737 06	Isolator	1	1	1	1	1	1	1
737 085	DC-blocker	--	--	--	--	--	--	1
737 09	Variable attenuator	--	--	--	--	--	--	1
737 10	Moveable short	--	--	--	--	--	1	--
737 12	Waveguide 200 mm	--	--	1	--	--	--	1
737 135	3-Screw transformer	--	--	1	1	--	1	1
737 14	Waveguide termination	--	--	--	--	--	1	1
737 15	Support for WG components	--	--	2	--	1	2	2
737 18	Cross directional coupler	--	--	--	--	--	--	1
737 197	E-Bend	--	--	--	--	1	--	1
737 20	Small horn antenna	--	--	1	--	--	--	--
737 21	Large horn antenna	1	1	2	1	1	1	1
737 22	Set 4 slit diaphragms	--	--	--	--	--	--	1
737 27	Physics microwave accessories	--	--	1	--	1	--	--
737 390	Set of microwave absorbers	1	1	1	1	1	1	1
737 405	Rotating antenna platform	1	1	1	1	1	1	1
737 415	Set of wire antennas	1	1	--	1	--	--	--
737 424	Slot antenna	--	--	--	--	--	1	--
737 427	Microstrip antenna	--	--	--	--	--	1	--
737 440	Helical antenna kit	--	--	--	--	1	--	1
737 452	Dish antenna	--	--	--	1	--	--	--
301 21	Stand base MF	2	2	4	2	3	4	4
301 26	Stand rod 25 cm	1	1	1	1	1	1	1
311 77	Steel tape measure	1	1	1	1	1	1	1
501 02	BNC cable, l = 1 m	--	--	1	--	1	1	1
568 702	Book: Antenna Technology	1	1	1	1	1	1	1
648 07	Storage tray S24-FN	1	1	1	1	1	1	1
648 08	Partition ZW 24	3	3	3	3	3	3	3
	PC Windows XP or higher version	1	1	1	1	1	1	1

## Symbols and abbreviations

Multiple use is possible.

$\alpha$	Opening angle of the aperture
A	Geometric aperture surface, transverse dimension of the horn, tilt angle of the polarizer
$A_{\text{eff}}$	Effective area
AR	Axial ratio
b	Transverse dimension of the horn, distance between the elements of the dipole antenna
D	Reflector diameter, director, pipe diameter, diameter of the helix, side reflection from the distance, conductor diameter
$d_0$	Slot distance
$D_0$	Directivity
$d_Q$	largest longitudinal or transversal dimension of the source antenna
$d_T$	largest longitudinal or transversal dimension of the test antenna
$\epsilon_{\text{eff}}$	Effective permittivity
$\epsilon_R$	Relative permittivity
f	Focal distance
$G_0$	Gain
h	Antenna height above the plane of the table, dielectric layer thickness
H	Directional diagram for the horizontal antenna array
k	Turn or wave number
$\lambda_0$	Free-space wavelength
$\lambda_G$	Wavelength in the waveguide
l	Dipole length, length, slot length
$L_L$	Line length
$L_R$	Radiator length
M	Characteristics exponent
N	Number of turns
$\eta$	Antenna efficiency
PLF	Polarisation attenuation
$P_{R/T}$	Receiving power / Transmission power
q	Aperture efficiency
r	Radius axis in directional diagrams, distance between source and test antenna
R	Reflector
$R_R$	Radiation resistance
s	Degree of slenderness
V	Directional diagram for the vertical antenna array
w	Conductor wire or line width
$w_L$	Line width of the microstrip line
$w_R$	Radiator width
x	Slot offset
$Z_0$	Characteristic impedance
$Z_m$	Characteristic impedance of the microstrip line
$Z_s$	Slot impedance

## Antenna measurement station



### Antenna rotation platform

Antennas serve to transmit or receive electromagnetic waves. For this they have to convert the conducted wave of the feeding line into a free-space wave. Antennas therefore are transition structures, which couple transmission lines to the free space. The radiation characteristics of an antenna are of particular interest. They can vary considerably, depending on their use in broadcasting, microwave transmission or Radar. Here the use of the antenna measuring station in conjunction with the rotating antenna platform (737 405) is explained. A  $\lambda/2$ -dipole antenna serves as an example of how to record a directional diagram. Additional remarks are obtained from the instruction sheet 737 405. Use the following instructions:

- Load the CASSY Lab 2 files from the CASSY help to start the antenna rotation platform. Save your own measurements under any name or the names proposed in the experiment.
- The axis of symmetry of the test antenna and the centre of the rotary plate have to be in line. If the antenna has been inserted in the central mounting of the rotary plate, this is in general fulfilled. However, there are test antennas which are mounted by means of stand material. In this case, the antenna has to be aligned carefully over the centre of the rotary plate in order that during rotation no eccentric motion occurs (which would lead to asymmetries in the directional diagrams).
- If the main lobe of the test antenna is to be located at  $0^\circ$  in the directional diagram, the test antenna has to be aligned so that its main-beam direction points into the  $0^\circ$  direction. Furthermore it has to be aligned with the transmitting antenna. That means its "back" "looks over" to the exciting source antenna. The reason for this lies in the nature of the process: the main-beam direction is thus measured in one run instead of being divided into two halves. Environmental influences on the system thus have less effect on the important region of the main lobe.
- Depending on the test antenna, the measurement can be made at various degrees of angular resolution. In principle complicated antennas with many or narrow lobes have to be measured at high resolution.
- The measurement process can be observed simultaneously on the measuring instruments (e.g. for the angle  $\vartheta$ , voltage  $U$  and level  $a$ ), which can be inserted/hidden, and in the graphical display. In the graphical display, the directional diagram is constructed step by step (Cartesian coordinates or polar diagram with freely selectable axes). Scaling can be shifted with the left mouse button and it can be changed with the right mouse button.

- The actual antenna signal  $A$  from the detector cannot be measured directly. Only the voltage drop  $U$  generated by the detector current at the measuring amplifier is measurable. In general,  $U$  is not proportional to  $A$  but instead:

$$U \approx A^m$$

The exponent  $m$  describes the detector characteristic. If the antenna signal  $A(\vartheta)$  is normalized with *Normalize Level* in Settings A so that it is 1 in the maximum, we have:

$$A = \left( \frac{U}{U_{\max}} \right)^{\frac{1}{m}} \quad a = 20 \cdot \log(A)$$

where  $U_{\max}$  is the maximum voltage  $U$  measured. The exponent  $m$  depends on the power of the incoming microwaves. In the low-power range it is  $m=2$ , i.e.:

$$U \approx A^2$$

Experience has shown that the assumed square law (=quadratic) behaviour only applies at very low microwave powers or received voltages  $U < 5$  mV. However, the antenna measurement system makes it possible to enter other detector characteristics. Strictly speaking, the selected characteristic has to be checked. For this a variable attenuator (737 09) is required which enables the antenna signal in front of the detector to be attenuated in a well-defined way.

## Safety

Due to the low power of the Gunn oscillator (approx. 10 mW), there can be no danger to experimenters during antenna measurements. However, if stronger HF sources are used, the following rules should be kept to:

- Under no circumstances "look" directly into" the transmitting antenna while it is radiating. This also applies to free ends of waveguides and horn antennas.
- When waveguide components have to be exchanged during modifications of the experimental setup, the supply voltage of the Gunn oscillator has to be switched off.

## Definitions

### Horizontal and vertical diagrams

Directional diagrams can be measured in horizontal or vertical mode. Usually the horizontal mode means a rotation of the test antenna in E-Plane (exception: slot antenna). The vertical mode means a rotation of the test antenna in the H-plane (exception: slot antenna). In the subsequent experiments the short cuts horizontal and vertical diagram are used for convenience.

### Far field condition

In general, the distance between the source antenna and the test antenna must fulfil the far field condition. Consequently, a far field distance of  $r_0$  must be maintained.

$$r_0 \geq \frac{2(d_Q + d_T)^2}{\lambda_0}$$

Where the following applies:

$d_Q$ and $d_T$	largest dimensions (in the transverse or longitudinal direction) of the antennas
$r_0$	distance between the transmitting and receiving antenna
$\lambda_0$	wavelength of the radiated wave.

#### Front to back ratio

The front-to-back ratio (F/B-ratio) describes the ratio of the received power in forward to reverse direction. This is measured in linear values or in the log-dB scale. In the case of  $A(\vartheta)$ , or  $a(\vartheta)$ , the scale is normalized to the maximum of the major lobe of radiation in the forward direction. Thus, this corresponds to  $A = 1.00$  or  $a = 0$  dB. Therefore, the front-to-back ratio can be read directly off the directional diagram. Its quantity corresponds to  $-a(\vartheta = 180^\circ)$  or the inverse value of  $A(\vartheta = 180^\circ)$ . This means that measurement is conducted in the opposite direction to the maximum value of the major lobe.

#### Directivity

The directivity  $D_0$  is the ratio of the antenna's maximum to mean radiation intensity. Directivity is measured as the 3 dB-width. Using the CASSY Lab it is advantageous to convert the polar plot of the directional diagram into the Cartesian representation  $a(\vartheta)$ . Insert a horizontal line and position it on the level  $-3$  dB. Insert two vertical lines at the interception points of this reference line with the directional diagram. The angular difference equals to the 3 dB-width.

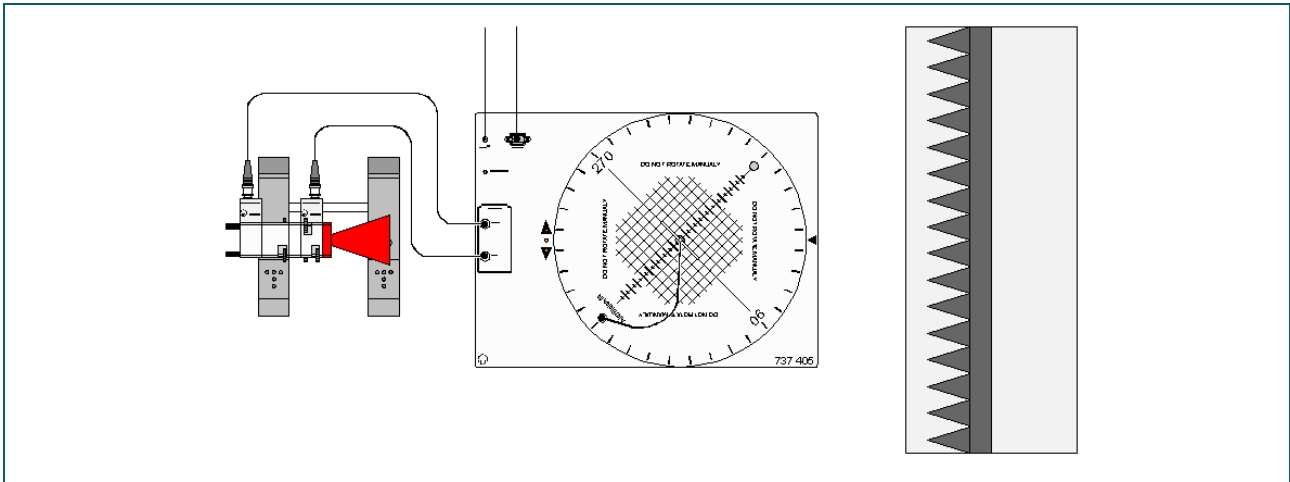
#### Gain

The gain  $G_0$  is given by the ratio of the maximum radiation intensity of the test antenna to the maximum radiation intensity of a reference antenna of equal power (the isotropic antenna is frequently used). In an ideal antenna, in which the efficiency is  $\eta = 100\%$ , gain and directivity are equal.

## Material

1	737 01	Gunn oscillator
1	737 05	PIN modulator
1	737 06	Isolator
1	737 21	Large horn antenna
1	737 390	Set of microwave absorbers
1	737 405	Rotating antenna platform including: 2x stand rod 345 mm, 2x BNC cable l=2m, plug in power supply, RS 232 cable
1	737 415	Set of wire antennas
1	737 21	Large horn antenna
2	301 21	Stand base MF
1		PC with Windows XP or higher version

## Experiment setup



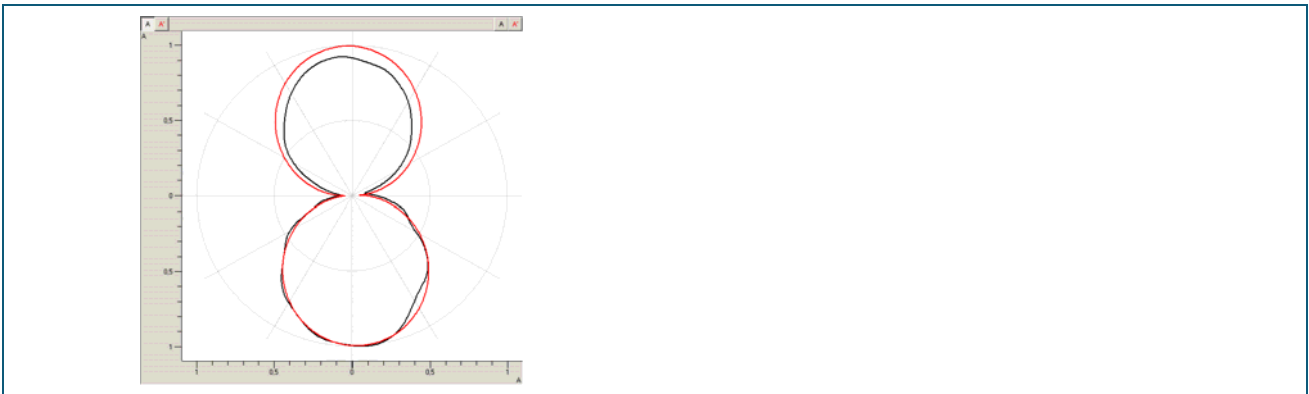
- Set up the experiment as shown in the drawing.
- Use the 345 mm stand rods supplied with the rotating antenna platform for setting up the transmitter (microwave components).
- For further remarks see instruction sheet 737 405.
- As a rule, the distance  $r_0$  between the transmitting and the test antenna should fulfil the far-field condition. For dipole antennas this is fulfilled for  $r_0 \approx 100$  cm in most cases. The Far-field computer to be found in the *Settings A* determines the minimum distance  $r_0$  for the transition to the far field after  $D_T$  has been entered.
- Insert the test antenna ( $\lambda/2$ -dipole) in the central mounting for plug-in axles in the rotating antenna platform so that the axis is aligned with the reference lines on the rotary plate.
- Connect the BNC output socket of the test antenna to the BNC socket TEST ANTENNA IN in the rotary plate via a coaxial cable.
- Align the antenna so that its main-beam direction is in the  $0^\circ$  position.
- Switch the rotating antenna platform on by connecting the plug-in unit. The rotary plate moves to the starting position  $-180^\circ$ .



## Experiment procedure

- Load settings
- If you have not yet selected the rotating antenna platform as the connected device, do it now. For this connect the rotating antenna platform to the desired serial interface in *General settings*. After this has been done, *Save New Defaults* saves this assignment.
- If necessary, change the settings of the rotating antenna platform in *Settings A*. If the dipole antenna is used, the bias current has to be switched on. If no PIN modulator is available, you have to switch over to Gunn modulation.
- Start the measurement with *F9* (stop clock). After a short break, the rotary plate starts to run in the forward direction, whereby the actual measurement of the directional diagram takes place. Immediately after reaching the set final angle, the rotary plate begins to return to its starting position.
- Normalize  $A(\vartheta)$  with *Normalize Level* in *Settings A* so that it is 1 in the maximum.

## Results



The measurement example shows the horizontal directional diagram of a  $\lambda/2$ -dipole. In *Settings A* the maximum of the measured curve was rotated to  $0^\circ$ . The black curve represents the measured curve whereas the theoretical directional diagram is given by the red curve. The theoretical curve was obtained by means of a free fit (see below).

## Formulas in directional diagrams

Measuring results can be compared with theoretical directional diagrams if a suitable formula is available or can be derived. Formulas can be used in various ways:

- The formula can be defined as a new quantity. Then all parameters of the formula have to be entered explicitly.
- The formula can be entered for carrying out a free fit. In this case, up to 4 parameters of the formula are varied automatically so that the best agreement between the measuring results and the formula is obtained. The method is very elegant in the case of antenna measurements and shall be explained briefly in the following paragraphs.

### Free fit for directional diagrams

After the measurement with the rotating antenna platform has been carried out, the following steps are required for performing a *Free fit*.

- Select the Cartesian representation (Change Axis Assignment in the diagram with the right mouse button and switch off the Polar button under the x-axis).
- Select Free fit (click Fit Function in the diagram with the right mouse button and select Free fit).
- Enter the formula in the input field, select it from the list, or copy it via the clipboard (via copy and paste, e.g. the examples below) having marked just the formula.
- Having estimated sensible starting values for  $A$ ,  $B$ ,  $C$  and  $D$  (see examples below), enter them.
- Mark the result as a new channel (parameter). This leads to a new column in the table when the evaluation takes place with the calculated values of the theoretical directional diagram.
- Select *Mark range*, and mark the entire measuring curve with the left mouse button. Then the fit is performed, and the best approximation of the formula found during the fitting procedure is displayed.
- Select the polar representation. For that: change axis assignment in the diagram with the right mouse button and switch the Polar button under the x-axis on again.

### Formula pool

The following formulas can simply be marked with the cursor and copied into the input field.

#### 1. Technical dipoles

$$A \cdot \left| \frac{\cos\left(\frac{\pi \cdot l_{el}}{\lambda_0}\right) \sin(\vartheta + \vartheta_0) - \cos\left(\frac{\pi \cdot l_{el}}{\lambda_0}\right)}{\cos(\vartheta + \vartheta_0)} \right|$$

The formula describes the dependence of the directional diagram on the polar angle in the case of a dipole antenna for which a sinusoidal distribution of the currents on the antenna conductors has been assumed. Distortions by the current displacement, which is due to a low reduction factor (finite thickness of the antenna conductors), are not taken into account.

- $\vartheta$  polar angle  
 $\vartheta_0$  angular misalignment  
 $l_{el}$  electric length of the dipole (shortening not taken into account)  
 $\lambda_0$  wavelength in free space

Formula to copy:  **$A \cdot \text{abs}((\cos(180 \cdot B/32 \cdot \sin(x+D)) - \cos(180 \cdot B/32)) / \cos(x+D))$**

- $x$  polar angle  $\vartheta$   
 32 wavelength in free space in mm ( $\lambda_0 = 32$  mm for 9.40 GHz).

From the measured values, the program obtains optimum values for:

- $A$  amplitude fit  
 $B$  electric length  $l_{el}$   
 $D$  angular misalignment  $\vartheta_0$  (deviation of the antenna from the direction of reference)

Starting values

Antenna	A	B/mm	D/deg
$\lambda/2$ -dipole	1	16	0
$\lambda$ -dipole	1	32	0
$3\lambda/2$ -dipole	1	48	0
$2\lambda$ -dipole	1	64	0
$4\lambda$ -dipole	1	128	0

## 2. Yagis with one parasitic element:

- Yagi-R: dipole and 1 reflector
- Yagi-D: dipole and 1 director

Both cases are approximately described by the directional diagram of a conducting sheet (reflector):

$$A \cdot |\cos(\vartheta + \vartheta_0)| \cdot \left| \cos\left(\frac{\pi}{2} + \frac{\pi \cdot a}{\lambda_0} \cdot \cos(\vartheta + \vartheta_0)\right) \right|$$

- A      amplitude fit  
 a      distance between the dipole and the reflector  
 $\vartheta$      polar angle  
 $\lambda_0$     wavelength in free space

Formula to copy:  **$A \cdot \text{abs}(\cos(x+B)) \cdot \text{abs}(\cos(C+D \cdot \cos(x+B)))$**

The factor  $A \cdot \cos(x+B)$  corresponds to the directional diagram of a Hertzian dipole. This ideal transmitting antenna is so short as compared with the wavelength that the current distribution on it can be assumed to be constant. The factor  $\text{abs}(\cos(C+D \cdot \cos(x+B)))$  describes the effect of the parasitic element (reflector or director).

- x      polar angle  $\vartheta$

Starting values

- A      = 1      amplitude fit  
 B      = 0      angular misalignment  $\vartheta_0$ , deviation of the antenna from the direction of reference  
 C      = 90     phase  
 D      = 60     factor depending on the construction, takes into account the ratio  $a/\lambda_0$

### 3. Yagis with several parasitic elements

These cases are approximately described by the directional diagram of a single dipole and so-called array factors (here: horizontal array factor):

$$A \cdot |\cos(\vartheta)| \cdot \left| \frac{\cos\left(n\left(\frac{\beta_0}{2} + \frac{\pi \cdot a}{\lambda_0} \cdot \cos(\vartheta)\right)\right)}{\cos\left(\frac{\beta_0}{2} + \frac{\pi \cdot a}{\lambda_0} \cdot \cos(\vartheta)\right)} \right|$$

- A     amplitude fit
- n     number of Yagi elements, including the dipole
- a     average distance between the parasitic elements (directors, reflector)
- $\beta_0$     phase angle
- $\vartheta$      polar angle
- $\lambda_0$     wavelength in free space

Formula to copy: **A\*abs(cos(x))\*abs(cos(B\*(C+D\*cos(x)))/cos(C+D\*cos(x)))**

x     polar angle  $\vartheta$

Starting values

- A     = 0.4            amplitude fit
- B     = 3 (6)         number  $n$  of transmitting elements, including dipole (select constant)
- C     = -60 (-20)    phase angle  $\beta_0$
- D     = 50 (36)     factor depending on the construction, takes into account the ratio  $a/\lambda_0$

#### 4. Slot antenna

The horizontal directional diagram of a slot antenna contains the factors  $D*H*R$ :

$$A * |\sin(\vartheta + \vartheta_0)| * \left| \frac{\sin\left(\frac{n * \pi * b}{\lambda_0} * \cos(\vartheta + \vartheta_0)\right)}{\sin\left(\frac{\pi * b}{\lambda_0} * \cos(\vartheta + \vartheta_0)\right)} \right| * \left| 2 * \cos\left\{\frac{\pi}{4} * (-1 + \sin(\vartheta + \vartheta_0))\right\} \right|$$

$$A * |\sin(\vartheta + \vartheta_0)|$$

D: directional diagram of the individual radiator

$$\frac{\sin\left(\frac{n * \pi * b}{\lambda_0} * \cos(\vartheta + \vartheta_0)\right)}{\sin\left(\frac{\pi * b}{\lambda_0} * \cos(\vartheta + \vartheta_0)\right)}$$

H: horizontal array factor

$$2 * \cos\left\{\frac{\pi}{4} * (-1 + \sin(\vartheta + \vartheta_0))\right\}$$

R: reflector factor

- A amplitude fit
- n number of transmitting slots
- b slot spacing (half of the guided wavelength  $\lambda_G/2$ )
- $\vartheta$  polar angle
- $\vartheta_0$  angular displacement
- $\lambda_0$  free space wavelength

Formula to copy:  **$A * \text{abs}(\sin(x+B)) * \text{abs}((\sin(D * 180 * C / 32 * \cos(x+B)) / \sin(180 * C / 32 * \cos(x+B))) * \cos(45 * (-1 + \sin(x+B))))$**

- x polar angle  $\vartheta$

Starting values

- A = 1 amplitude fit
- B = 0 angle fit  $\vartheta_0$
- C = 23 distance between slots
- D = 7 number  $n$  of slots (select constant)

## Dipole antennas

### Fundamentals

The dipole is one of the oldest and simplest forms of antenna. It is used for microwave frequencies and even up to the long-wave range. Its radiation properties are dependent on the ratio  $l/h$  (dipole length/wavelength). Normally the antenna length is between  $1/3 \lambda$  and  $5/4 \lambda$  and only rarely exceeds  $2\lambda$ . Since LD antenna experiments are carried out in the X-band ( $f = 9.40 \text{ GHz}$ ,  $\lambda_0 = 32 \text{ mm}$ ) even long dipoles with  $l = 4\lambda$  have small dimensions suitable for work in the laboratory. Dipoles consist of two linear wire segments of equal length, the axes of which run collinearly. The distance between the wires ( $2\delta$ ) is assumed to be infinitely small and the center of the antenna is located at the origin of the coordinate system, whereby the dipole wires (conductors) run along the z-axis, (fig. 1).

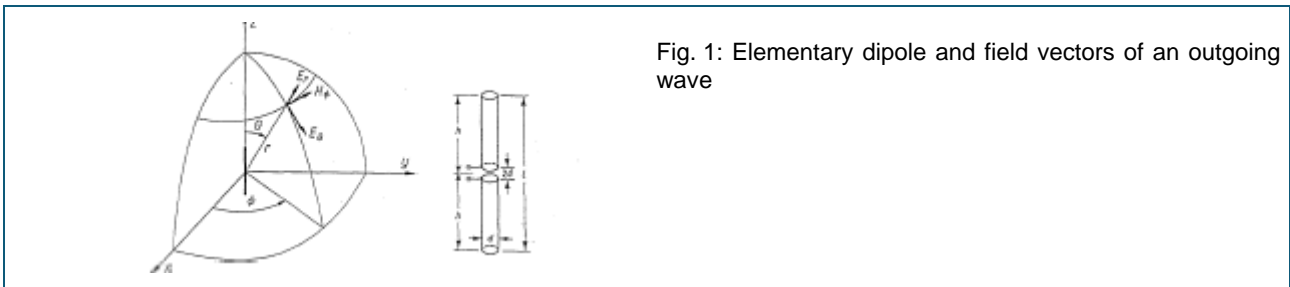


Fig. 1: Elementary dipole and field vectors of an outgoing wave

In theory wire length and diameter of a dipole can be of almost any value. Thus frequently the model of an infinitely short dipole (Hertzian dipole) is discussed. Dipoles possess a distinct directivity. They emit or receive linearly polarized waves. The vector of polarization evidently runs parallel to the dipole axis (z-axis). The radiation properties of a dipole are dependent on the current distribution in the antenna. The directivity of the dipole antenna can be derived mathematically based on the following (ideal) assumptions:

1. the dipole is infinitely thin ( $d \ll \lambda_0$ )
2. its wires are ideal conductors ( $\sigma = \infty$ ) and
3. the current distribution flows sinusoidal along the conductors.

From this we can derive the equation for the directional diagram of ideal dipole antennas in the far field.

$$E = \frac{60I_0}{r} \left| \frac{\cos(kh \cdot \cos \vartheta) \cdot \cos(kh)}{\sin \vartheta} \right|$$

where:

$$k = 2\pi/\lambda_0$$

$I_0$  = maximum current flowing through the antenna

$r$  = distance from the antenna

Typical directional diagrams of dipole antennas with various lengths are depicted in fig. 2. The equation (2) is used in many text books on antennas. However, errors can arise due to the fact that the approximations are neglected.

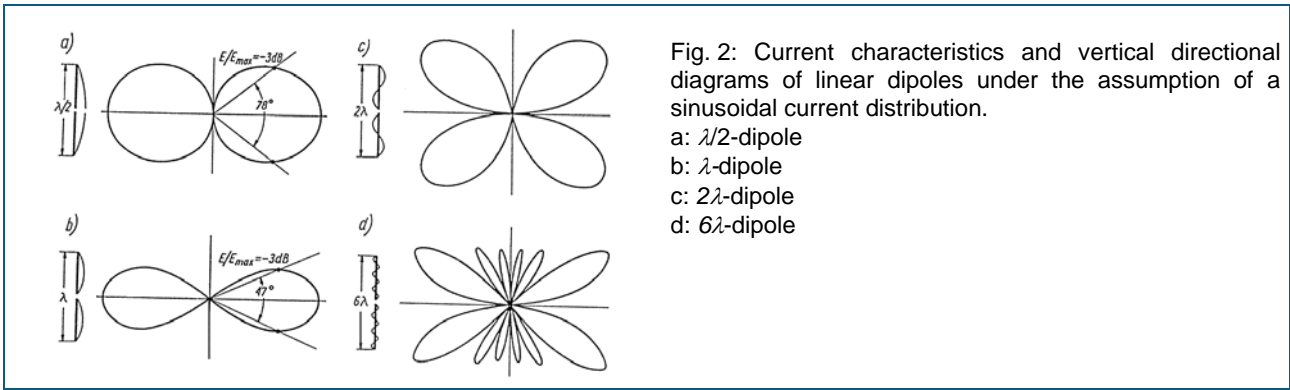


Fig. 2: Current characteristics and vertical directional diagrams of linear dipoles under the assumption of a sinusoidal current distribution.

- a:  $\lambda/2$ -dipole
- b:  $\lambda$ -dipole
- c:  $2\lambda$ -dipole
- d:  $6\lambda$ -dipole

The conductors of a real antenna are not ideal. This leads to a non-sinusoidal current distribution along the antenna conductors. Directional diagrams of ideal and a real antenna also differ due to the different current distributions on their wires. For mechanical reasons the wires of a real antenna must have a certain strength. The diameter of the wire must also be larger, if we need a broadband dipole. Both requirements reduce the slenderness of technical antennas. The degree of slenderness is given by the ratio:

$$s = \frac{l}{d}$$

Here the following applies:

- $l = 2h =$  dipole length
- $d =$  wire diameter

A change in thickness causes a change in the current distribution in the antenna. Thus, the conductor thickness affects the radiation properties of a dipole antenna too. The deviations increase with increasing wire thickness (Fig. 3).

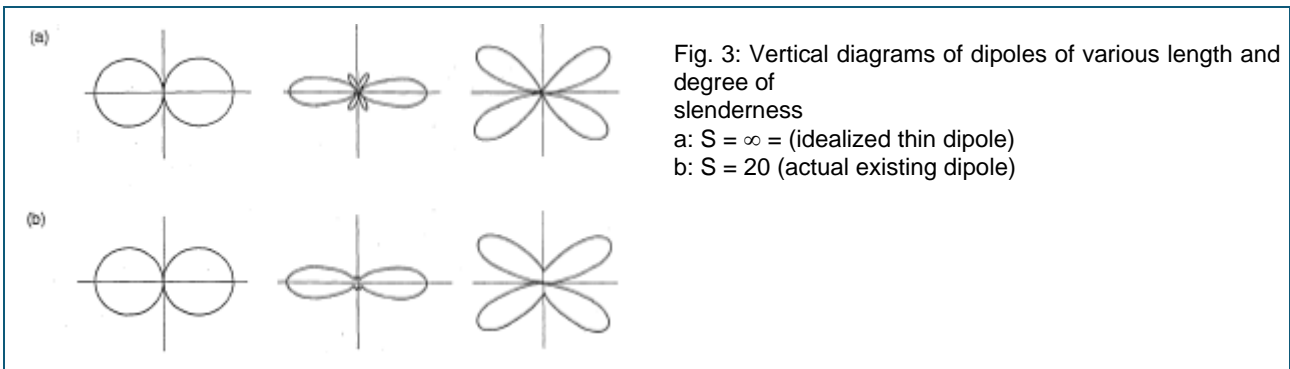


Fig. 3: Vertical diagrams of dipoles of various length and degree of slenderness

- a:  $S = \infty =$  (idealized thin dipole)
- b:  $S = 20$  (actual existing dipole)

Obviously our previous model of the dipole has been simplified too much for actual practice. The classical model of the dipole is flawed due to the assumption of a sinusoidal current distribution, which does not exist in real antennas. Notice: thick antennas suppress some of the nulls and minor lobes. Antennas must be matched either to a feeding oscillator or to the load of a receiver. For this reason it is important to know the impedance at the base of the antenna. The input impedance of an infinitely thin dipole ( $s = l/d = \infty$ ), which is exactly  $\lambda/2$  long, is a complex impedance with  $Z_{in} = (73 - j42) \Omega$ . The imaginary component of the input impedance of the dipole can be eliminated by selecting its length somewhat shorter than  $\lambda/2$ . The dipole then operates in its first resonance mode, whereby the input impedance then becomes real  $Z_{in} = R_{in}$ . The following empirical equations apply for the  $\lambda/2$ -dipole:

$$l \approx \frac{\lambda_0}{2} \cdot \frac{s}{s+1} \quad R_{in} = 67 \Omega$$



The frequency bandwidth of a dipole is dependent on its slenderness, whereby wider dipoles are broad-band.

## Material

1	737 01	Gunn oscillator
1	737 05	PIN modulator
1	737 06	Isolator
1	737 21	Large horn antenna
1	737 390	Set of microwave absorbers
1	737 405	Rotating antenna platform
1	737 415	Set of wire antennas
1	568 702	Book: Antenna Technology
2	301 21	Stand base MF
1	311 77	Steel tape measure
1		PC with Windows XP or higher version

## Experiment set-up

Typical experiment set-ups for excitation with a horizontally polarized, or vertically polarized wave.

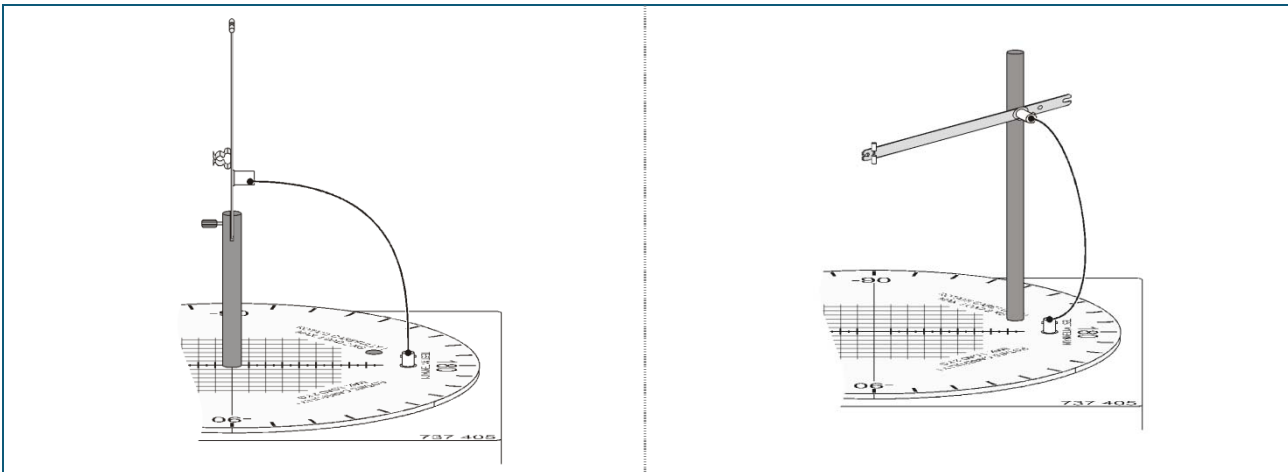


Fig. 9: Experiment set up for excitation with a horizontally polarized wave (E-plane).

Fig. 10: Experiment set up for excitation with a vertically polarized wave (H-plane). Rotation of the test antenna takes place in the H-plane of the exciting source field.

## Experiment procedure

### 1. Horizontal diagrams of the $\lambda/2$ -dipole

- Assemble the experiment set-up as specified in fig. 9. The  $\lambda/2$ -dipole is the basic configuration of the dipole antenna, i.e. without extension.
- Connect the dipole rod (this contains the dipole and the detector diode), with the holder provided. Insert the holder into the central mounting bore for the stand rods in the rotating antenna platform so that the axis is aligned to the reference lines on the rotating base.
- Connect the plug of the antenna output with a coaxial cable (25 cm) to the BNC input socket on the rotating base.

- Record the directional diagram with the following settings:
  - Range from:  $-180^\circ$  to:  $+180^\circ$
  - Angular Increment:  $1^\circ$
  - Bias Current: on
  - Detector characteristic: Quadratic,  $m = 2$
  - Graphic display:  $A(\vartheta)$  and  $a(\vartheta)$  respectively
- Insert the theoretical plot. To do this, refer to chapter *Formulas in directional diagrams*.
- Switch to Cartesian coordinates and determine the 3 dB-width using the graphic cursor. The 3 dB-width characterizes the angular positions of the main radiation lobe where the power has dropped by -3 dB. In linear representation this corresponds to 0.707 of the maximum value. Insert the values onto the screen.
- Comment on the results.

## 2. Horizontal diagrams of the $\lambda$ -dipole

- Attach the extension for the  $\lambda$ -dipole onto the two ends of the dipole. Do not alter the alignment of the experiment set-up.



- The experiment procedure corresponds to the procedure followed in point 1.
- Start the measurement. Evaluate the recorded measurement data graphically. Using the graphic cursor determine the 3 dB-width of the two lobes of the dipole.

## 3. Horizontal diagrams of the $3\lambda/2$ -dipole

- Carefully attach the extension for the  $3\lambda/2$ -dipole to the two ends of the dipole.
- Proceed with the instructions outlined in point 1.

## 4. Horizontal diagrams of the $2\lambda$ -dipole

- Carefully attach the extension for the  $2\lambda$ -dipole to the two ends of the dipole.
- Proceed with the instructions outlined in point 1.

## 5. Horizontal diagrams of the $4\lambda$ -dipole

- Carefully attach the extension for the  $4\lambda$ -dipole to the ends of the dipole.
- Proceed with the instructions outlined in point 1.

## 6. Attenuation of cross-polarized waves

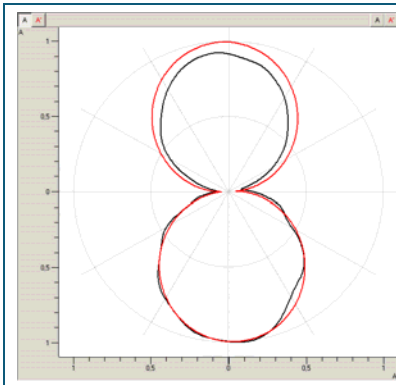
- By cross-polarization attenuation we are referring to the ratio of co-polarized incoming signals to cross-polarized incoming signals, i.e. the ratio of components lying in a perpendicular position with respect to each other.
- Here, the  $\lambda/2$ -dipole serves as the experiment object. Therefore carefully remove all extension from the dipole antenna.
- Set the antenna coupled to the rotating antenna platform in the  $0^\circ$  angular position. A maximum incoming signal should now appear on the level meter **a/dB**. Leave the test antenna unchanged in this position.
- Change the polarization of the exciting field by turning the waveguide circuit of the transmitter by  $90^\circ$  along its axis. Don't change the position or orientation of the transmitter! The horn antenna now radiates a vertically-polarized wave. The signal now received by the test antenna must be minimal (see level meter **a/dB**).
- Read the incoming signal on the level meter **a/dB**.
- The difference in dB between the co-polarized and cross-polarized measurement gives the attenuation of the cross-polarized waves.

## 7. Vertical diagrams of the $\lambda/2$ -dipole

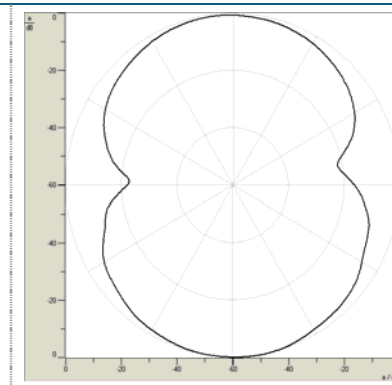
- A  $\lambda/2$ -dipole antenna serves as the experiment object. Determine the directional diagram in the H-plane. Therefore, the experiment set-up found in fig. 10 is used.
- Connect the antenna rod (this contains the dipole and the detector diode) with the arm for vertical diagrams (components from cat. no. 737 415). Mount the modified test antenna on the rotating antenna platform. Align the test antenna so that it is orientated over the center of the platform.
- For excitation of the test antenna, use the transmitter in the rotated configuration of experiment 6.
- Proceed with the instructions outlined in point 1.

## Results

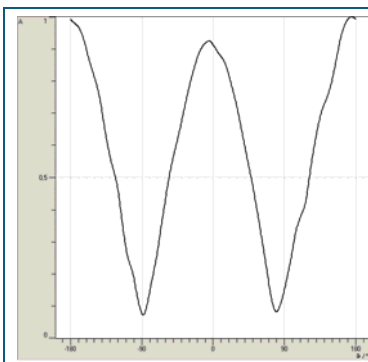
### 1. Horizontal diagrams of the $\lambda/2$ -dipole



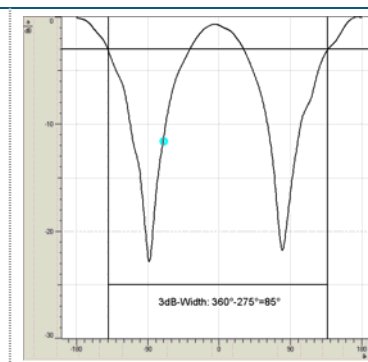
E-plane  
Polar coordinates  
Linear representation:  $A(\vartheta)$   
Black: measurement  
Red: Best fit approximation



E-plane  
Polar coordinates  
Logarithmic representation:  $a(\vartheta)$   
Black: measurement  
Red: Best fit approximation



E-plane  
Cartesian coordinates  
Linear representation:  $A(\vartheta)$   
Black: measurement



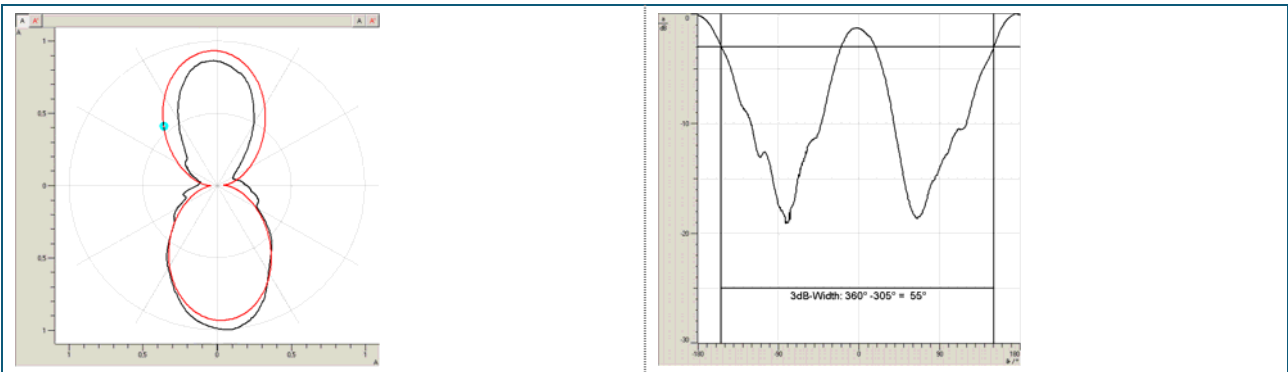
E-plane  
Cartesian coordinates  
Logarithmic representation:  $a(\vartheta)$   
3 dB-Width:  $360^\circ - 275^\circ = 85^\circ$  (Theory:  $78^\circ$ )

The directional diagram of a  $\lambda/2$ -dipole in the E-plane in polar representation shows the form of an even symmetrical eight. If the dipole is tested in an inhomogeneous field, the recorded directional diagram would deviate (asymmetrical form) from the theoretical form. Inhomogeneous fields in the area of the test antennas are caused by standing waves. They are formed by the superimposing of progressive and reflecting waves, which are arriving from different directions. They can arise longitudinally or laterally to the measurement path. The asymmetry of the directional diagram increases further if the test antenna carries out eccentric movements. These kind of distortion is especially noticeable in the case of small antennas like the  $\lambda/2$ -dipole.

**Far field condition**

Test antenna:	$\lambda/2$ -dipole	Remarks
$r_0$ :	1000 mm	Mean distance measured between the source and the test antenna
$\lambda_0$ :	32 mm	Wavelength of the radiated wave
$d_Q$ :	100 mm	Largest transverse measurement of the radiating horn
$d_T$ :	15 mm	Extension of the $\lambda/2$ -dipole
$r_0 \geq \frac{2(d_Q + d_T)^2}{\lambda_0}$	$r_0 > 827\text{mm}$	Far field condition is fulfilled.

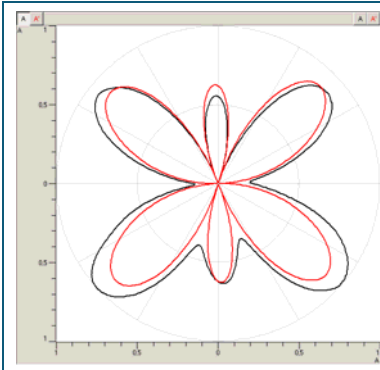
**2. Horizontal diagrams of the  $\lambda$ -dipole**



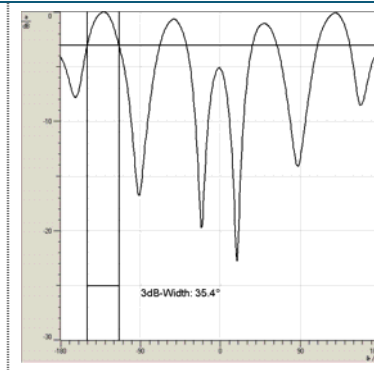
E-plane  
 Polar coordinates  
 Linear representation:  $A(\vartheta)$   
 Black: measurement  
 Red: Best fit approximation

E-plane  
 Cartesian coordinates  
 Logarithmic representation:  $a(\vartheta)$   
 3 dB-Width:  $360^\circ - 305^\circ = 55^\circ$  (Theory:  $47^\circ$ )

### 3. Horizontal diagrams of the $3/2\lambda$ -dipole

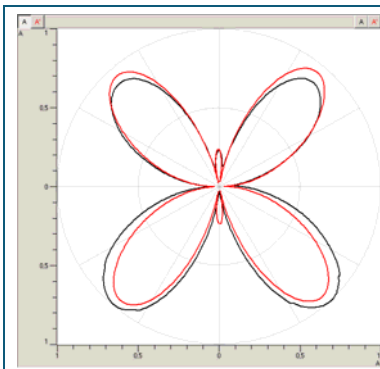


E-plane  
 Polar coordinates  
 Linear representation:  $A(\vartheta)$   
 Black: measurement  
 Red: Best fit approximation

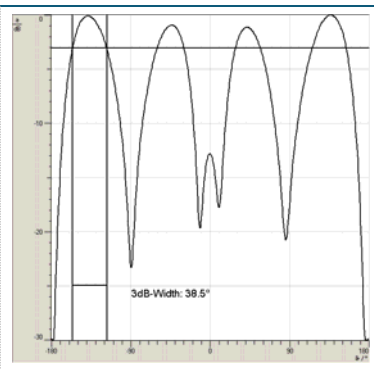


E-plane  
 Cartesian coordinates  
 Logarithmic representation:  $a(\vartheta)$   
 3 dB-Width: 35 °

### 4. Horizontal diagrams of the $2\lambda$ -dipole

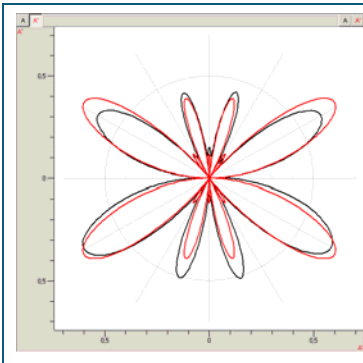


E-plane  
 Polar coordinates  
 Linear representation:  $A(\vartheta)$   
 Black: measurement  
 Red: Best fit approximation

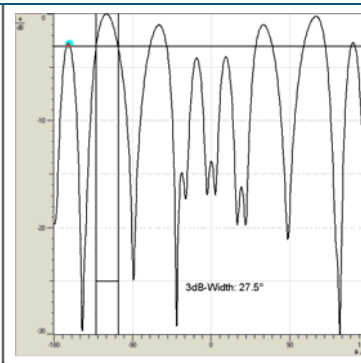


E-plane  
 Cartesian coordinates  
 Logarithmic representation:  $a(\vartheta)$   
 3 dB-Width: 38,5 °(main lobe)

5. Horizontal diagrams of the  $4\lambda$ -dipole



E-plane  
 Polar coordinates  
 Linear representation:  $A(\vartheta)$   
 Black: measurement  
 Red: Best fit approximation



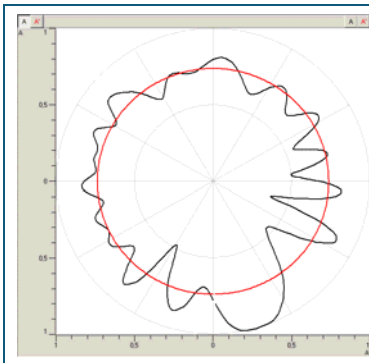
E-plane  
 Cartesian coordinates  
 Logarithmic representation:  $a(\vartheta)$   
 3 dB-Width: 27,5 °(main lobe)

6. Attenuation of cross-polarized waves (PLF)

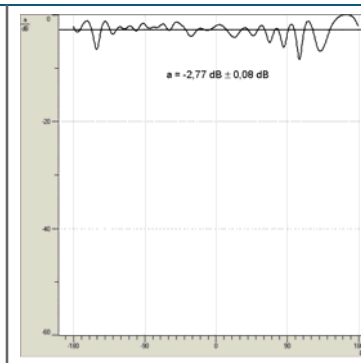
Co-polarization  
 Cross polarization  
 PLF

**a/dB**  
 $a_1 =$   
 $a_2 =$   
 $a_1 - a_2 = 30$

7. Vertical diagrams of the  $\lambda/2$ -dipole



H-plane  
 Polar coordinates  
 Linear representation:  $A(\vartheta)$   
 Black: measurement  
 Red: Best fit approximation



H-plane  
 Cartesian coordinates  
 Logarithmic representation:  $a(\vartheta)$   
 Mean value: -2.8 dB

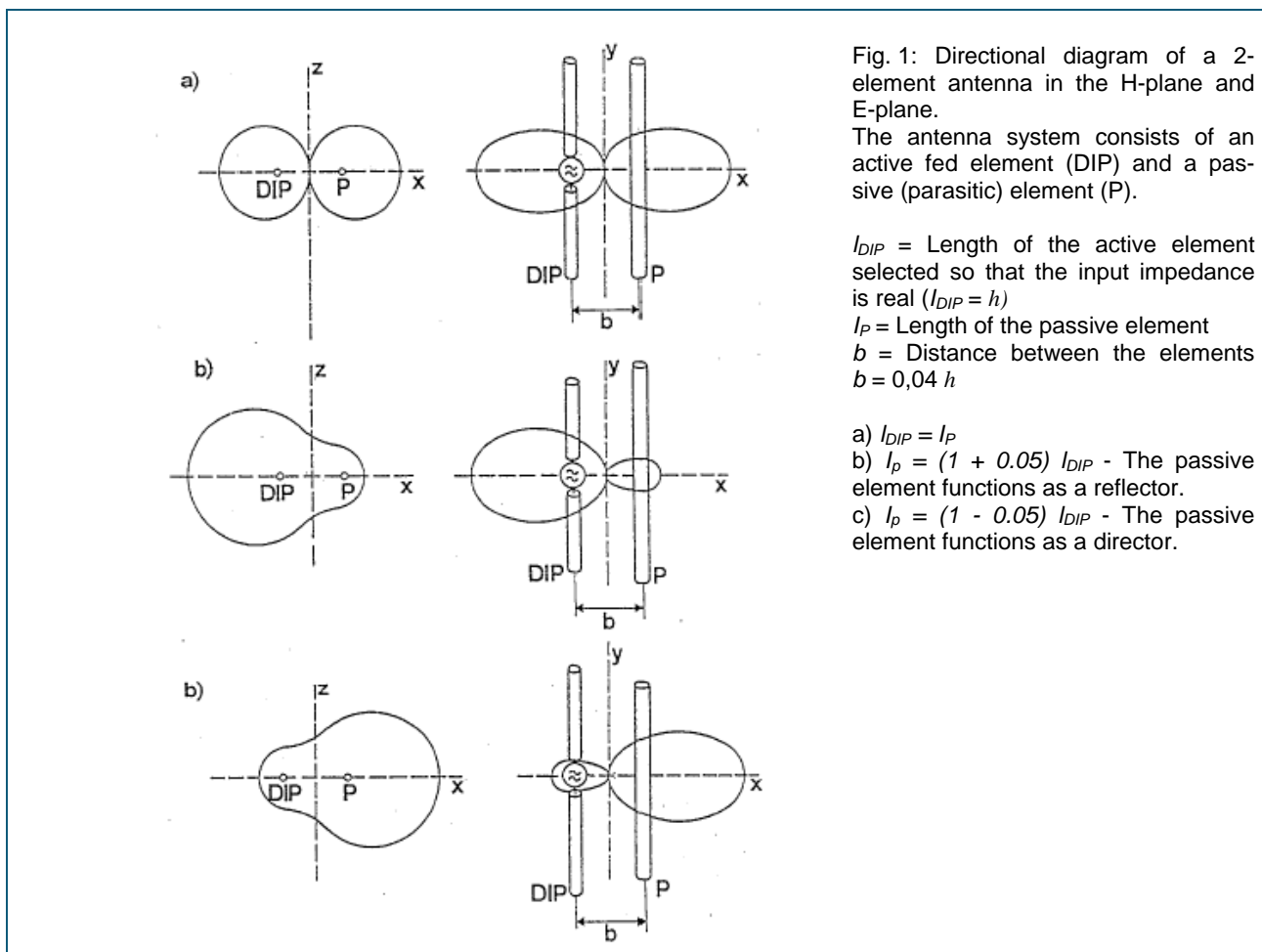
The arm for the vertical diagram causes unwanted reflections. They are responsible for the periodic fluctuations within the vertical directional diagram of the  $\lambda/2$ -dipole.



## Yagi antennas

### Fundamentals

The Yagi antenna represents a form of the multi-element antenna. Only one single active element is used for feeding: the dipole. All other elements are radiation coupled or parasitic. Thus, they do not require any feed lines or matching elements. Radiation coupling means the parasitic elements are only excited by the electromagnetic field of the dipole. The parasitic elements influence both the input impedance of the active element - the dipole - as well as the directional diagram of the entire antenna system. By selecting suitable dimensions for the parasitic elements, it is possible to shape the directional diagram of the antenna (see fig. 1). Behind the dipole we have a slightly longer element, which reflects the power radiated from the dipole in the direction of the major lobe. Using optics as an analogy, this is called a reflector. The director is, in comparison to the dipole, a shorter, parasitic element which concentrates the radiated energy in the major lobe direction. Its counterpart in optics is the focusing lens.



The directional properties of the simple Yagi- antenna shown in fig. 1 can be improved by combining the two passive elements  $R$  and  $D$ . We then obtain a system with a reflector behind the dipole and a director in front of it (see fig. 2).

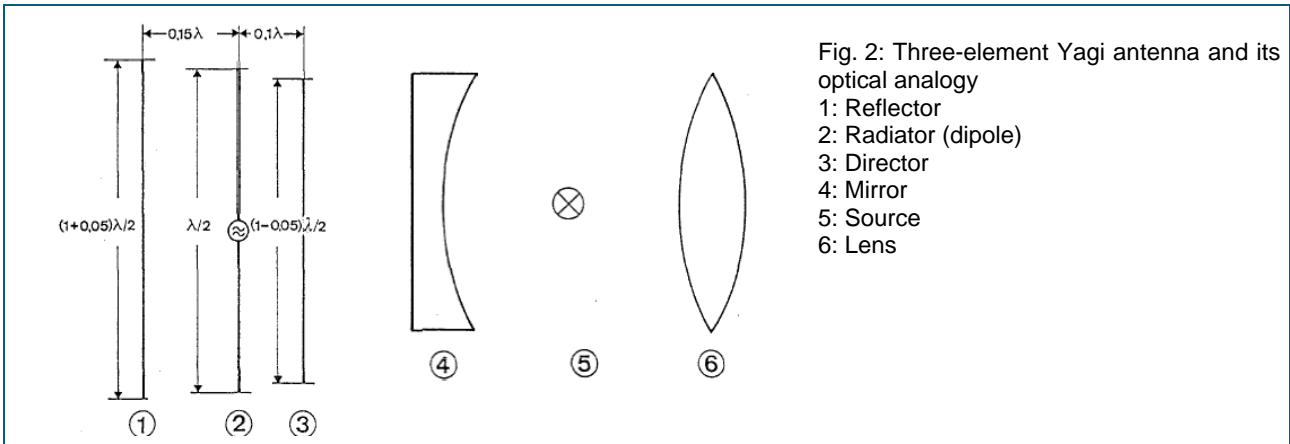


Fig. 2: Three-element Yagi antenna and its optical analogy  
 1: Reflector  
 2: Radiator (dipole)  
 3: Director  
 4: Mirror  
 5: Source  
 6: Lens

When the length of the parasitic elements and the distances between them have been suitably selected, it is possible to alter the shape of the directional diagram, thus optimizing, for example, the gain or the front-to-back ratio of the antenna. The possibilities of optimization are increased with the number of reflectors and directors. A larger number of directors causes an increased flattening off of the wave fronts in the direction of the major lobe. Fig. 3 demonstrates this phenomena. Directly at the dipole the wave fronts are still extremely curved. At the outer directors the waves have almost reached the transition to a plane wave and in this manner a more focused beam is achieved.

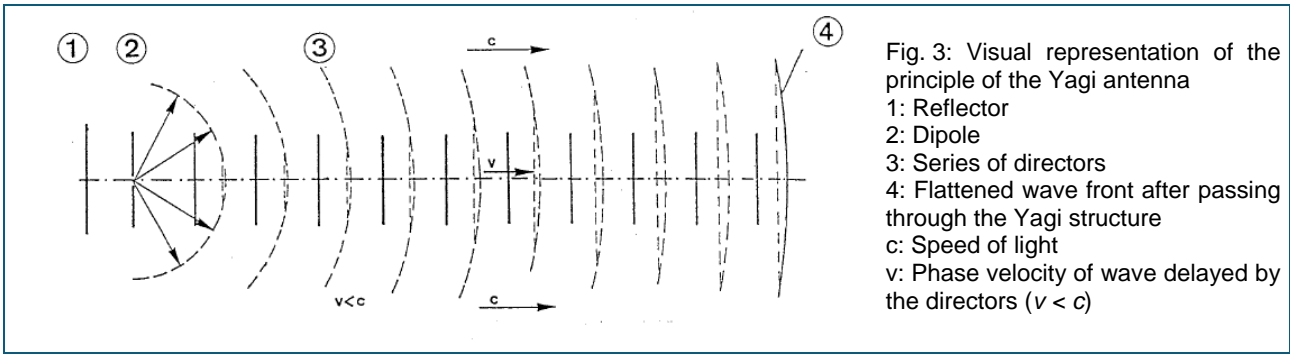
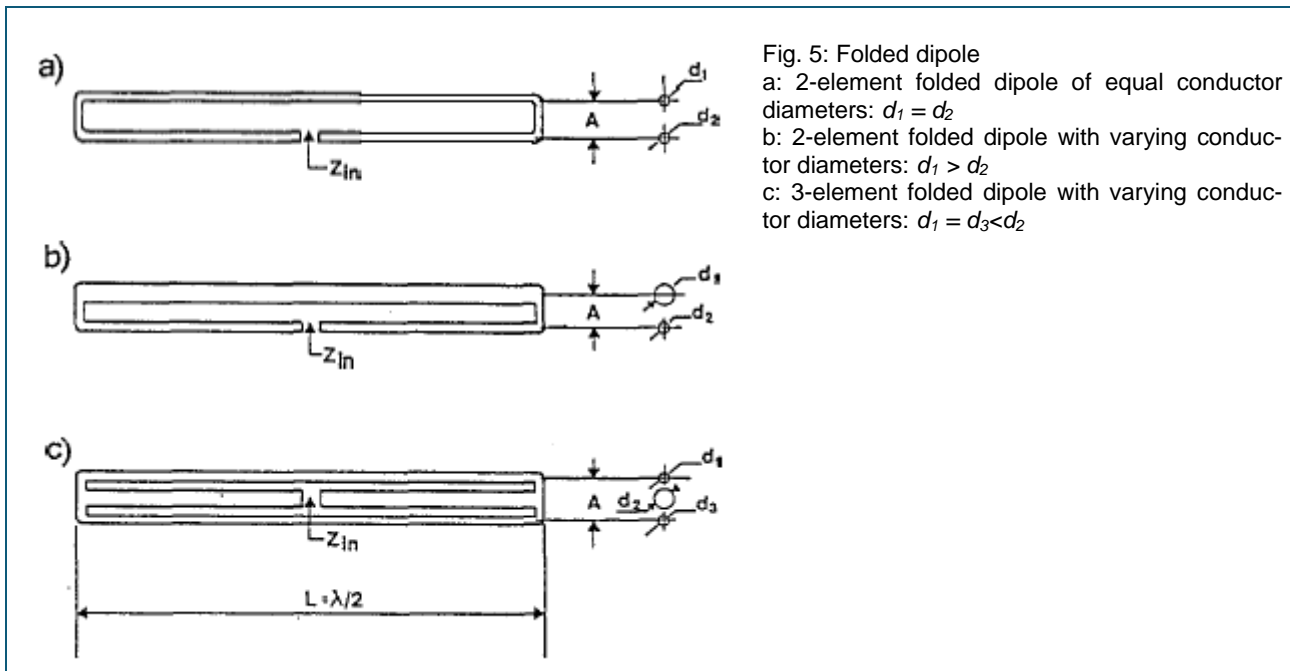


Fig. 3: Visual representation of the principle of the Yagi antenna  
 1: Reflector  
 2: Dipole  
 3: Series of directors  
 4: Flattened wave front after passing through the Yagi structure  
 c: Speed of light  
 v: Phase velocity of wave delayed by the directors ( $v < c$ )

The Yagi antenna radiates or receives linearly polarized waves, where the polarization vector runs parallel to the dipole axis (Y-axis). The radiation properties as well as the input impedance are dependent on the current distribution in all elements of the antenna including the parasitic elements. The input impedance of a Yagi antenna deviates considerably from that of its active base element - the dipole. This is brought about by the interaction of the additional radiators. Furthermore, the input impedance is generally a complex number. The frequency response depends on the antenna's geometry in a complicated way. The input impedance is lower compared to the single dipole. Therefore, in order to make matching easier, the folded dipole replaces the single dipole in a practical Yagi antenna. It is normal to find a 2-element or generally  $n$ -element folded dipole in use (see fig. 5). The input impedance is then  $n^2$ -times larger than in the case of a single-rod dipole, provided that the dipoles are insulated and  $(\lambda/2)$  in length.



By using a 2-element folded dipole, the input impedance of a 6-element Yagi antenna (Yagi-4DR), increases from  $20 \Omega$  to almost  $80 \Omega$ , which approximates the characteristic impedance of  $75 \Omega$  of a standard TV-cable and thus simplifies the construction of a matching transformer. Folded dipoles with conductor rods of various thickness, cause deviations from the  $n^2$ -law. Thus, it is possible to dimension the folded dipole even without any matching elements.

## Material

1	737 01	Gunn oscillator
1	737 05	PIN modulator
1	737 06	Isolator
1	737 21	Large horn antenna
1	737 390	Set of microwave absorbers
1	737 405	Rotating antenna platform
1	737 415	Set of wire antennas
1	568 702	Book: Antenna Technology
2	301 21	Stand base MF
1	311 77	Steel tape measure
1		PC with Windows XP or higher version

## Experiment set-up

A typical experiment set-up is shown in fig. 6 with excitation using a horizontally-polarized wave. For vertically-polarized waves turn the transmitter by 90°.

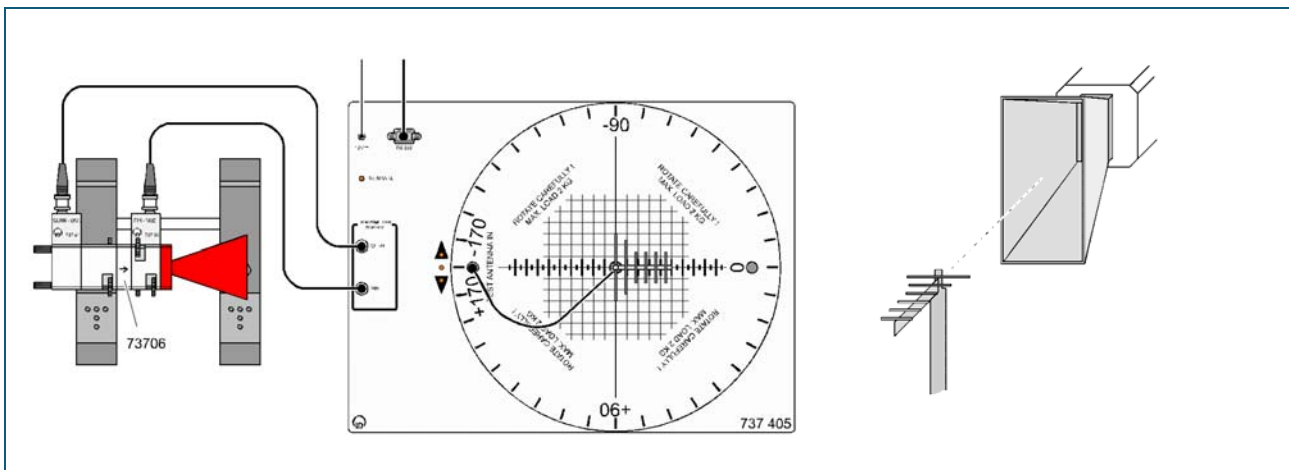


Fig. 6: Experiment set-up for excitation with horizontally-polarized waves. Test antenna is rotating in the E-plane of the source antenna.

## Experiment procedure

The influence of parasitic elements of the Yagi antenna (reflector and directors) on directional diagrams is determined experimentally.

### 1. Horizontal diagrams of the Yagi-R antenna

- The 2-element Yagi antenna consisting of a  $\lambda/2$ -dipole and a reflector  $R$  is used as the object of the experiment.
- Carefully insert the holder with the reflector into the dipole rod. At the same time be careful not to turn the antenna rod in the center bore mount of the rotating platform. In the starting position of the rotating platform the reflector should be pointed at the source antenna.

- Record the directional diagram with the following settings:
  - Range from:  $-180^\circ$  to:  $+180^\circ$
  - Angular Increment:  $1^\circ$
  - Bias Current: on
  - Detector characteristic: Quadratic,  $m = 2$
  - Graphic display:  $A(\vartheta)$  and  $a(\vartheta)$  respectively
- Insert the theoretical plot. To do this, refer to chapter *Formulas in directional diagrams*.
- Switch over to Cartesian coordinates and determine the 3 dB-width.
- Load the file of the  $\lambda/2$ -dipole additionally. Compare the directional diagrams.
- Save the measurement e.g.: Yagi-R.labx
- Determine the front-to-back ratio of the Yagi-R antenna. For this, position the cursor at the maximum of the back lobe, opposite the maximum of major lobe. The values are also to be entered into table 1.
- Jointly display the directional diagrams of the  $\lambda/2$ -dipole and the Yagi-R antenna on the screen. Compare the displayed directional diagrams to each other and draw conclusions with respect to the effects of the reflector. Is the far field condition fulfilled for the Yagi-R antenna?

## 2. Horizontal diagrams of the Yagi-D antenna

- The 2-element Yagi antenna consisting of a director  $D$  and a  $\lambda/2$ -dipole is used as the experiment object.
- Carefully insert the holder with director onto the dipole rod. Be careful not to turn the dipole rod in the central bore mount of the rotating platform. In the rotating platform's starting position, the director must point away from the source antenna.
- Repeat the measurement described in point 1.
- Save the measurement e.g.: Yagi-D.labx
- Jointly display the directional diagrams of the  $\lambda/2$ -dipole and the Yagi-D antenna on the screen. Compare the displayed directional diagrams to each other and draw conclusions with respect to the effects of the director on the directional diagram.

## 3. Horizontal diagrams of the Yagi-DR antenna

- A 3-element Yagi antenna consisting of a director  $D$ , a  $\lambda/2$ -dipole and a reflector  $R$  is used as the experiment object.
- Carefully insert the holder with director and reflector onto the antenna rod.
- Repeat the measurement described in point 1.
- Save the measurement e.g.: Yagi-DR.labx
- Jointly display the directional diagrams of the  $\lambda/2$ -dipole and the Yagi-DR antenna on the screen. Compare the displayed directional diagrams to each other and draw conclusions with respect to the effects of the director and reflector on the directional diagram.

## 4. Horizontal diagrams of the Yagi-4DR antenna

- The 6-element Yagi antenna consisting of 4 directors of equal length  $4D$ , a  $\lambda/2$ -dipole and a reflector  $R$  is used as the object of the experiment.
- Carefully insert the holder with four directors and a reflector onto the antenna rod. In the rotating platform's starting *position*, the directors must *point* away from the source antenna while the reflector is aligned toward the source antenna.
- Is the far field condition fulfilled?
- Repeat the measurement described in point 1.
- Save the measurement e.g.: Yagi-4DR.labx.

- Jointly display the directional diagrams of the  $\lambda/2$ -dipole and the Yagi-4DR antenna on the screen. Compare the displayed directional diagrams to each other and draw conclusions with respect to the effects of the 4 directors and the reflector on the directional diagram.
- Comment on your measurement results.

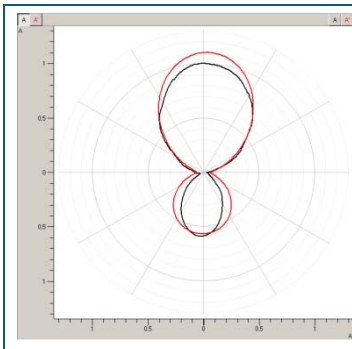
Antenna	3 dB-Width / deg	F/B-Ratio / dB
Yagi-R		
Yagi-D		
Yagi-DR		
Yagi-4DR		

### Variant

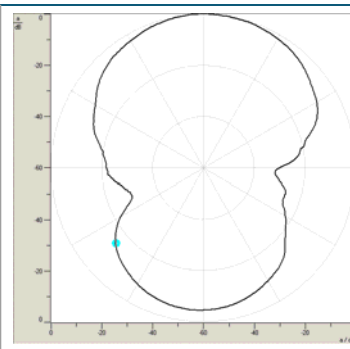
Measure the vertical directional diagrams of the Yagi antennas.

## Results

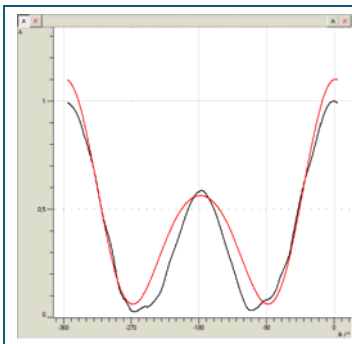
### 1. Horizontal diagrams of the Yagi-R antenna



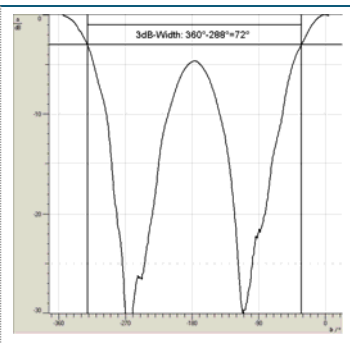
E-plane  
Polar coordinates  
Linear representation:  $A(\vartheta)$   
Black: measurement  
Red: Best fit approximation



E-plane  
Polar coordinates  
Logarithmic representation:  $a(\vartheta)$

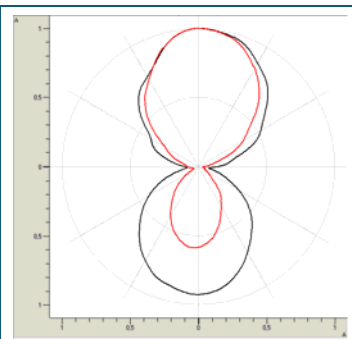


E-plane  
Cartesian coordinates  
Linear representation:  $A(\vartheta)$   
Black: measurement  
Red: Best fit approximation



E-plane  
Cartesian coordinates  
Logarithmic representation:  $a(\vartheta)$   
3 dB-Width: 72°

### Joint display of the directional diagrams of a $\lambda/2$ -dipole and a Yagi-R antenna.

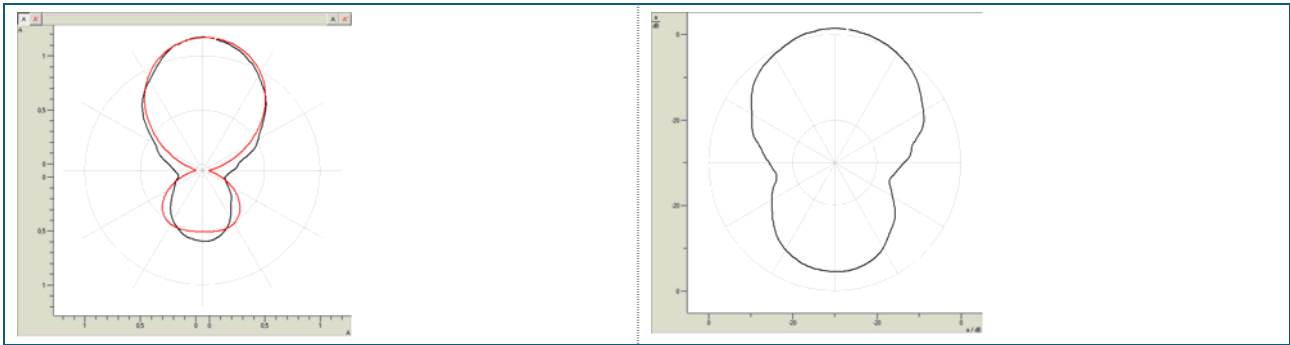


E-plane  
Polar coordinates  
Linear representation:  $A(\vartheta)$   
Black:  $\lambda/2$ -dipole  
Red: Yagi-R

#### Observation

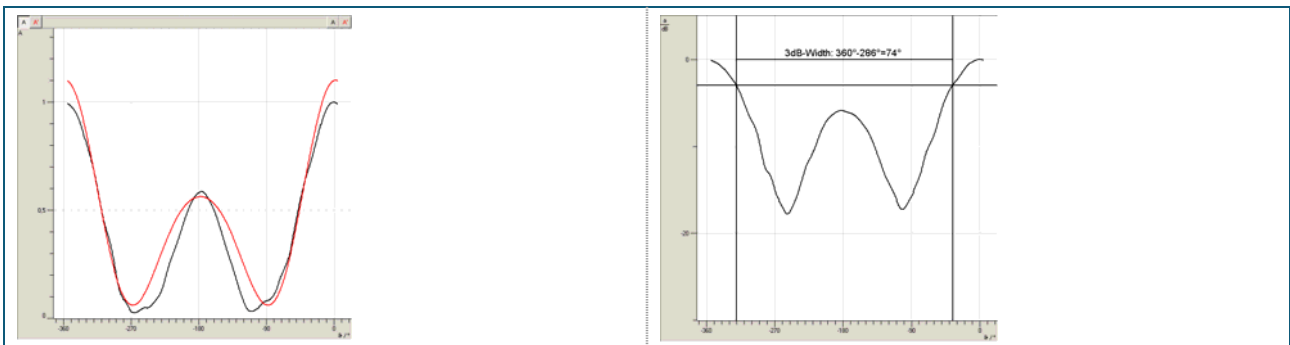
By using a reflector behind the dipole, the front-to-back ratio is increased considerably. However, the shape of the major lobe remains practically unchanged; it becomes somewhat thinner, see also table 1.

2. Horizontal diagrams of the Yagi-D antenna



E-plane  
 Polar coordinates  
 Linear representation:  $A(\vartheta)$   
 Black: measurement  
 Red: Best fit approximation

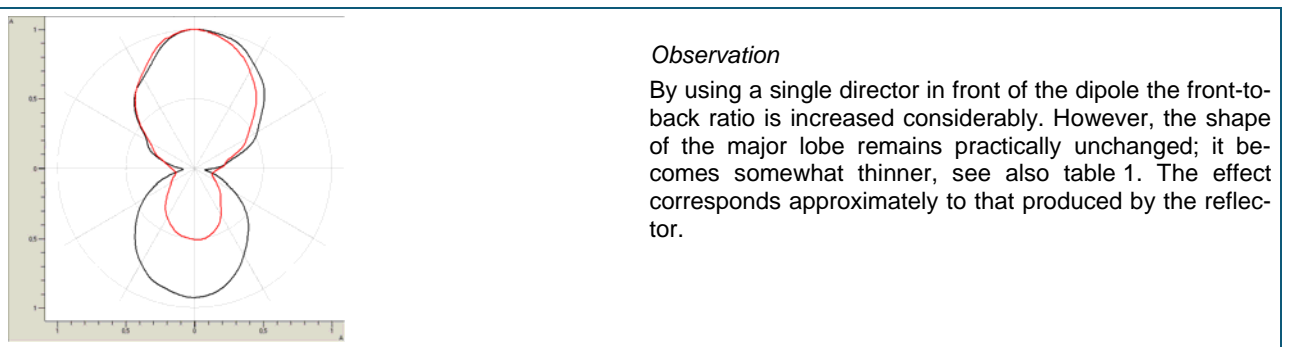
E-plane  
 Polar coordinates  
 Logarithmic representation:  $a(\vartheta)$



E-plane  
 Cartesian coordinates  
 Linear representation:  $A(\vartheta)$   
 Black: measurement  
 Red: Best fit approximation

E-plane  
 Cartesian coordinates  
 Logarithmic representation:  $a(\vartheta)$   
 3 dB-Width: 74°

Joint display of the directional diagrams of a  $\lambda/2$ -dipole and a Yagi-D antenna.



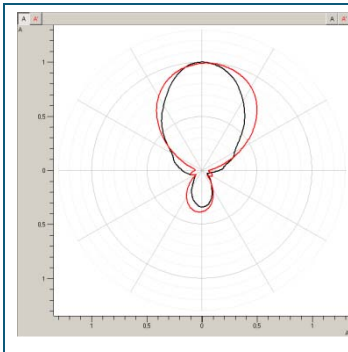
*Observation*

By using a single director in front of the dipole the front-to-back ratio is increased considerably. However, the shape of the major lobe remains practically unchanged; it becomes somewhat thinner, see also table 1. The effect corresponds approximately to that produced by the reflector.

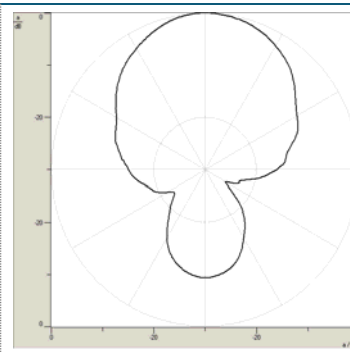
E-plane  
 Polar coordinates  
 Linear representation:  $A(\vartheta)$   
 Black:  $\lambda/2$ -dipole  
 Red: Yagi-D



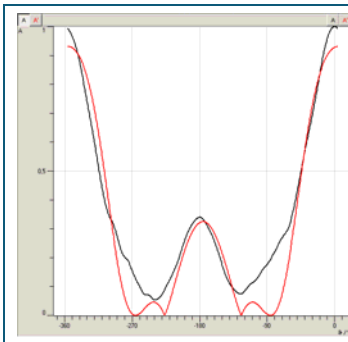
### 3. Horizontal diagrams of the Yagi-DR antenna



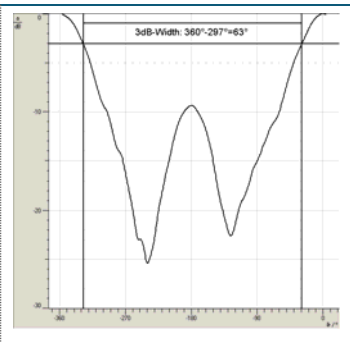
E-plane  
Polar coordinates  
Linear representation:  $A(\vartheta)$   
Black: measurement  
Red: Best fit approximation



E-plane  
Polar coordinates  
Logarithmic representation:  $a(\vartheta)$

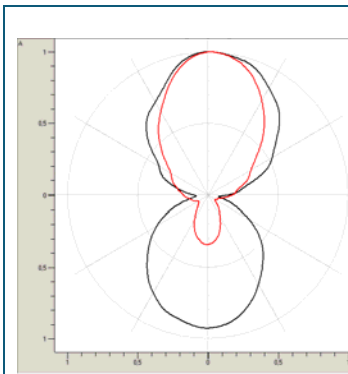


E-plane  
Cartesian coordinates  
Linear representation:  $A(\vartheta)$   
Black: measurement  
Red: Best fit approximation



E-plane  
Cartesian coordinates  
Logarithmic representation:  $a(\vartheta)$   
3 dB-Width: 63°

Joint display of the directional diagrams of a  $\lambda/2$ -dipole and a Yagi-DR antenna.

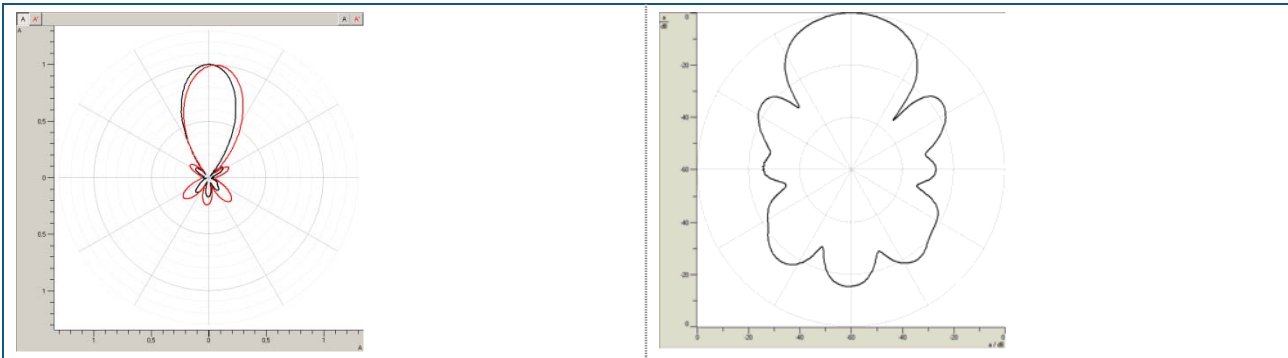


E-plane  
Polar coordinates  
Linear representation:  $A(\vartheta)$   
Black:  $\lambda/2$ -dipole  
Red: Yagi-DR

#### Observation

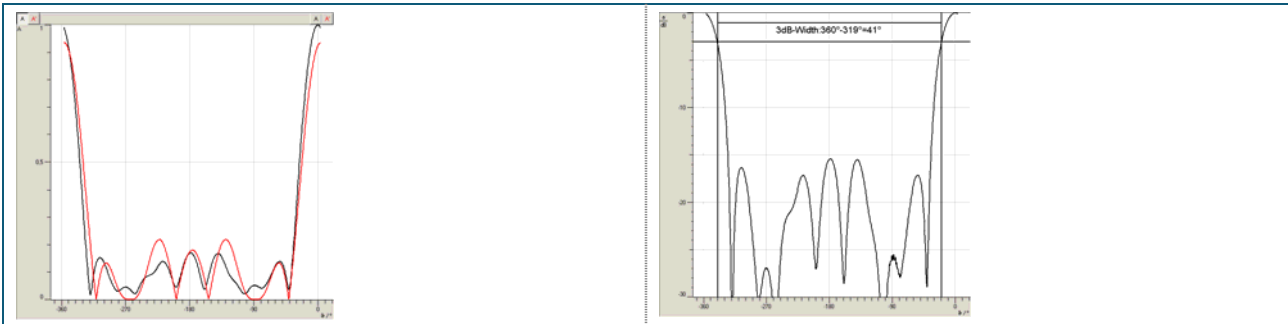
By jointly using a single director and a reflector, the front-to-back dipole is considerably improved in comparison to the dipole. The shape of the major lobe remains practically unchanged, almost as in the experiments with the Yagi-R or Yagi-D. It becomes somewhat more narrow, see also table 1.

4. Horizontal diagrams of the Yagi-4DR antenna



E-plane  
 Polar coordinates  
 Linear representation:  $A(\vartheta)$   
 Black: measurement  
 Red: Best fit approximation

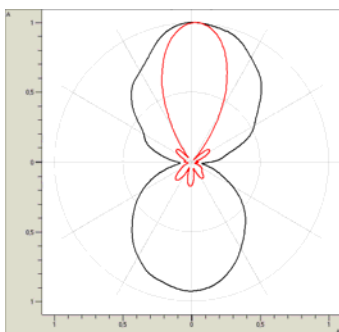
E-plane  
 Polar coordinates  
 Logarithmic representation:  $a(\vartheta)$



E-plane  
 Cartesian coordinates  
 Linear representation:  $A(\vartheta)$   
 Black: measurement  
 Red: Best fit approximation

E-plane  
 Cartesian coordinates  
 Logarithmic representation:  $a(\vartheta)$   
 3 dB-Width: 41°

Joint display of the directional diagrams of a  $\lambda/2$ -dipole and a Yagi-4DR antenna.



E-plane  
 Polar coordinates  
 Linear representation:  $A(\vartheta)$   
 Black:  $\lambda/2$ -dipole  
 Red: Yagi-4DR

*Observation*

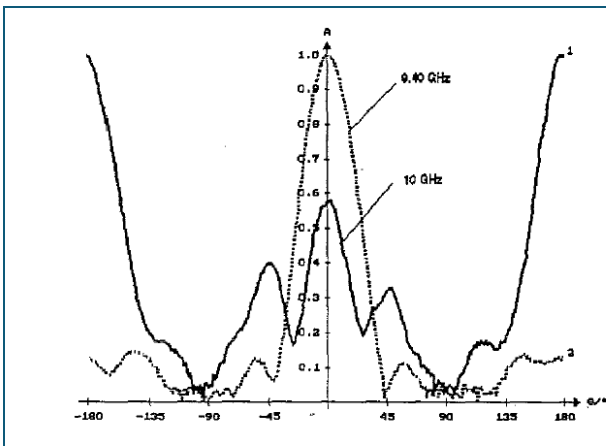
By increasing the number of directors to 4 and utilizing a reflector, a 6-element Yagi antenna is produced. Its front-to-back ratio increases considerably than in the case of the 3-element antenna. Even the shape of the major lobe is more distinct. Here a real directional antenna is created, which operates primarily in the direction of the major lobe. For the first time, two smaller secondary lobes appear in the forward direction.

## Far field condition

Test antenna:	Yagi-4DR	Remarks
$r_0$ :	1000 mm	Mean distance measured between the source and the test antenna
$\lambda_0$ :	32 mm	Wavelength of the radiated wave
$d_Q$ :	100 mm	Largest transverse measurement of the radiating horn
$d_T$ :	54 mm	Longitudinal extension of the Yagi-4DR antenna
$r_0 \geq \frac{2(d_Q + d_T)^2}{\lambda_0}$	$r_0 > 1482\text{mm}$	Far field condition is not fulfilled.

Antenna	3 dB-Width /deg	F/B-Ratio / dB
Yagi-R	72	
Yagi-D	74	
Yagi-DR	63	
Yagi-4DR	41	

### Note:



The properties of Yagi antennas are strongly frequency dependent. This applies even more, the more parasitic elements are used. This frequency dependency also influences the directional diagram. For example the Yagi-4DR practically inverts its directional diagram (main lobe on the backside) for an operating frequency of approx. 10 GHz.

## Aperture antennas

### Fundamentals

Aperture antennas include different elementary radiators such as:

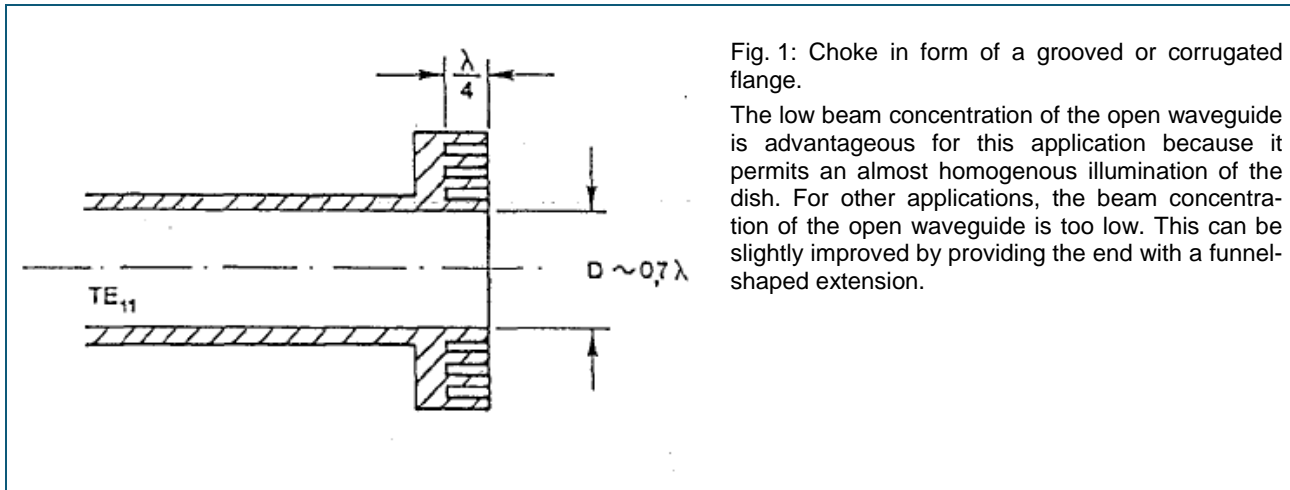
- open waveguide ends
- horns
- reflectors and
- lenses of the most varied kind.

Aperture antennas are employed in many applications. To avoid aerodynamic disturbances in aircraft, aperture antennas can be integrated directly into the external metallic skin and fitted with dielectric windows. The metal cladding can then be considered a base plate of an aperture antenna. Another well-known representative of an aperture antenna is the reflector antenna fed via a horn radiator (because it consists of a mirror and feed antenna, we prefer to designate this type as non-elementary.) The type of parabola dish antenna is frequently used as a radar antenna for aviation and marine navigation purposes. Additional important fields of application for this kind of antenna are microwave links, radio astronomy, measurement technology and police traffic control. The characteristics of this kind of mirror antenna with large apertures are investigated later. The radiating and receiving characteristics of aperture antennas are determined by their field distribution (i.e. the distribution of the displacement current) in the aperture. For review: in wire antennas these characteristics are determined by the current distribution in the wires. Normally the fields (including the displacement currents) are regarded to be zero outside the aperture. The discussion of aperture antennas is similar to the optic problem of light diffraction at a diaphragm. Because the dimensions of an optical diaphragm are much greater relative to the wavelength of light than the dimensions of the aperture in comparison to the wavelength of a radiated microwave, the results and conclusions made in optics can only be an initial approximation to antenna technology. This is particularly true for short slot antennas, which can be dealt with better in terms of a dipole antenna using Babinet's principle. The limitations mentioned above when transferring results obtained in optics to microwave technology also apply to the size of the base plate. The popular assumption in optics is that the base plate can be extended infinitely. This assumption is not fulfilled for microwaves. The diffraction at the edges of the base plate affects the directional diagram of the radiating aperture. This effect is even greater, the smaller the base plate dimensions are in relation to the wavelengths.

### Open waveguides and horns

Open-ended waveguides and horn antennas are widely used aperture radiators. They are primarily employed as feed elements for various reflector type antennas. Any open end of a waveguide, which guides the fundamental wave, acts like an aperture radiator. Field lines emerge into free space at its open end. Therefore, it can be expected that the power fed into the waveguide, is radiated. The radiation is maximum in the longitudinal direction of the waveguide. The radiated wave is not concentrated into a particularly focused beam, because the dimensions of the aperture opening are small in comparison with the wavelength. Therefore, only a portion of the wave is radiated, while the remaining portion is reflected at the aperture plane. This kind of mismatching can be reduced using a matching element, i.e. a 3-stub tuner or a slide screw transformer.

The directional diagram of an open waveguide is determined not only by its aperture dimensions, but also by the ground plane (ideal: infinitely extended ground plane). In actual practice diffraction effects at the edges of the reflector plate distort the directional diagram. They have a particularly strong impact on the side lobes. Diffraction effects at the edges can be minimized by equipping the flanges with chokes. Thus for round open-ended waveguides carrying the  $TE_{11}$ -mode, corrugated flanges (see fig. 1) are common. This type is frequently used for the primary feeder of TV dish antennas.



**Note:** Waveguide antennas are simple open-ended waveguides. Horn antennas are waveguides whose mouths gradually open into funnel-shaped extensions.

The field distribution in a rectangular waveguide excited with the fundamental mode  $TE_{10}$  is shown in fig. 2.

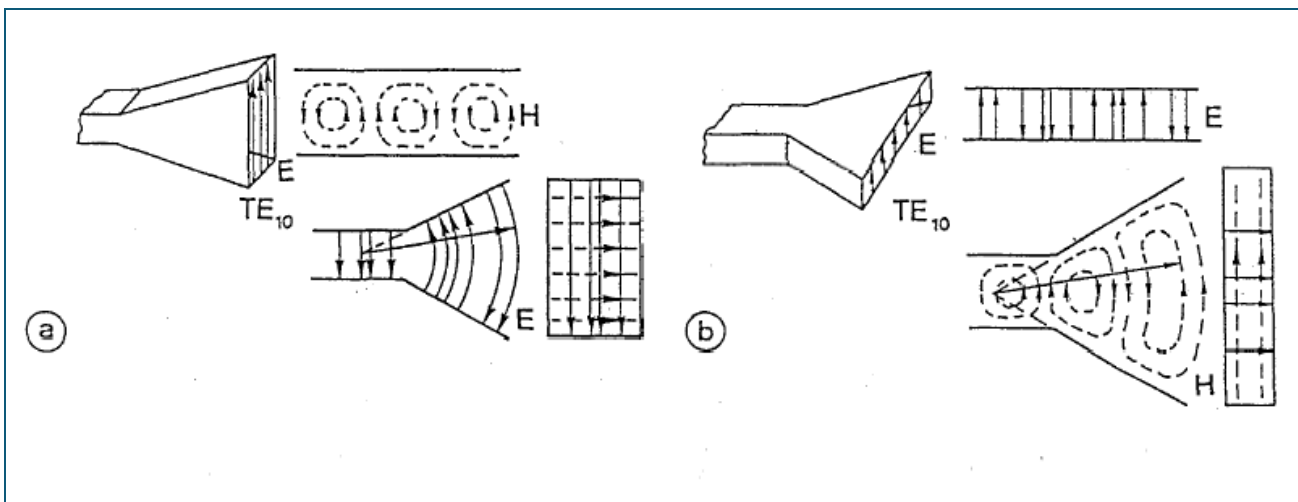


Fig. 2: Distribution of the E- and H-Fields in an E and H sectoral horn (with smooth walls).

- a: E sectoral horn
- b: H sectoral horn

The extension of the feeding waveguide in the E and H planes leads to the pyramidal horn. A conical horn is produced by extending a round waveguide. The most important horn antennas are depicted in fig. 3.

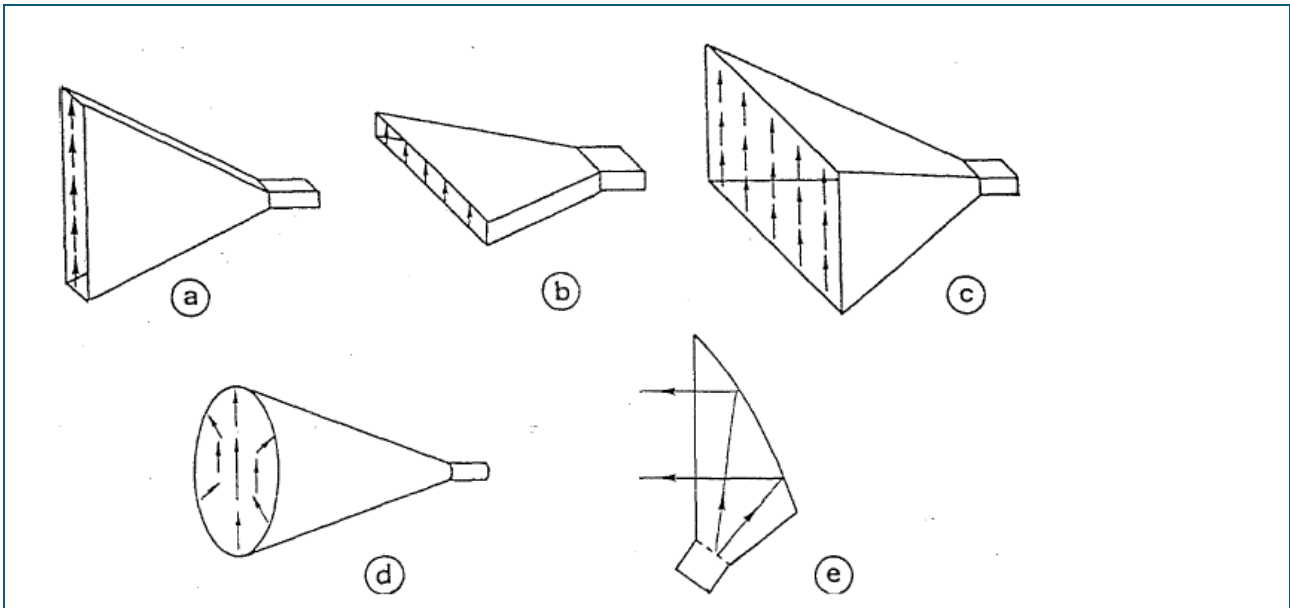


Fig. 3: Typical horn antennas (with smooth walls)

- a: E sectoral horn
- b: H sectoral horn
- c: Pyramidal horn
- d: Conical horn
- e: Hoghorn antenna

Normal horn antennas have smooth walls. More sophisticated horn antennas have grooves (see fig. 4). The grooved or corrugated structure has the effect of reducing the side and back lobes caused by the diffraction at the horn funnel edge. Thus a parabola antenna fed by a corrugated horn has considerably smaller side lobes than one with a smooth horn. Also the radiation of orthogonal polarized waves is weakened. The corrugated horn is especially suitable for TV reception, as in this case it is important to increase the signal-noise ratio and to minimize the interference signal from other satellites.

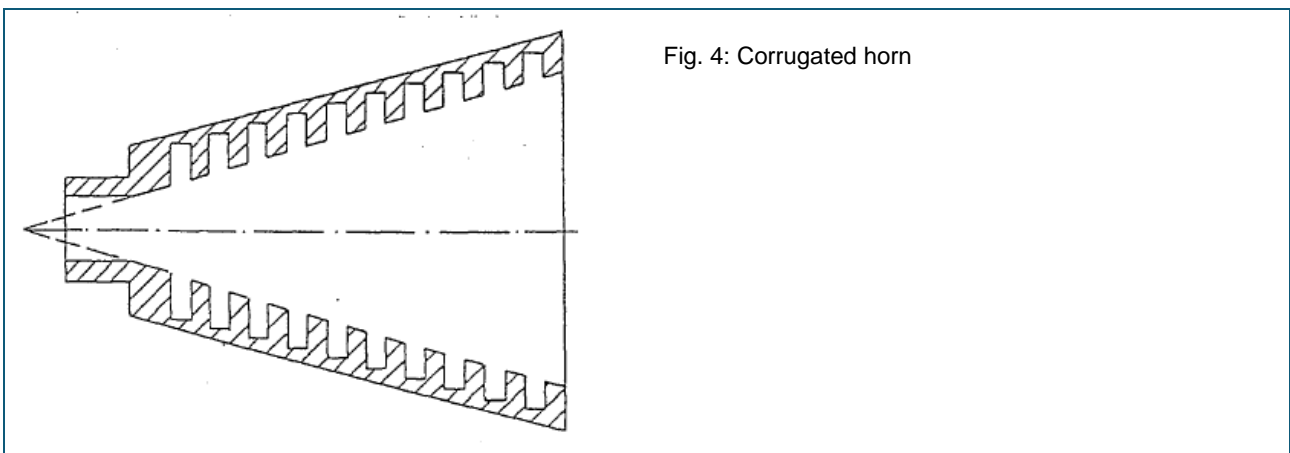


Fig. 4: Corrugated horn

## Material

1	737 01	Gunn oscillator
1	737 03	Coax detector
1	737 035	Transition waveguide/coax
1	737 05	PIN modulator
1	737 06	Isolator
1	737 12	Waveguide 200 mm
1	737 135	3-Screw transformer
2	737 15	Support for waveguide components
1	737 20	Small horn antenna
2	737 21	Large horn antenna
1	737 390	Set of microwave absorbers
1	737 405	Rotating antenna platform
1	501 02	BNC cable, $l = 1$ m
1	568 702	Book: Antenna Technology
4	301 21	Stand base MF
1	311 77	Steel tape measure
1		PC with Windows XP or higher version

For Variants only

1	737 27	Physic microwave accessories
---	--------	------------------------------

## Experiment set up

The experiment set-up is shown in fig. 7.

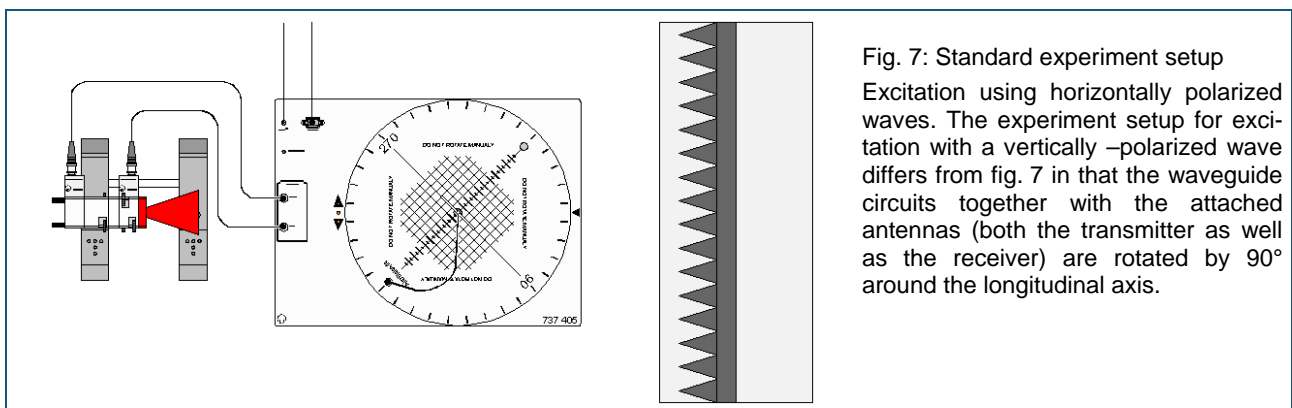


Fig. 7: Standard experiment setup

Excitation using horizontally polarized waves. The experiment setup for excitation with a vertically -polarized wave differs from fig. 7 in that the waveguide circuits together with the attached antennas (both the transmitter as well as the receiver) are rotated by  $90^\circ$  around the longitudinal axis.

## Experiment procedure

### 1. Horizontal diagrams of the large horn antenna

- The Large horn antenna 737 21 serves as the test antenna. Both horn antennas (the source and test antenna) radiate horizontally-polarized waves.
- Assemble the test antenna in accordance with fig. 8. Before installing the 3-screw transformer make sure that the screws are not protruding into the waveguide.

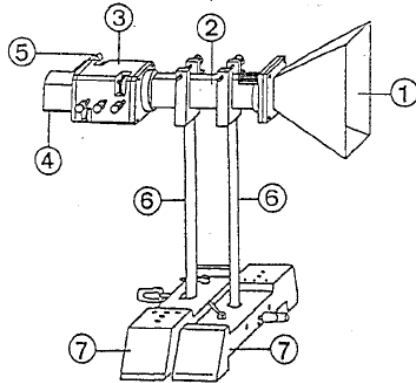


Fig. 8: Assembly of the test antenna

- 1: Large horn antenna 737 21
- 2: Waveguide 200 mm 737 12
- 3: Three screw transformer 737 135
- 4: Transition WG/Coax 737 035
- 5: Coax detector 737 03
- 6: Stand rod 245 mm
- 7: Stand base MF 300 21

- The horn of the test antenna is oriented at  $-180^\circ$  (opposite direction) to the source antenna.
- Connect the BNC cable to the BNC output socket of the coax-detector and to the BNC socket on the rotating platform.
- Match the test antenna in the maximum of the major lobe to the coax detector. Faulty matching always causes a reduction in reception power.
- Record the directional diagram with the following settings:
  - Range from:  $-180^\circ$  to:  $+180^\circ$
  - Angular Increment:  $1^\circ$
  - Bias Current: off
  - Detector characteristic: Quadratic,  $m = 2$
  - Graphic display:  $A(\vartheta)$  and  $a(\vartheta)$  respectively
- Switch over to Cartesian coordinates and determine the 3 dB-width.
- Save the measurement.
- Using the graphics cursor determine the 3 dB-width of the horn antenna's major lobe in the measurement plane.
- Comment on your matching attempts using the 3-screw transformer.

### 2. Polarization loss of the large horn antenna

- The decoupling between the orthogonal (cross-polarized) modes of the antenna determines the polarization loss. It describes the ratio of cross-polarized and copolarized reception signals of the antenna.
- Set the antenna coupled to the platform to the  $0^\circ$  angle position. Maximum receiving signal should now appear on the level meter  **$a/dB$**  (CASSY-Lab). **Reduce the power to  $a_1 = 0 dB$  with the 3-screw transformer.** Leave the test antenna unchanged in this position.



- Mark the previous position of the source antenna. Now change the experiment set up by rotating the waveguide circuit with the source antenna by  $90^\circ$  around its longitudinal axis. The horn now radiates a vertically-polarized wave. Be careful not to shift the set-up. The signal received by the test antenna should now be at a minimum level.
- Note the minimum signal  $a_2$  of the level meter. The value indicates the polarization loss factor of the antenna.
- Comment on the result.

	a/dB
Co-polarization	$a_1 = 0$
Cross polarization	$a_2 =$
PLF	$a_1 - a_2 =$

### 3. Vertical diagrams of the large horn antenna

- Mark the previous position of the test antenna. Then carefully rotate the experiment set-up by  $90^\circ$  around the longitudinal axis. Now the test antenna receives a vertically polarized wave. Make sure that the circuit has not slipped out of position.
- Repeat the procedure of measurement 1.
- Jointly represent the directional diagrams of the horn antenna in the E-plane and H-plane (horizontal and vertical diagrams). Compare the directional diagrams to each other. Comment on your results.

### 4. Vertical diagrams of the small horn antenna

- The large horn antenna remains as source antenna, the test antenna is replaced by the small horn antenna 737 20.
- Repeat the procedure of measurement 3.

### 5. Horizontal diagrams of the small horn antenna

- Repeat the procedure of measurement 1.

### 6. Horizontal diagrams of waveguide antennas

- Measurement object: open waveguide
- Record the horizontal and vertical directional diagrams. Compare the directional diagrams. Comment on the differences in the directional diagrams and in the matching of the antennas.

## Variants

### Polarization effects on the transmission channel

This experiment needs additional material and therefore is meant as an option. In this experiment the effect of rain on crosstalk between two communication channels is investigated. Both channels are operated at the same carrier frequency and only decoupled by frequency reuse technique (polarization decoupling). The water drops absorb the RF power and attenuate the radiated waves. Because the attenuation increases almost proportionally to the frequency, microwaves are strongly affected by this phenomenon. Rain drops, due to the wind falling at a certain angle to ground, have a similar effect on the microwave as a polarization grid. The rotation angle of the polarization grid corresponds to the tilt angle of the rain drops brought about by the wind.

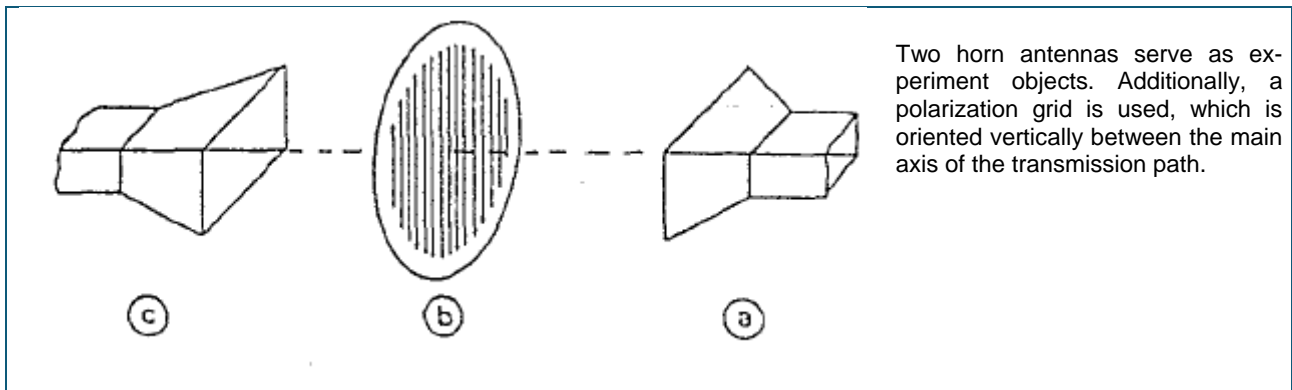


Table 2:

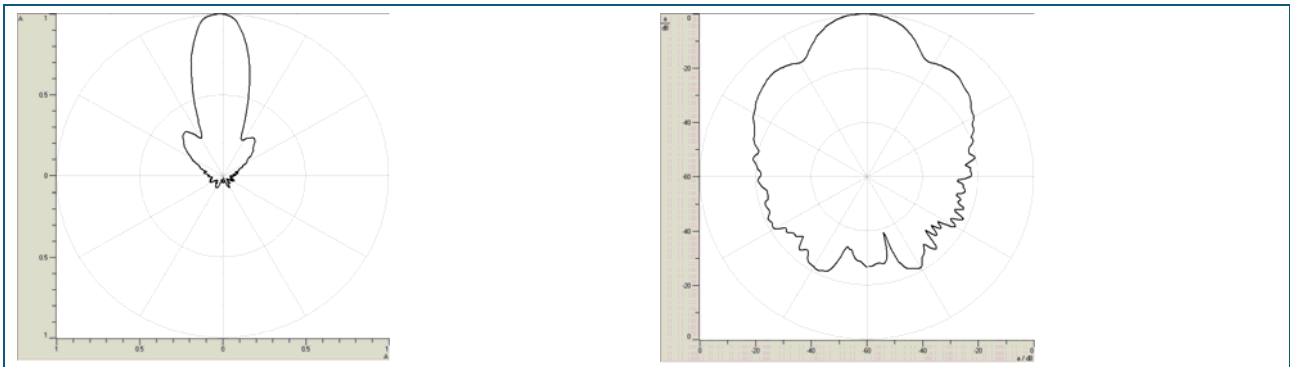
$\alpha/\text{deg}$	$a/\text{dB}$
0	
10	
20	
30	
40	
50	
60	
70	
80	
90	

### Vertical diagrams of open waveguides

- When recording the vertical diagrams follow step 3.

## Results

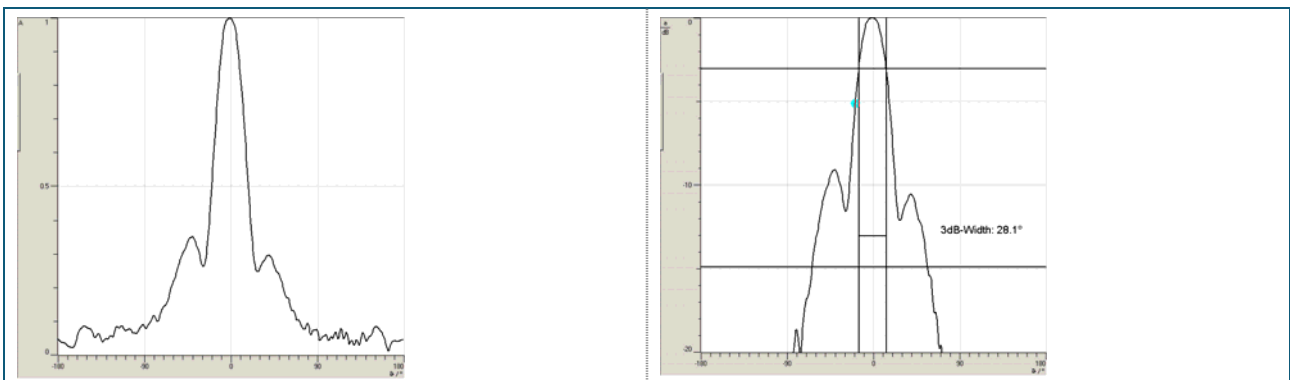
### 1. Horizontal diagrams of the large horn antenna



E-plane  
Polar coordinates  
Linear representation:  $A(\vartheta)$

E-plane  
Polar coordinates  
Logarithmic representation:  $a(\vartheta)$

- In all measurements the mean distance between the test and source antennas is  $r_o = 1000$  mm
- Due to matching approx. + 20% stronger receiving signal.
- Attention: Horns need to be in “vertical” orientation. Horizontal diagram means rotation in the E-plane!



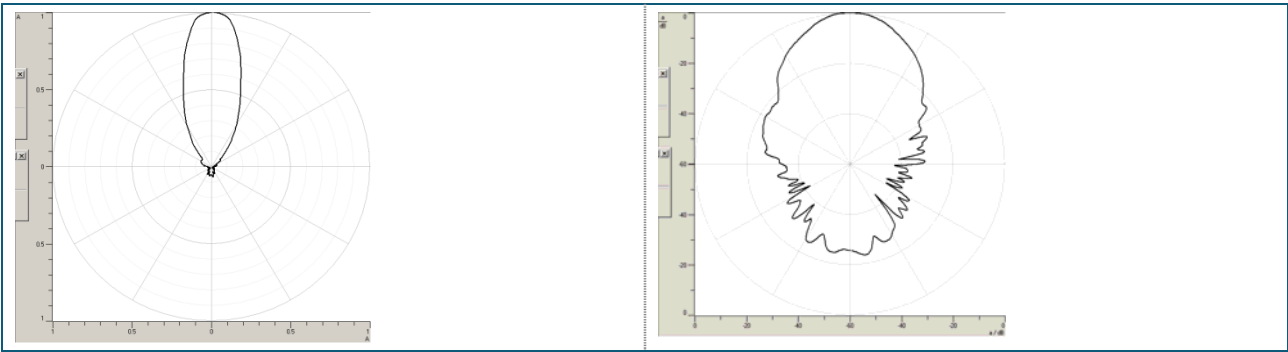
E-plane  
Cartesian coordinates  
Linear representation:  $A(\vartheta)$   
Black: measurement

E-plane  
Cartesian coordinates  
Logarithmic representation:  $a(\vartheta)$   
3 dB-Width: 28.1°

### 2. Polarization loss of the large horn antenna (PLF)

	a/dB
Co-polarization	$a_1 = 0$
Cross polarization	$a_2 = -36$
PLF	$a_1 - a_2 = 36$

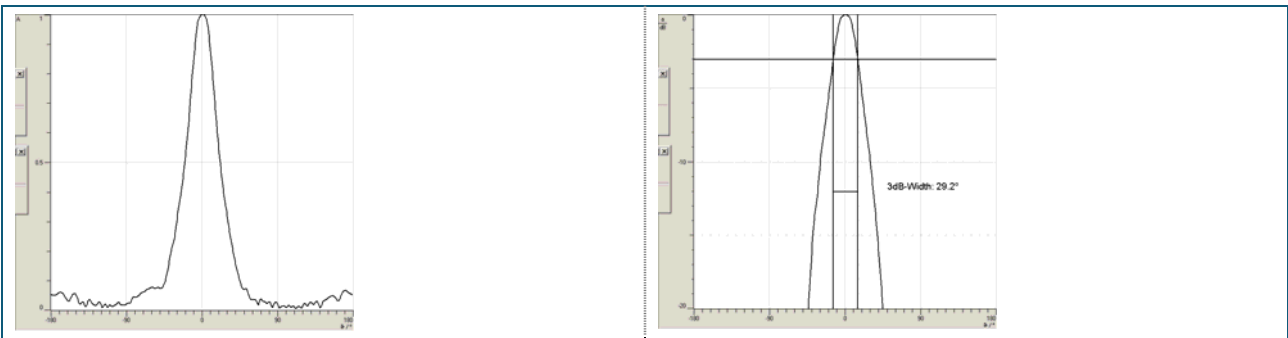
### 3. Vertical diagrams of the large horn antenna



H-plane  
Polar coordinates  
Linear representation:  $A(\theta)$

H-plane  
Polar coordinates  
Logarithmic representation:  $a(\theta)$

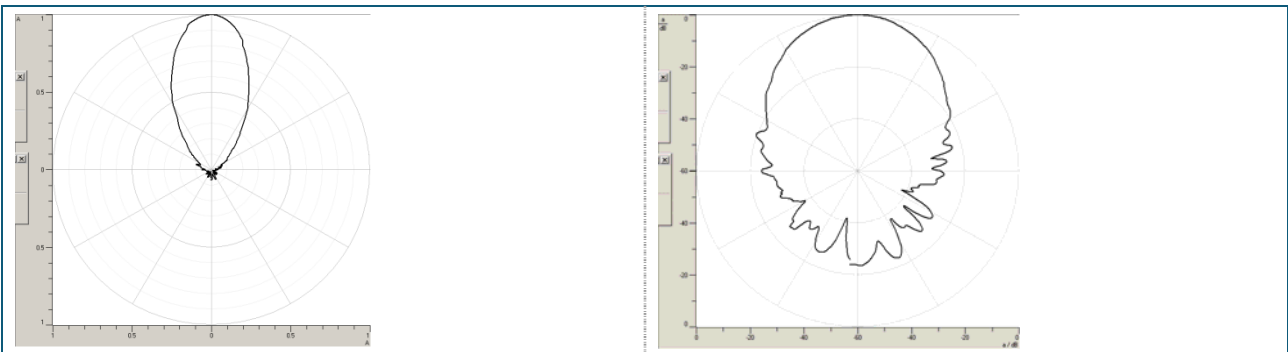
Attention: Horns need to be in “horizontal” orientation. Vertical diagram means rotation in the H-plane!



H-plane  
Cartesian coordinates  
Linear representation:  $A(\theta)$

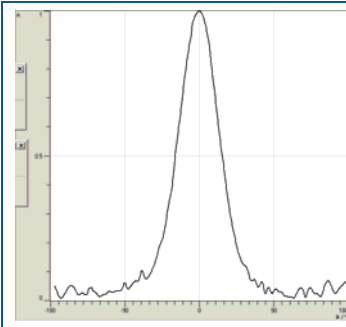
H-plane  
Cartesian coordinates  
Logarithmic representation:  $a(\theta)$   
3 dB-Width: 29.2°

### 4. Vertical diagrams of the small horn antenna

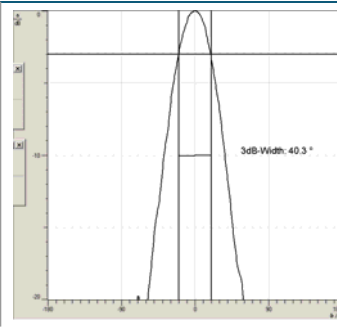


H-plane  
Polar coordinates  
Linear representation:  $A(\theta)$

H-plane  
Polar coordinates  
Logarithmic representation:  $a(\theta)$

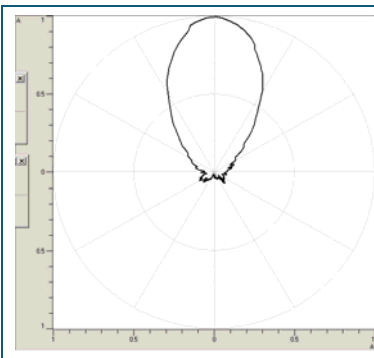


H-plane  
Cartesian coordinates  
Linear representation:  $A(\vartheta)$

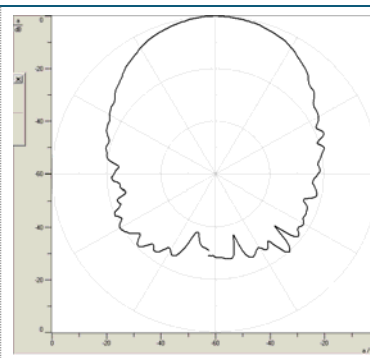


H-plane  
Cartesian coordinates  
Logarithmic representation:  $a(\vartheta)$   
3 dB-Width: 40.3°

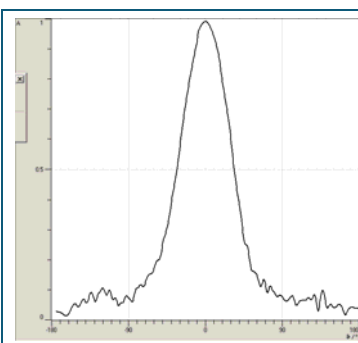
5. Horizontal diagrams of the small horn antenna



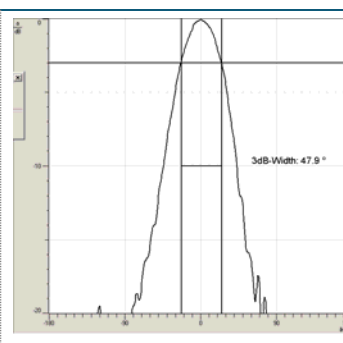
E-plane  
Polar coordinates  
Linear representation:  $A(\vartheta)$



E-plane  
Polar coordinates  
Logarithmic representation:  $a(\vartheta)$

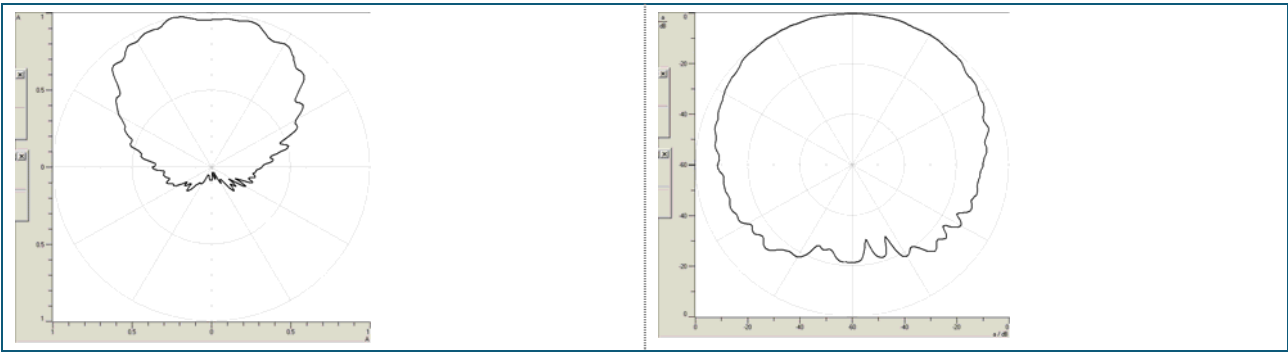


E-plane  
Cartesian coordinates  
Linear representation:  $A(\vartheta)$



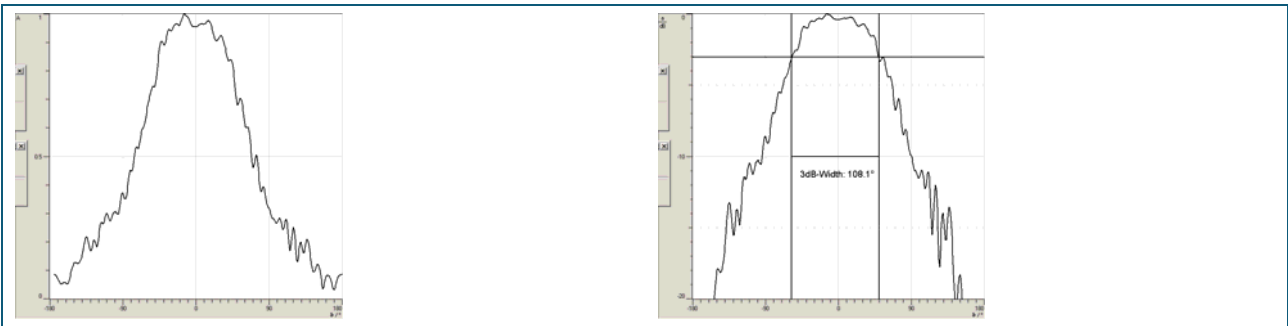
E-plane  
Cartesian coordinates  
Logarithmic representation:  $a(\vartheta)$   
3 dB-Width: 41°

6. Horizontal diagrams of waveguide antennas



E-plane  
Polar coordinates  
Linear representation:  $A(\vartheta)$

E-plane  
Polar coordinates  
Logarithmic representation:  $a(\vartheta)$



E-plane  
Cartesian coordinates  
Linear representation:  $A(\vartheta)$

E-plane  
Cartesian coordinates  
Logarithmic representation:  $a(\vartheta)$   
3 dB-Width: 108.1°

## Variants

Polarization effects on the transmission path

Table 2:

$\alpha/\text{deg}$	$a/\text{dB}$
0	-16.7
10	-19.1
20	-25.1
30	-17.1
40	-10.2
50	-6.6
60	-4.1
70	-2.3
80	-1.0
90	-0.9

The transmission conditions change radically when a polarization grid is installed between the two antennas. The linearly polarized wave incidenting on the grid can be broken down into two linear orthogonal base fields in the direction of the main axis of the polarizer. The polarization grid suppresses the field which is parallel to the grid wires. Thus the grid rotates the plane of polarization in the incidenting wave. Consequently the wave propagating behind the grid demonstrates a linear SOP perpendicular to the grid wires. The SOP conversion occurring at the grid is linked with power losses, because one of the linear components is not transmitted.

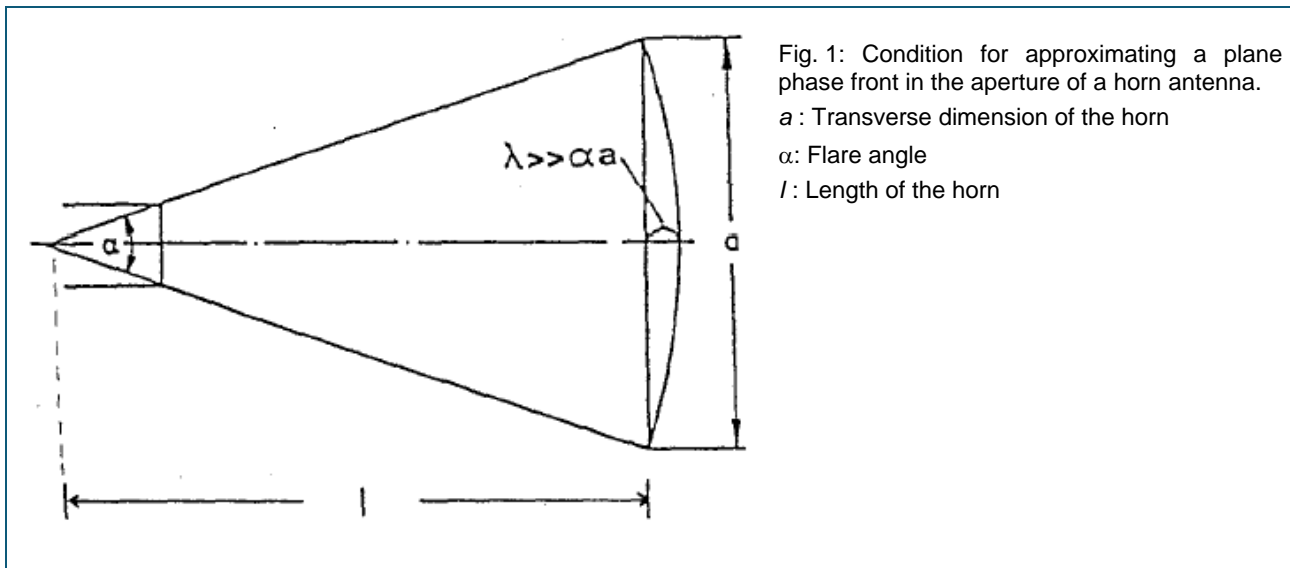
## Reflector antennas

### Fundamentals

Microwave antennas which can radiate a focused beam are increasingly used in the following applications:

- Terrestrial radio links
- Satellite communication
- Radio astronomy
- Telemetry
- Navigation
- Radar

Various antenna types have been designed to fit the requirements of these applications. Reflector antennas are very popular, because of their simple and robust mechanical construction. In order to achieve a distinct directivity with a focused beam and high gain, a plane phase distribution must be present in the radiating aperture. When the phase fronts are shaped like spherical curves, beam dispersion arises resulting in a rapid drop in beam focus and gain. In actual practice the approximation reproduced in fig. 1 can be used for evaluating phase distribution in the horn antenna.



As can be seen in fig. 1, almost even phase fronts apply for:

$$\alpha \cdot a \ll \lambda_0$$

For a horn with the given transverse dimension  $a$ , a constant phase illumination in the aperture requires that the horn is of considerable length  $l$ . When the aperture has sufficiently large dimensions with respect to the wavelength, microwave antennas can be designed quite similar to optical systems. Like concave mirrors in geometric optics, reflectors can be used for beam focusing of microwaves. The reflector is used, to transform curved wave fronts into planar phase fronts in the reflector aperture.



Reflector antennas are frequently distinguished according to the manner in which they are excited:

- Front feeding
- Cassegrain excitation using a subreflector
- Offset-feed reflectors

The shape of the main reflector is also an important feature. Fig. 2 depicts several types of reflector antennas.

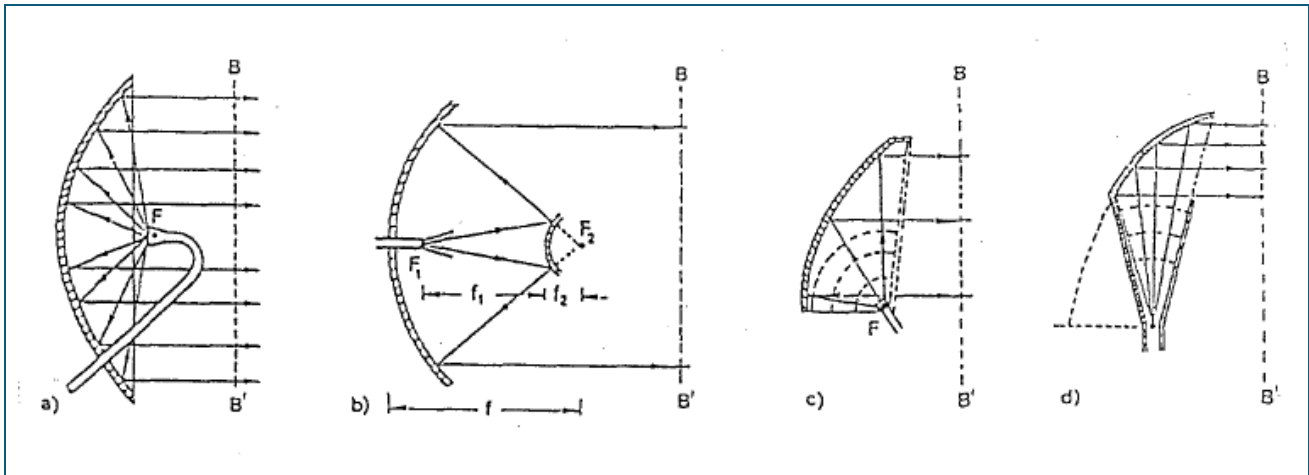


Fig. 2: Various models of reflector antennas

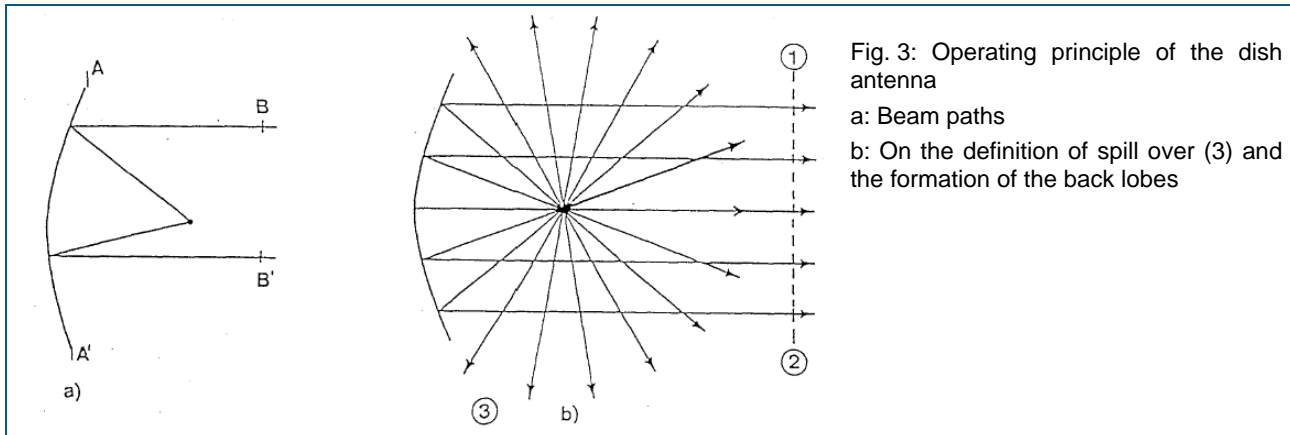
- Direct-feed dish antenna
- Cassegrain feed system with hyperboloid subreflector
- Offset-feed dish antenna with parabolic reflector
- Hog horn antenna

## Parameters of the dish antenna

The simplest form of a highly focusing reflector antenna in microwave technology is the direct-feed dish antenna. It consists of a symmetrical parabolic reflector (main reflector) and the primary radiator arranged at the focal point (feeder). According to the laws of geometrical optics, the feeder transmits spherically-shaped waves from the focus of the main reflector, which are then transformed into a collimated beam in the aperture  $A-A'$ , or any parallel plane to this  $B-B'$  of the main reflector (and vice versa). The prerequisites for this are:

- The radiator is negligibly small (ideally point-shaped)
- There is a parabolic curvature of the main reflector.

Under these assumptions the “path length” of different beams from the radiator to the aperture are equal, thus resulting in the desired constant phase distribution. Fig. 3 shows the beam path in a dish antenna.



The dish antenna is normally excited by horn radiators, Yagis, or  $\lambda/2$ -dipoles with small subreflectors and coaxial feeding. In order to achieve large bandwidths, double-ridged horn radiators are used. The radiator should illuminate the reflector homogeneously. The aim is to obtain a constant illumination over the entire aperture, which rapidly drops to zero at the rim so that only little radiation from the feeder spills over the reflector. When the dish antenna is operated in receiving mode, the spill over increases the noise and thus diminishes the transmission quality. This is a real problem for satellite ground stations. A certain part of the power transmitted by the primary radiator is radiated in the forward direction and can interfere destructively with the desired parallel beam. Back-radiation can be minimized by suitably selecting the radiator or by taking additional measures with respect to the antenna construction like the attachment of a subreflector behind the feeder. The directivity of the dish antenna is dependent on the following factors:

- Gain function of the primary radiator
- Ratio of the focal distance to the diameter of the reflector  $f/D$  (numerical aperture)

In order to achieve nearly plane phase fronts in the aperture, the dish antenna requires a relatively large diameter. Using the Cassegrain antenna depicted in fig. 2b high directivity is attained by using a passive reflector to transform the focal distance while keeping the construction length small. The effective focal distance amounts to:

$$f = \frac{f_1}{f_2} F$$

The offset feed according to fig. 2c or 2d serves to reduce the mismatching caused by reflections into the radiator. The 3 dB-width as a measure for antenna directivity depends on the special choice of the primary radiator and its position in front of the main reflector. The following approximately holds true for most radiator types:

$$\frac{3dB - Width}{degrees} = \frac{70 \cdot \lambda_0}{D}$$

The definition of the effective area of an antenna is valid generally and not restricted to reflector antennas. The effective area is the surface through which a plane homogeneous wave of a power density  $S$  just transports the power received  $P_R$ . Furthermore, there is a relationship applicable for all antennas between the antenna's effective area  $A_{eff}$  and the gain  $G$ :

$$\frac{A_{eff}}{G} = \frac{\lambda_0^2}{4\pi}$$

As the radiator does not illuminate the reflector ideally, the effective area  $A_{eff}$  is smaller than the geometric aperture surface  $A$ . The quotient from the antenna's effective area and the geometric surface defines the illumination or aperture efficiency  $q$ . In dish antennas it is in the range of  $0.5 < q < 0.6$ .

## Questions

1. Explain the principle of a dish antenna.  
 2. How is the directivity of a dish antenna determined? Determine the 3 dB-width of the experiment antenna. Technical specifications of the main reflector:

- Focal distance  $f = 160$  mm
- $D = 400$  mm
- Free-space wavelength for 9.40 GHz:  $\lambda_0 = 32$  mm

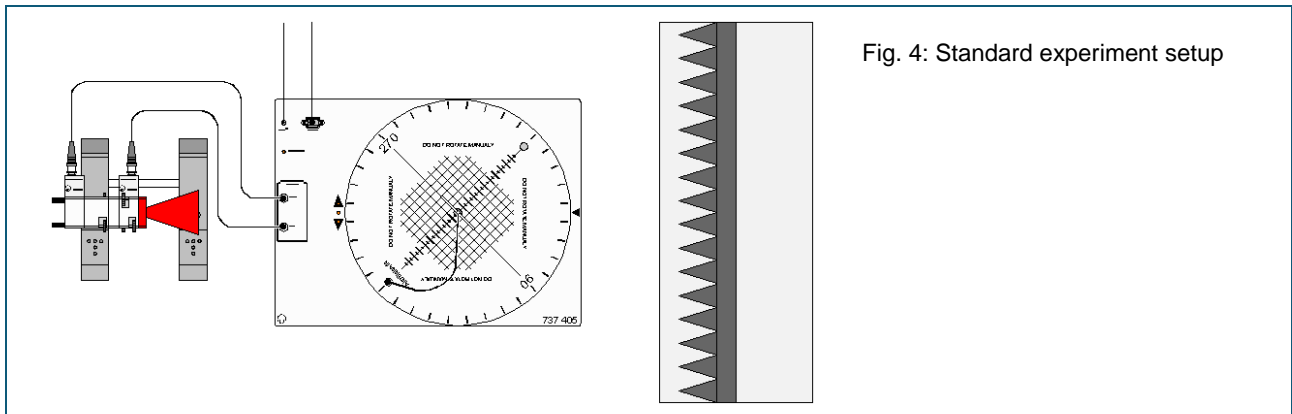
Approximately determine the gain of the dish antenna to be expected based on the following assumptions:

- Operating frequency  $f = 9.40$  GHz, corresponding to a free-space wavelength of  $\lambda_0 = 32$  mm
- Reflector diameter  $D = 400$  mm
- Aperture efficiency  $q = 0.5$

## Material

1	737 01	Gunn oscillator
1	737 05	PIN modulator
1	737 06	Isolator
1	737 135	3-Screw transformer
1	737 21	Large horn antenna
1	737 390	Set of microwave absorbers
1	737 405	Rotating antenna platform
1	737 415	Set of wire antennas
1	737 452	Dish antenna
1	568 702	Book: Antenna Technology
1	311 77	Steel tape measure
2	301 21	Stand bases MF
1		PC with Windows XP or higher version

## Experiment set-up



## Experiment procedure

### 1. Horizontal diagrams of the parabolic reflector with $\lambda/2$ -dipole

- Assemble the experiment set-up in accordance with fig. 4. Additionally insert the 3-screw transformer **between** PIN-modulator and horn antenna. The source antenna radiates horizontally-polarized waves, i.e. the broad sides of the waveguide components are in a vertical position.
- Does the distance between the source and test antenna fulfil the far field condition?

$$r_0 > \frac{2(d_Q + d_T)^2}{\lambda_0}$$

$d_Q$  and  $d_T$ : largest dimension of the antenna (transversal or longitudinal)

$r_0$ : distance between the antennas

$\lambda_0$  free space wavelength.

- Insert the dish antenna into its holder and mount this onto the rotating base. The assembly is shown in fig. 5.
- Manually turn the rotating base into the position of the main lobe. Reduce the transmitted power by means of the 3-screw transformer, until you get the received signal to  $U = 30 \text{ mV}$ .

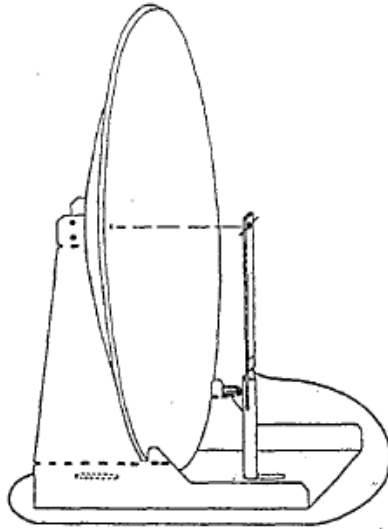


Fig. 5: The dish antenna with dipole radiator

Assembling the primary radiator. Connect the supplied antenna rod (this carries the dipole and the detector diode) to the carrier rod made of PVC. Insert the dipole antenna into the central bore mount in the rotating antenna platform.

Connect the plug of the antenna output cable to the BNC socket on the rotating base plate. Check whether the set-up on the rotating base collides with any objects.

- Record the directional diagram with the following settings:  
Range from:  $-180^\circ$  to:  $+180^\circ$   
Angular Increment:  $0.5^\circ$   
Bias Current: on  
Detector characteristic: Quadratic,  $m = 2$   
Graphic display:  $A(\vartheta)$  and  $a(\vartheta)$  respectively
- Switch over to Cartesian coordinates and determine the 3 dB-width.
- Load the file of the  $\lambda/2$ -dipole additionally. Compare the directional diagrams.
- Save the measurement files.
- Determine the front-to-back ratio and the 3 dB-width of the dish-antenna. Enter the values into table 1.

Primary Radiator	3 dB-Width	F/B-Ratio
$\lambda/2$ -dipole		
Yagi-R		
Yagi-D		
Yagi-DR		
Yagi-4DR		

## 2. Horizontal diagrams of the parabolic reflector with Yagi-R

- The Yagi-R serves as primary radiator.
- The experiment corresponds to the one described in point 1.

## 3. Horizontal diagrams of the parabolic reflector with Yagi-D

- The Yagi-D serves as primary radiator.
- The experiment corresponds to the one described in point 1.

4. Horizontal diagrams of the parabolic reflector with Yagi-DR
  - The Yagi-DR serves as primary radiator.
  - The experiment corresponds to the one described in point 1.
5. Horizontal diagrams of the parabolic reflector with Yagi-4DR
  - The Yagi-4DR serves as primary radiator.
  - The experiment corresponds to the one described in point 1.

## Variant

The use of different radiators

In the same way as described above, the parabolic reflector can be excited by several other radiators, e.g.:

- helical antennas
- horn antennas

Try yourself!

## Answers

1.

Spherical waves transmitted by the radiator in the focal point of the primary reflector are transformed into plane waves in the aperture of the parabolic reflector. Thus a wave front with constant amplitude and phase exists in the aperture of an ideal reflector. The major lobe is formed by a parallel focused beam and the 3 dB-width is very small.

2.

The directivity of the parabolic antenna is determined by:

- Gain function of the primary radiator
- The ratio of the focal distance to the diameter of the primary reflector  $f/D$ .

Estimation of gain  $G$  of the parabolic antenna

$$\frac{A_{eff}}{G} = \frac{\lambda_0^2}{4\pi}$$

$$G = 4\pi \frac{A_{eff}}{\lambda_0^2}$$

$$A_{eff} = qA$$

$$A = \frac{\pi D^2}{4}$$

$$A_{eff} = qA$$

$$G = q \left( \frac{\pi D}{\lambda_0} \right)^2$$

$$G_{dB} = 10 \cdot \log G = 10 \cdot q + 20 \cdot \log \left( \frac{\pi D}{\lambda_0} \right)$$

Inserting the numerical values gives:

$$G = -3 + 32 = 29 \text{ dB}$$

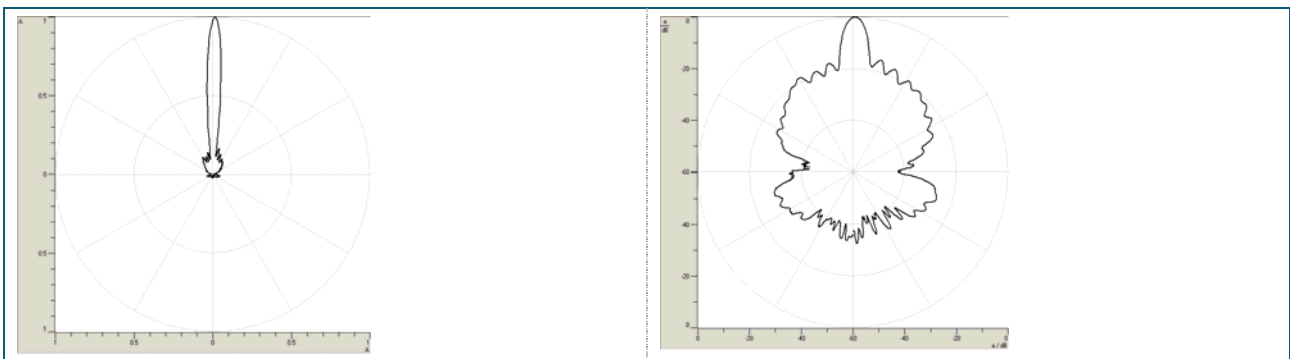


## Results

### Far field Condition

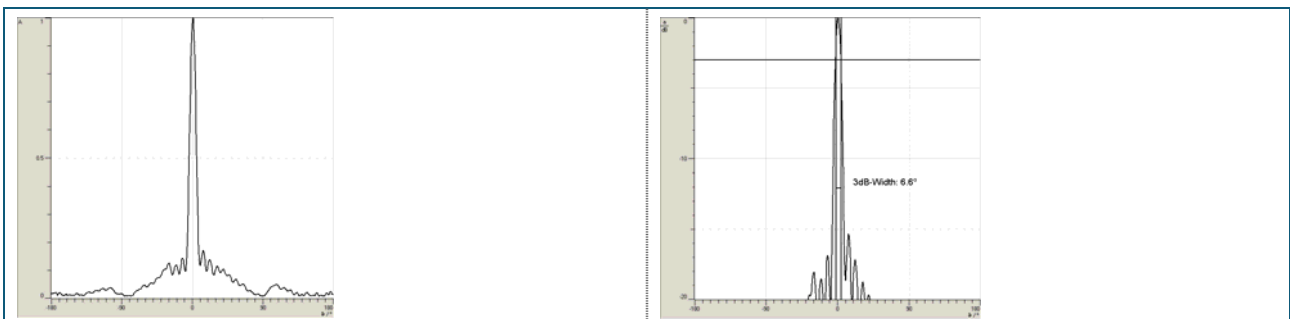
Test antenna:	Yagi-4DR	Remarks
$r_o$ :	1000 mm	Mean distance measured between the source and the test antenna
$\lambda_0$ :	32 mm	Wavelength of the radiated wave
$d_Q$ :	100 mm	Largest transverse measurement of the radiating horn
$d_T$ :	400 mm	Reflector diameter
$r_o \geq \frac{2(d_Q + d_T)^2}{\lambda_0}$	$r_o > 15625 \text{ mm}$	Far field condition is not fulfilled. The measurements with the parabolic antenna are conducted in the near field!

#### 1. Horizontal diagrams of the parabolic dish antenna with $\lambda/2$ -dipole



E-plane  
Polar coordinates  
Linear representation:  $\mathbf{A}(\vartheta)$

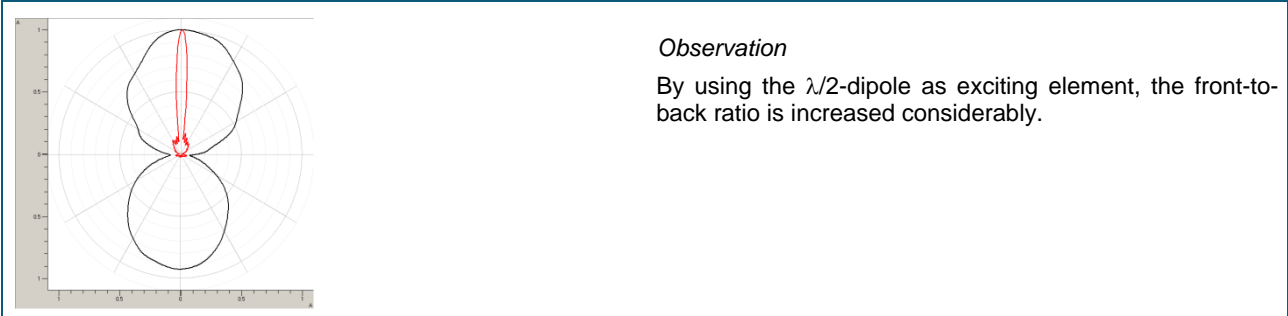
E-plane  
Polar coordinates  
Logarithmic representation:  $\mathbf{a}(\vartheta)$   
F/B-Ratio: 35.7 dB



E-plane  
Cartesian coordinates  
Linear representation:  $\mathbf{A}(\vartheta)$

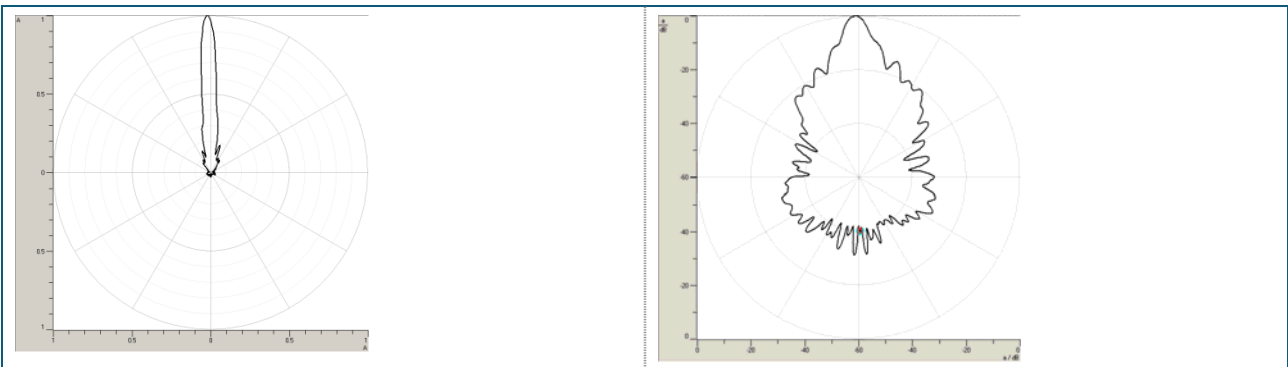
E-plane  
Cartesian coordinates  
Logarithmic representation:  $\mathbf{a}(\vartheta)$   
3 dB-Width: 6.6°

Joint display of the directional diagrams of a  $\lambda/2$ -dipole with / without parabolic reflector.



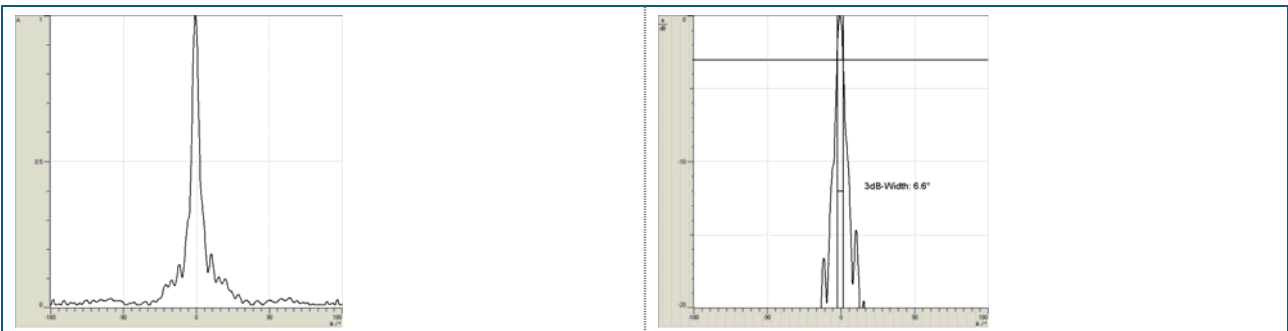
E-plane  
Polar coordinates  
Linear representation:  $A(\vartheta)$   
Black:  $\lambda/2$ -dipole  
Red: Parabolic dish in front of  $\lambda/2$ -dipole

2. Horizontal diagrams of the parabolic dish antenna with Yagi-R



E-plane  
Polar coordinates  
Linear representation:  $A(\vartheta)$

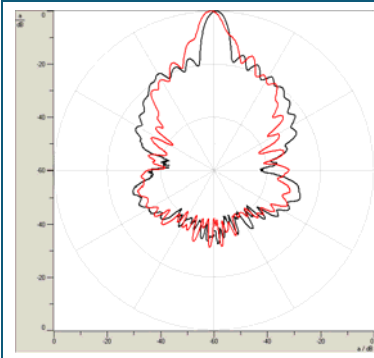
E-plane  
Polar coordinates  
Logarithmic representation:  $a(\vartheta)$   
F/B-Ratio: 40 dB



E-plane  
Cartesian coordinates  
Linear representation:  $A(\vartheta)$

E-plane  
Cartesian coordinates  
Logarithmic representation:  $a(\vartheta)$   
3 dB-Width:  $6.6^\circ$

Joint display: Parabolic reflector with  $\lambda/2$ -dipole and Yagi-R excitation.



*Observation*

Excitation with the Yagi-R reduces the side lobes, but enhances the 3 dB-Width.

E-plane

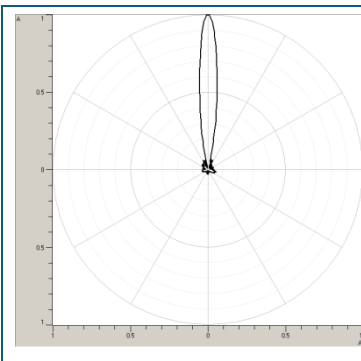
Polar coordinates

Logarithmic representation:  $a(\theta)$

Black: Excitation with  $\lambda/2$ -dipole

Red: Excitation with Yagi-R

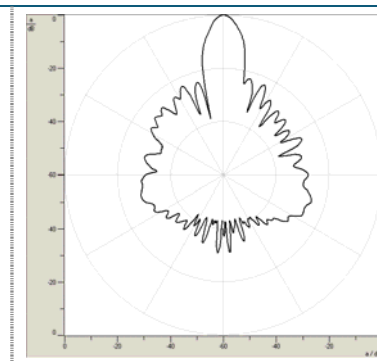
3. Horizontal diagrams of the parabolic dish antenna with Yagi-D



E-plane

Polar coordinates

Linear representation:  $A(\theta)$

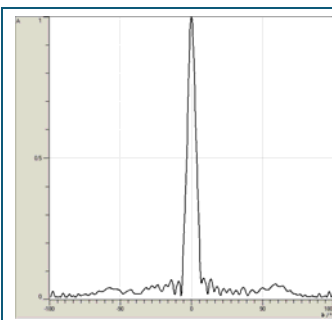


E-plane

Polar coordinates

Logarithmic representation:  $a(\theta)$

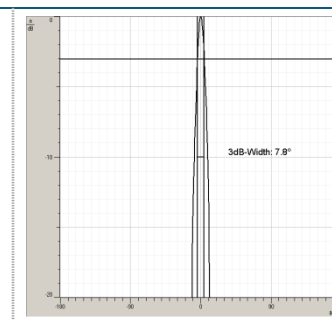
F/B-Ratio: 37.1 dB



E-plane

Cartesian coordinates

Linear representation:  $A(\theta)$



E-plane

Cartesian coordinates

Logarithmic representation:  $a(\theta)$

3 dB-Width: 7.8°

Joint display: Parabolic reflector with  $\lambda/2$ -dipole and Yagi-D excitation.



E-plane

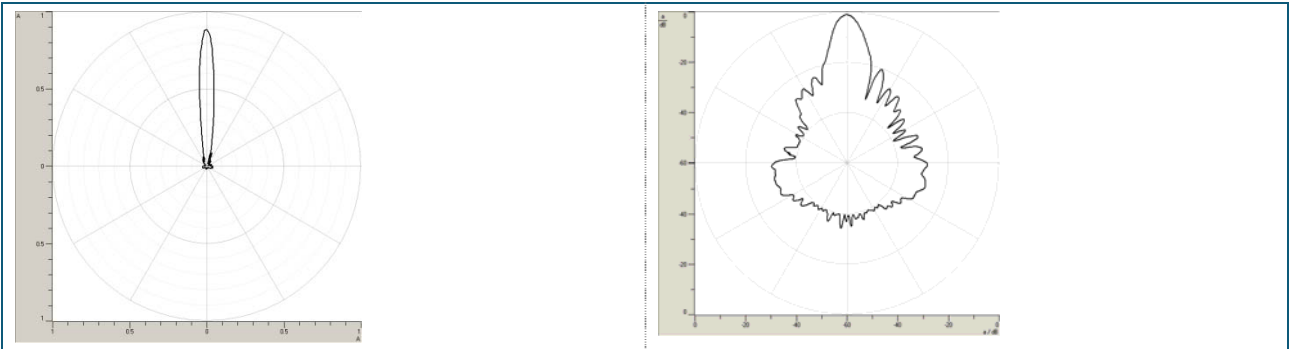
Polar coordinates

Linear representation:  $A(\vartheta)$

Black: Excitation with  $\lambda/2$ -dipole

Red: Excitation with Yagi-D

#### 4. Horizontal diagrams of the parabolic dish antenna with Yagi-DR



E-plane

Polar coordinates

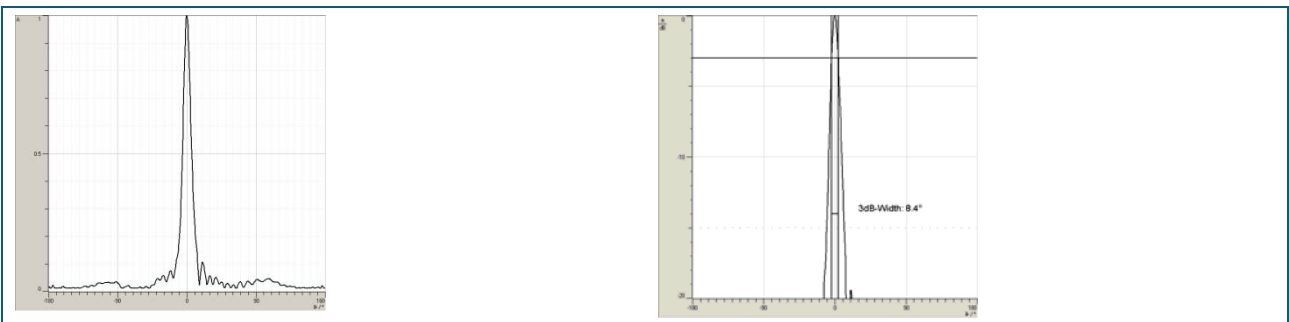
Linear representation:  $A(\vartheta)$

E-plane

Polar coordinates

Logarithmic representation:  $a(\vartheta)$

F/B-Ratio: 35.9 dB



E-plane

Cartesian coordinates

Linear representation:  $A(\vartheta)$

E-plane

Cartesian coordinates

Logarithmic representation:  $a(\vartheta)$

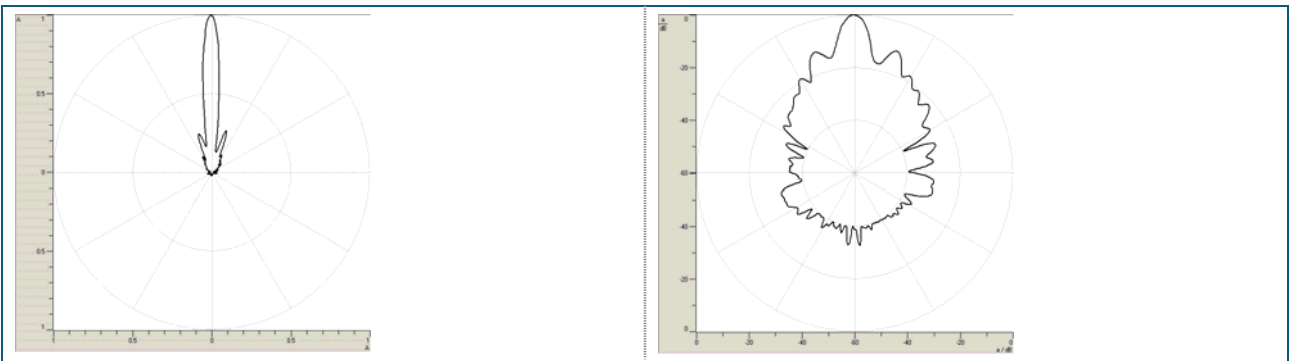
3 dB-Width: 8.4°

Joint display: Parabolic reflector with  $\lambda/2$ -dipole and Yagi-DR excitation.



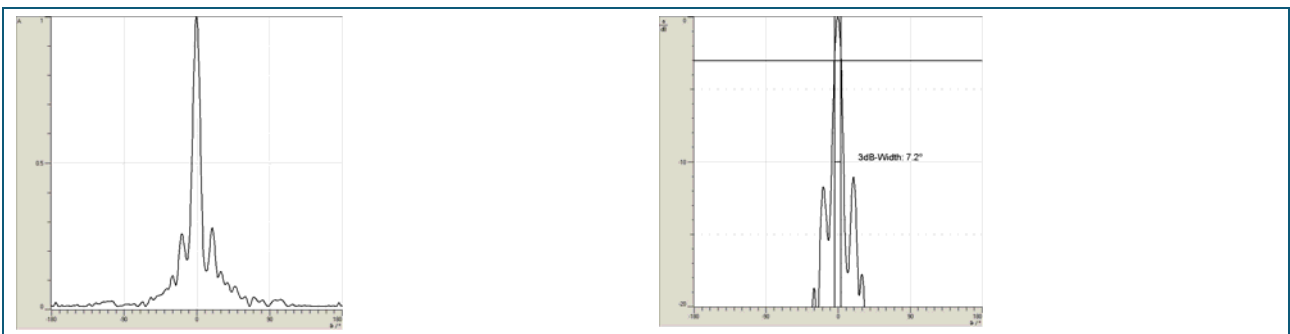
E-plane  
 Polar coordinates  
 Linear representation:  $A(\theta)$   
 Black: Excitation with  $\lambda/2$ -dipole  
 Red: Excitation with Yagi-DR

5. Horizontal diagrams of the parabolic dish antenna with Yagi-4DR



E-plane  
 Polar coordinates  
 Linear representation:  $A(\theta)$

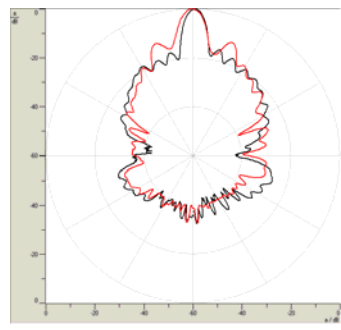
E-plane  
 Polar coordinates  
 Logarithmic representation:  $a(\theta)$   
 F/B-Ratio: 38.4 dB



E-plane  
 Cartesian coordinates  
 Linear representation:  $A(\theta)$

E-plane  
 Cartesian coordinates  
 Logarithmic representation:  $a(\theta)$   
 3 dB-Width: 7.2°

Joint display: Parabolic reflector with  $\lambda/2$ -dipole and Yagi-4DR excitation.



#### Observation

Yagi-4DR excitation brings no significant improvement of the radiation properties compared to the simple  $\lambda/2$ -dipole.

E-plane

Polar coordinates

Linear representation:  $A(\vartheta)$

Black:  $\lambda/2$ -dipole

Red: Yagi-4DR

Primary Radiator	3 dB-Width	F/B-Ratio
$\lambda/2$ -dipole	6.6°	35.7 dB
Yagi-R	6.6°	40 dB
Yagi-D	7.8°	37.1 dB
Yagi-DR	8.4°	35.9 dB
Yagi-4DR	7.2°	38.4 dB

#### Hints

- At levels around 40 dB below the primary maximum, the dynamic range of the measurement system no longer suffices for quantitative evaluations. Thus the determination of the front to-back ratio shows certain fluctuations and is to be interpreted with care.
- There are several weakly defined, asymmetrically positioned side lobes to be ignored.
- The absolute value of the front-to-back gain corresponds to the inverse value of  $A$  for  $\vartheta = 180^\circ$ . For a quadratic detector this is equal to the relationship of the field strength in the forward and backward direction. The dB value denotes the corresponding power ratio again under the assumption of a quadratic detector.

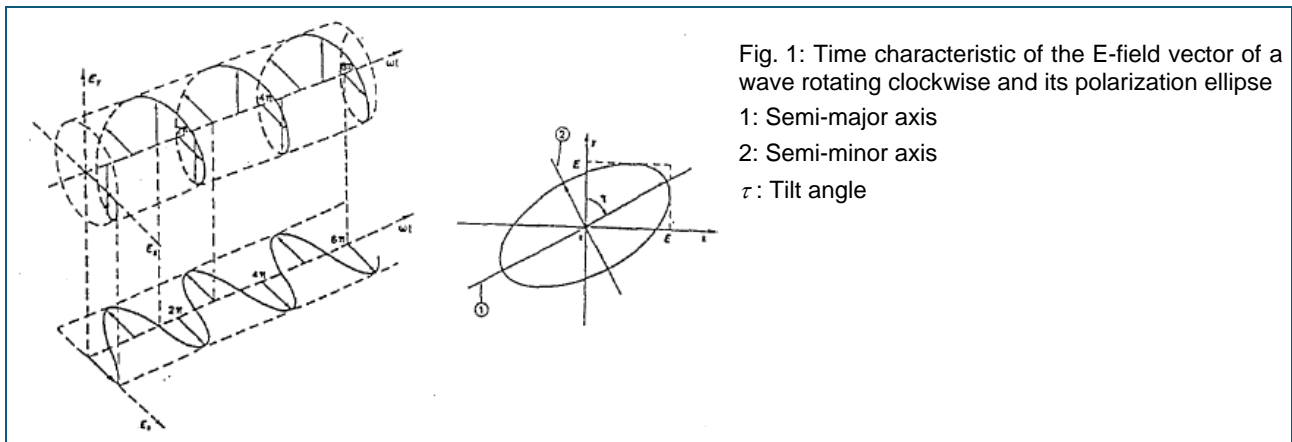
## Helix antennas

### Fundamentals

Of all the antennas which radiate circularly polarized waves, the helical antenna is of particular interest for didactic purposes. This is due to its simple geometric structure. The well known relationship in mechanics between the rotation sense of a screw and a nut can be transferred directly to the antenna geometry and the handedness of circularly polarized waves. The circularly polarized waves received or radiated by a helix antenna have the same handedness as the spiral sense of the helix. Thus, it is easy to imagine how a wave radiated from a clockwise wound helix rotates into a receiving antenna whose helix is also wound in the clockwise manner. In this case, the reception of the wave is excellent. However, if the wave is transmitted to an antenna with a counter clockwise wound helix, only poor reception is received. Although we will only be investigating helix antennas in the experiment, the experience gained here can also be applied to other antennas which transmit or receive circularly polarized waves.

### Polarization of antennas and waves

The polarization of a transmitting antenna is characterized by the polarization of the wave radiated from it in a certain direction. Normally the polarization of an antenna means the state of polarization (SOP) in the maximum of the major lobe. The polarization of an electromagnetic wave is characterized by the time dependent changes in the orientation and magnitude of the electrical field vector at a fixed point in space. In general an ellipse is described by the tip of the E-vector at a particular point in space as a function of time. Consequently, this kind of wave is elliptically polarized. A typical time characteristic of the E-field vector is depicted in fig. 1.



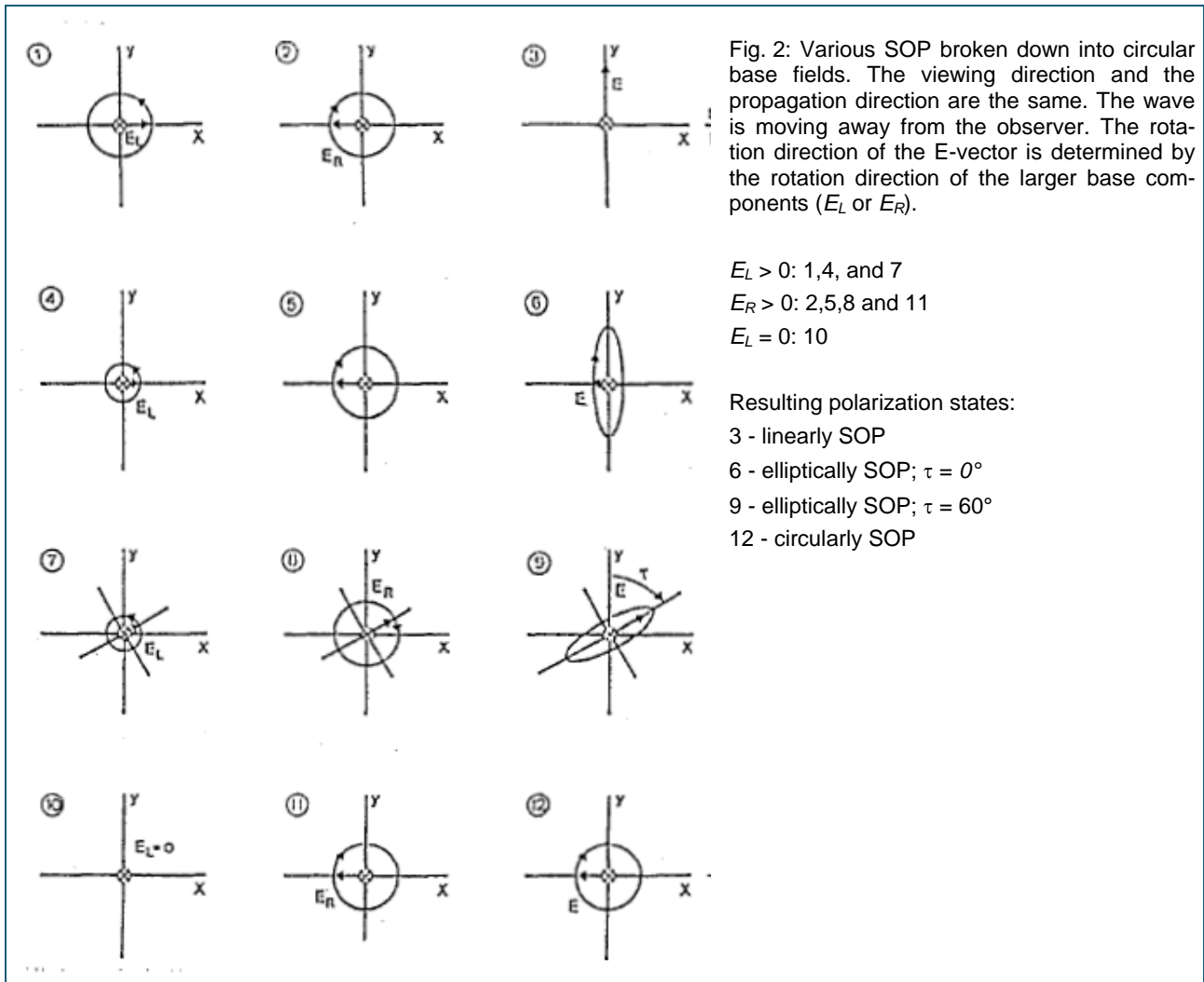
The rotation of the E-field vector can be either clockwise or counter-clockwise. Linearly and circularly polarized waves represent special cases of standard elliptical polarization. In the case of linear polarization the ellipse degenerates into a straight line and in circular polarization into a circle. Each elliptically polarized wave can be described not only by a linear vector base, but also by circularly polarized base fields. Thus, the polarization states depicted in fig. 2 are produced from the linear combination of one counter-clockwise (left handed) and one clockwise (right handed) rotating field ( $E_L$  and  $E_R$ ).

The polarization state is characterized by providing the following parameters:

- the axial ratio (AR) of the polarization ellipse, i.e. the quotients of the semi-major axis with respect to the semi-minor axis of the ellipse

$$AR = \frac{E_R + E_L}{E_R - E_L}$$

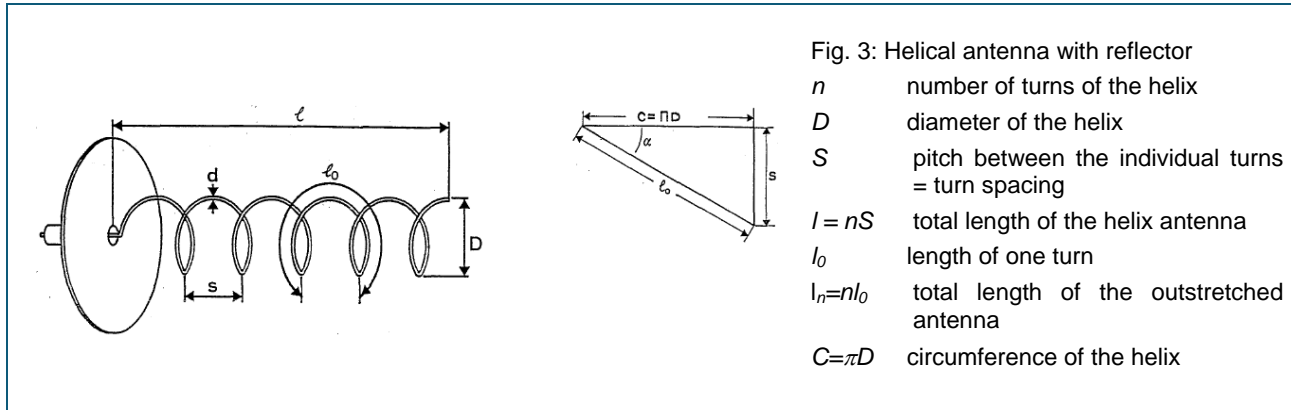
- the tilt angle  $\tau$  of the semi-major axis towards a reference line, e.g. the plane of the table.





## Helix antenna

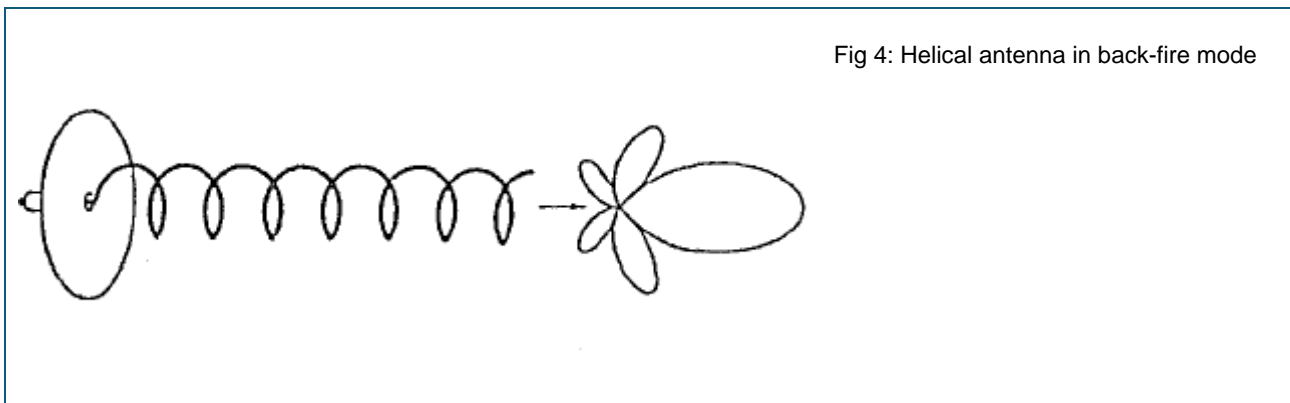
The helix antenna consists of a helix-shaped conductor, which turns like a screw thread. Normally the antenna is fed via a coaxial line. Furthermore, the antenna is operated with a reflector. At the feeding point, in the middle of the reflector, the internal conductor of the coaxial cable is connected to the helix. The external conductor is connected to the reflector (see fig. 3).



Practical modes of operation for helical antennas are:

- the normal mode (lateral radiation characteristic)
- back-fire (axial) mode.

Because of its popularity here only the back-fire mode is discussed. It receives or radiates along its axis. The handedness of the circularly polarized radiated wave is directly given by the spiral or turn direction of the antenna (see fig. 4).



Optimum values to excite the end-fire mode are:

- $C/\lambda = 1$  for the circumference of the helical spiral
- $C = \lambda/4$  for the turn spacing or pitch
- $D \geq \lambda/2$  for the diameter of the reflector.

Elliptically polarized waves can be regarded as a vector addition of two orthogonal linear base fields, whose phases are perpendicular (i.e.  $\Delta\Phi = 90^\circ$ ). Each one of these base fields can be received from an elliptically polarized field using a linearly polarizing antenna (for example with a dipole). If a linearly polarizing antenna radiates, the wave thus generated can likewise also be broken down into circularly polarized base fields. A base field can then be measured using a right-handed or clockwise circularly polarizing antenna. The other base field can be correspondingly measured out with the orthogonal (counter-clockwise or left-handed) antenna. In both cases only one component of the wave is received while the second wave component is suppressed. Thus a decoupling of transmission channels is achieved by means of polarization. Because of their immunity to changes in the polarization direction, circularly polarizing antennas are used for telemetry and communication with moving objects in space. The helical antenna receives circularly polarized waves only when they have the same handedness and suppresses the orthogonal SOP. Upon reflection of circularly polarized waves on the earth's surface, the handedness of these waves is reversed, because the reflection factor is  $r = -1$ . Therefore, a circularly polarizing receiving antenna can receive the wave of identical polarization, while reflections from the ground are suppressed. Thus, the fading effect is reduced for reception in directional radio links because of the absence of time fluctuating reflections.

## Material

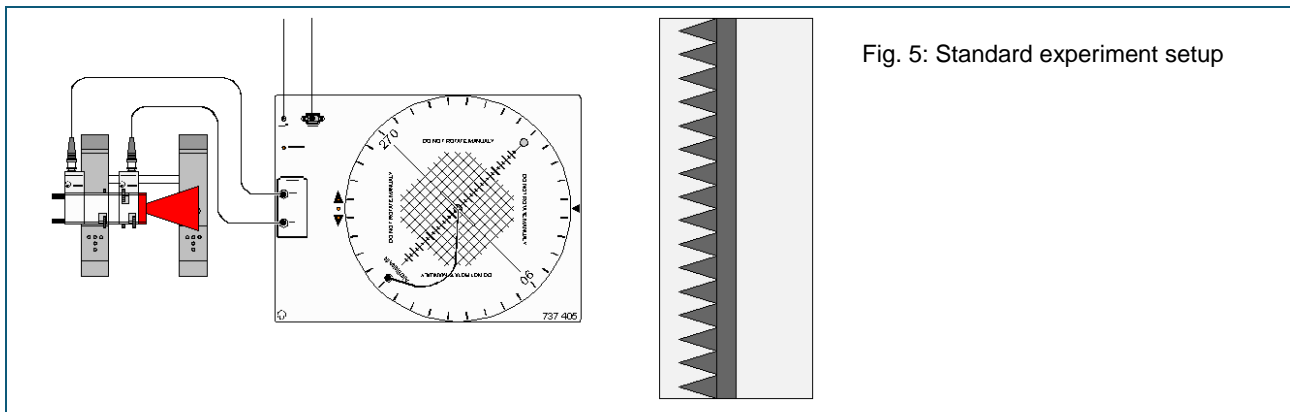
1	737 01	Gunn oscillator
1	737 03	Coax detector
1	737 035	Transition waveguide/coax
1	737 033	Coax Transition
1	737 05	PIN modulator
1	737 06	Isolator
1	737 15	Support for waveguide components
1	737 197	E-Bend
1	737 21	Large horn antenna
1	737 390	Set of microwave absorbers
1	737 405	Rotating antenna platform
1	737 440	Helical antenna kit
1	501 02	BNC Cable, l = 1 m
1	568 702	Book: Antenna Technology
3	301 21	Stand base MF
1	311 77	Steel tape measure
1		PC with Windows XP or higher version

For Variants only

1	737 27	Physics microwave Accessories
---	--------	-------------------------------

## Experiment set-up

The experiment set-up is shown in fig. 5. Helical antennas are used as test and source antennas. The source antenna radiates right-handed circularly polarized waves (R-type). The E-bend should be pointing sideward, this results in a more advantageous height alignment between the test and source antenna.



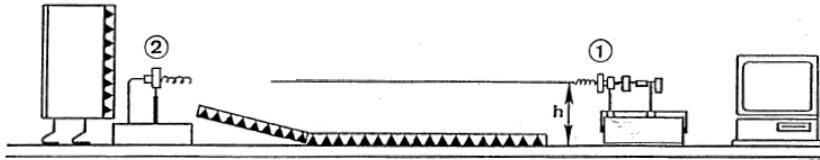


Fig. 6: Standard experiment setup

- 1: Transmitter  
2: Receiver



Fig. 7: Experiment assembly

**1: Source antenna**

- a: PIN-Modulator  
b: E-Bend  
c: Transition waveguide/coax with coax transition male/male 737 033  
d: Helical source antenna

**2: Test antenna**

- a: Helical test antenna  
b: Coax detector  
c: BNC cable

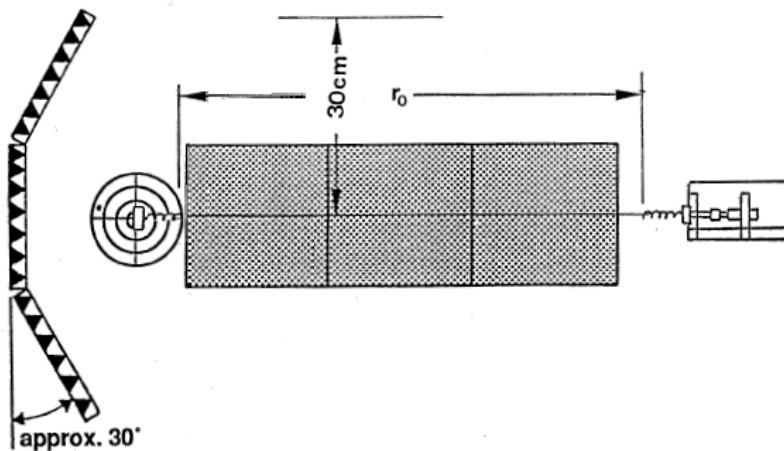


Fig. 8: Experiment assembly

Schematic view for the placement of the reflector plate. **Note:** The transmitter has to be turned "somewhat" towards the mirror.

## Experiment procedure

### 1. Directional diagram of helical antennas with same SOP

- Right-handed helical antennas (R-type) serve as source and test antennas.
- Assemble the experiment set-up as specified in fig. 5-7.
- Connect the helical antenna to the coax detector and the holder (stand rod 245 mm long). Insert the holder into the central mounting bore in the rotating antenna platform. The 245 mm long stand rod is contained in Support for waveguide components 737 15.
- Connect the coaxial cable to the BNC output of the coax detector and to the input of the rotating platform.

- Record the directional diagram with the following settings:
  - Range from:  $-180^\circ$  to:  $+180^\circ$
  - Angular Increment:  $1^\circ$
  - Bias Current: off
  - Detector characteristic: Quadratic,  $m = 2$
  - Graphic display:  $A(\vartheta)$  and  $a(\vartheta)$  respectively
- Switch over to Cartesian coordinates and determine the 3 dB-width.
- Save the measurement.
- Determine the front-to-back ratio of the helix-antenna.

## 2. Directional diagram of helical antennas with orthogonal SOP

- Replace the source antenna with the L-type helix antenna.
- Repeat the measurement according to point 1.
- Jointly display:  $U(\vartheta)$  for the directional diagrams of helical antennas with same and orthogonal SOP.
- Determine the isolation between the right handed and left handed helical antenna (cross polarization) by measuring  $U(\vartheta)$  in the main lobes of the two directional diagrams. **Note:** Ideal helical antennas only handle purely circular polarized waves. A reception is only possible with a reception antenna of the same handedness as the transmitting antenna. Real helical antennas even radiate a small amount of waves with the orthogonal SOP. The decoupling between the R-type and L-type antennas is called polarization loss factor (PLF). It is given by the equation:

$$PLF_{dB} = 20 \log \left( \frac{E_{R-R}}{E_{R-L}} \right) = 10 \log \left( \frac{U_{R-R}}{U_{R-L}} \right)$$

$U_{R-R}$ : maximum receiving signal  $U(\vartheta)$  in the main lobe for transmitter and receiver with same spiral type (R-R)

$U_{R-L}$ : maximum receiving signal  $U(\vartheta)$  in the main lobe for transmitter and receiver with opposite spiral type (R-L)

## 3. The influence of reflections for antennas with orthogonal SOP

- The test antenna is right-handed. Thus it suppresses the signal arriving directly from the left handed source antenna.
- Set up a metal reflector (backside of one the microwave absorbers or component of 737 27) to the side of the measurement path as shown in fig. 7. Optimize the received signal by alternately rearranging the reflector, the antenna platform and the transmitter.
- Select *Approach Reference Point* from Settings (CASSY Lab software).
- Repeat the measurement according to point 1.

#### 4. Influence of reflections for antennas with the same SOP

- Again test and source antenna have the same handedness (SOP). Repeat the measurement according to point 3.
- Give a joint representation for the R-R and R-L configuration under the influence of reflections. Comment your results.

### Variants

#### Polarizer between two helical antennas with orthogonal SOP

- Here two helical antennas of opposite handedness are used. Additionally a polarization grid is inserted between source and test antenna.
- Repeat the measurement according to point 1 for various settings of the polarizer.

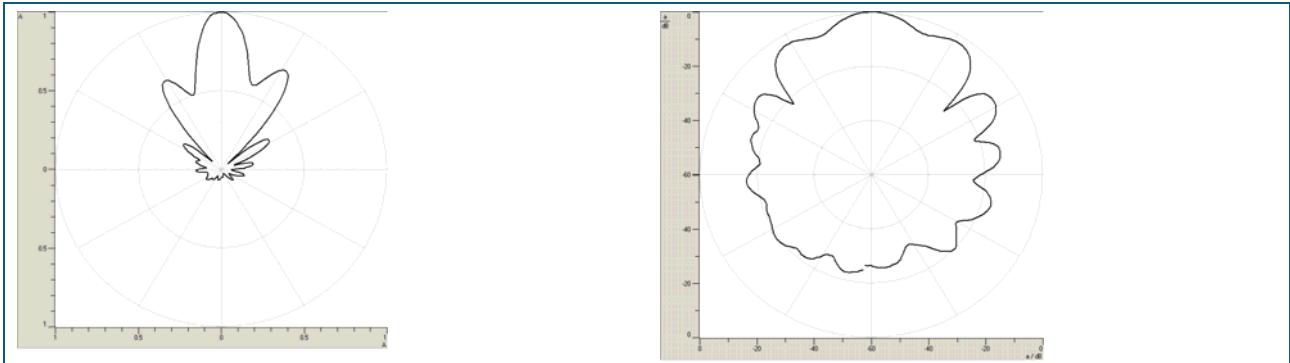
#### Measuring the SOP of a nearly circular polarized wave

Determine the following polarization parameters:

- Axial ratio (AR) of the polarization ellipse
- Tilt angle  $\tau$  of the polarization ellipse
- Handedness (left- or right-handed) of the wave

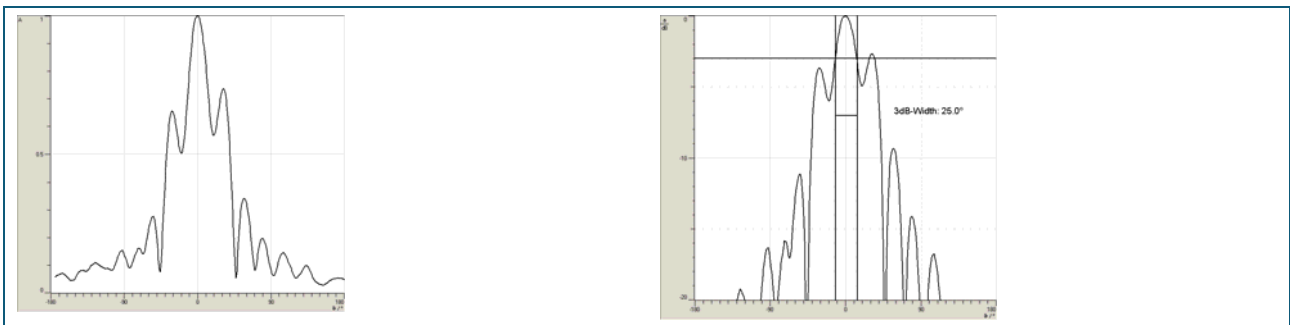
## Results

### 1. Directional diagram of helical antennas with same SOP



Source antenna: R-type. Test antenna: R-type  
Polar coordinates  
Linear representation:  $A(\vartheta)$

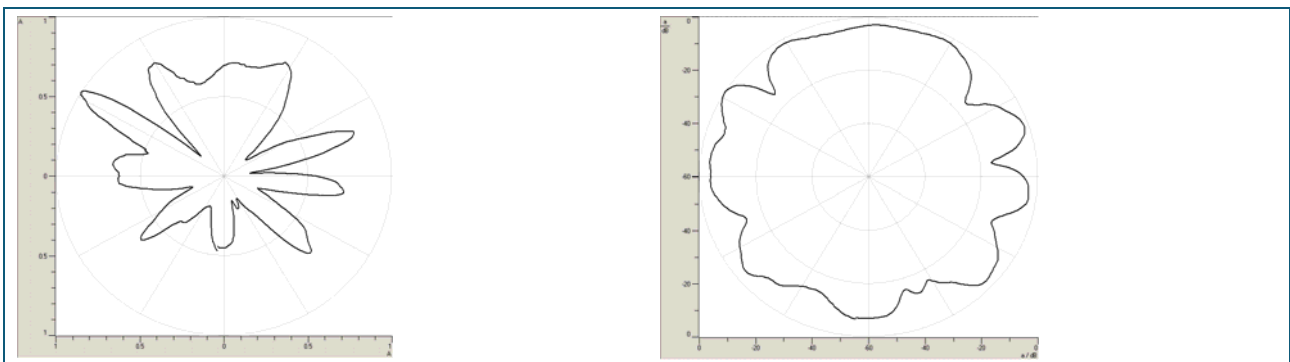
Source antenna: R-type. Test antenna: R-type  
Polar coordinates  
Logarithmic representation:  $a(\vartheta)$



Source antenna: R-type. Test antenna: R-type  
Cartesian coordinates  
Linear representation:  $A(\vartheta)$

Source antenna: R-type. Test antenna: R-type  
Cartesian coordinates  
Logarithmic representation:  $a(\vartheta)$   
3 dB-Width: 25°

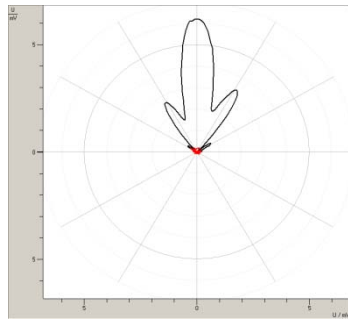
### 2. Directional diagram of helical antennas with orthogonal SOP



Source antenna: L-type. Test antenna: R-type  
Polar coordinates  
Linear representation:  $A(\vartheta)$

Source antenna: L-type. Test antenna: R-type  
Polar coordinates  
Logarithmic representation:  $a(\vartheta)$

Joint display of the directional diagrams R-R and R-L configuration



The directional diagram for cross polarization (red curve) is hardly to see.

**Note:** Representation with auto scaling. Click left into the gray vertical axis and activate: *Find Minimum and Maximum*.

Polar coordinates

Linear representation:  $\mathbf{U}(\vartheta)$

Black: Antennas with same SOP (R-R configuration)

Red: Antennas with orthogonal SOP (R-L configuration)

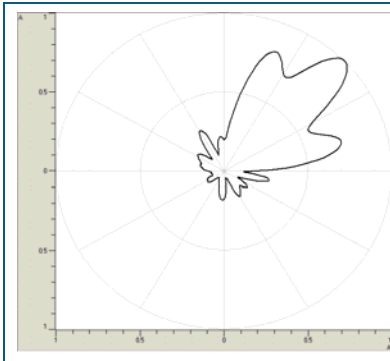
$$U(\vartheta)_{R-R}: 6.21 \text{ mV}$$

$$U(\vartheta)_{R-L}: 0.13 \text{ mV}$$

$$PLF_{dB} = 20 \log \left( \frac{E_{R-R}}{E_{R-L}} \right) = 10 \log \left( \frac{U_{R-R}}{U_{R-L}} \right) = 10 \log \frac{6.21}{0.13} = 16.8$$

$$AR = \frac{E_{R-R} + E_{R-L}}{E_{R-R} - E_{R-L}} = \frac{\sqrt{U_{R-R}} + \sqrt{U_{R-L}}}{\sqrt{U_{R-R}} - \sqrt{U_{R-L}}} = 1.33$$

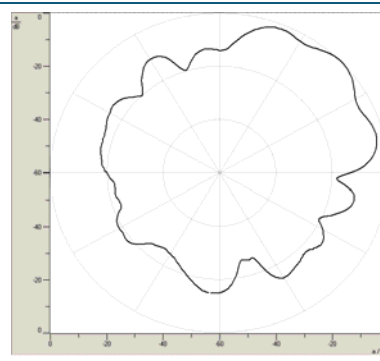
3. The influence of reflections for antennas with orthogonal SOP



Source antenna: L-type. Test antenna: R-type

Polar coordinates

Linear representation:  $\mathbf{A}(\vartheta)$

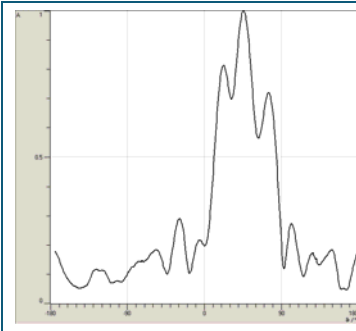


Source antenna: L-type. Test antenna: R-type

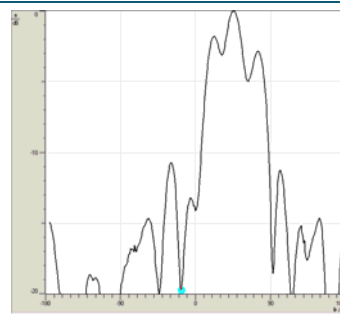
Polar coordinates

Logarithmic representation:  $\mathbf{a}(\vartheta)$





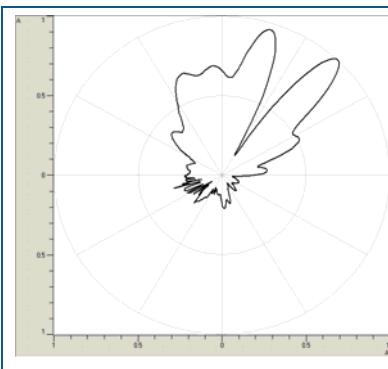
Source antenna: L-type. Test antenna: R-type  
Cartesian coordinates  
Linear representation:  $\mathbf{A}(\vartheta)$



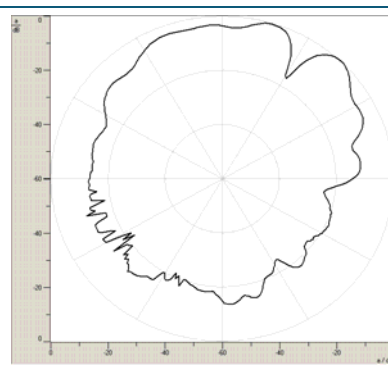
Source antenna: L-type. Test antenna: R-type  
Cartesian coordinates  
Logarithmic representation:  $\mathbf{a}(\vartheta)$

Due to the reversal of the handedness caused by the reflection at a metal plate, the reflected wave is received. This is shown by a strong lobe into the direction towards the reflector. Note: Apart from the direct transmission between transmitter and receiver real radio links additionally suffer from reflected waves at the earth's surface.

#### 4. Influence of reflections for antennas with the same SOP

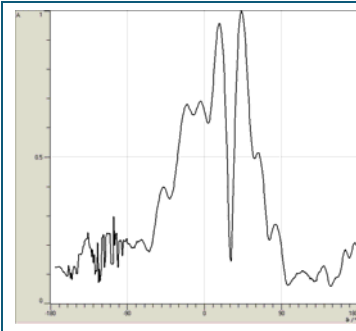


Source antenna: R-type. Test antenna: R-type  
Polar coordinates  
Linear representation:  $\mathbf{A}(\vartheta)$

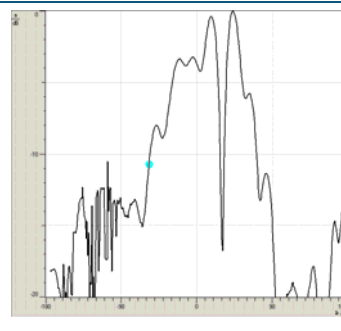


Source antenna: R-type. Test antenna: R-type  
Polar coordinates  
Logarithmic representation:  $\mathbf{a}(\vartheta)$

The reflections are simulated by a metal plate next to the measurement station. The helices of the test and source antenna are wound clockwise. Counter clockwise polarized waves are thus be suppressed. Because the reflector inverts the handedness of the reflected circular wave, there is really no directional diagram detectable (only a "potato" graph).

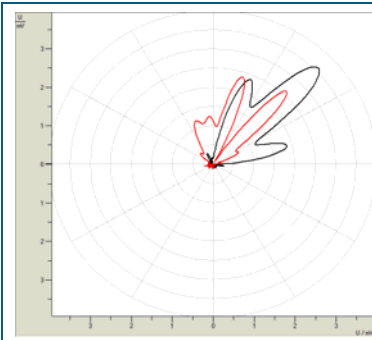


Source antenna: R-type. Test antenna: R-type  
 Cartesian coordinates  
 Linear representation:  $\mathbf{A}(\vartheta)$



Source antenna: R-type. Test antenna: R-type  
 Cartesian coordinates  
 Logarithmic representation:  $\mathbf{a}(\vartheta)$   
 3 dB-Width: not detectable

### Joint display of the directional diagrams R-R and R-L configuration



Polar coordinates  
 Linear representation:  $\mathbf{U}(\vartheta)$

Because of the reversal of the SOP upon reflection at the reflector, it is now possible for the left-handed helical antenna to receive the signal. It can be clearly seen that the main lobe of the directional diagram is aligned toward the metal reflector.

**Note:** Representation with auto scaling. Click left into the grey vertical axis and activate: *Find Minimum and Maximum*.

Red: Antennas with same SOP (R-R configuration)

Black: Antennas with orthogonal SOP (R-L configuration)

## Variants

### Polarizer between two helical antennas with orthogonal SOP

- Without the grid the situation is described by cross polarization. The degree of decoupling gives the polarization loss factor (PLF). This situation changes, when a polarization grid is installed between the two antennas. The incidenting circular polarized wave at the grid is broken down into two linear base fields, whose phases are in quadrature (phase shift:  $90^\circ$ ). The polarization grid suppresses one of two orthogonal components. The linear polarized wave exiting the grid can be regarded as the superposition of two circular polarized wave (L-Type and R-type).
- The losses should amount to  $-6$  dB due to the twofold suppression of a base component, i.e. the receiving signal is reduced to 25%.
- The linearly polarized wave arising behind the polarizer can be broken down again into left- and right-handed components of equal magnitude. Thus the receiving antenna behind the polarizer can be left- or right-handed. Causes for deviations from the theoretical  $-6$  dB loss are:
  - standing wave between the metal grid of the polarizer and the helical antennas
  - finite conductivity of the grid wires
  - dielectric losses in the printed circuit board.

Measuring the SOP of a nearly circular polarized wave

### 1 Determination of the axial ratio (AR) of the polarization ellipse

Determination of the AR needs the measurement of the two orthogonal components  $E_R$  and  $E_L$ .

$$AR = \frac{E_{R-R} + E_{R-L}}{E_{R-R} - E_{R-L}} = \frac{\sqrt{U_{R-R}} + \sqrt{U_{R-L}}}{\sqrt{U_{R-R}} - \sqrt{U_{R-L}}}$$

This equation applies for detectors operating in the square law region. Hint: The measurements need test and source antennas of the same gain. A prerequisite which is not 100% fulfilled.

### 2 Determination of the tilt angle

The determination of the tilt angle  $\tau$  with respect to the horizon is carried out with the polarizer. The polarizer must be set up to between source and test antenna and it must be able to rotate around its symmetry axis. The signal received by a circularly polarized antenna is independent of  $\tau$ , if the wave radiated by the source antenna is also circularly polarized. The magnitude of the received signal remains constant during grid rotation. If the source antenna radiates linearly polarized waves, then a distinct maximum can be observed when the wires of the grid are positioned perpendicularly to the polarization plane of the source antenna. For an elliptical SOP, there are two maxima corresponding to the semi axes of the polarization ellipse.

### 3 Determination of the handedness

Determination of the handedness requires the  $E_L$  and  $E_R$  measurements:

- The radiated wave is polarized left-handed for:  $E_L > E_R$
- The radiated wave is polarized right-handed for:  $E_L < E_R$
- The radiated wave is linearly polarized for:  $E_L = E_R$

Rotating direction:  $U_R > U_L$ ; i.e. right handed.

*Conclusion:*

The beam is nearly right handed circularly polarized. The ideal AR would be  $AR = 1.0$

## Array antennas

### Fundamentals

The radiation characteristic can be considerably improved when an array is used instead of a single radiator. In contrast to the parasitic elements of the Yagi antenna, the radiators of an array are combined together by a feeder system. In this chapter experiments are carried out on a 1-dimensional array arranged in a single row and a 2-dimensional array in the form of a plane. The total directional diagrams for these configurations can be calculated by multiplication of the directional diagram of the individual radiators and array factors. The array factors are determined for the horizontal and vertical configuration of the radiators and are dependent on their geometrical arrangement. Fig. 1 shows a planar dipole configuration formed out of individual radiators in a vertical arrangement. This configuration is used to explain the principle of factorization of directional diagrams. The directional diagram of the array is described by the following equation:

$$\left| \frac{A}{A_0} \right| = 2 |\sin \vartheta| \left| \frac{\sin\left(\frac{m\pi b}{\lambda_0} \cos \vartheta\right)}{\sin\left(\frac{\pi b}{\lambda_0} \cos \vartheta\right)} \right| \left| \frac{\sin\left(\frac{n\pi a}{\lambda_0} \sin \varphi \sin \vartheta\right)}{\sin\left(\frac{\pi a}{\lambda_0} \sin \varphi \sin \vartheta\right)} \right| \left| \cos\left(\frac{\pi}{2} - \frac{2\pi h}{\lambda_0} \cos \varphi\right) \right|$$

$$D = |\sin \vartheta|$$

Directional diagram of the individual dipole

$$H = \left| \frac{\sin\left(\frac{n\pi a}{\lambda_0} \sin \varphi \sin \vartheta\right)}{\sin\left(\frac{\pi a}{\lambda_0} \sin \varphi \sin \vartheta\right)} \right|$$

Directional diagram for the horizontal array, n radiators

$$V = \left| \frac{\sin\left(\frac{m\pi b}{\lambda_0} \cos \vartheta\right)}{\sin\left(\frac{\pi b}{\lambda_0} \cos \vartheta\right)} \right|$$

Directional diagram for the vertical array, m radiators

$$R = \left| \cos\left(\frac{\pi}{2} - \frac{2\pi h}{\lambda_0} \cos \varphi\right) \right|$$

Reflector characteristic of the ground plane

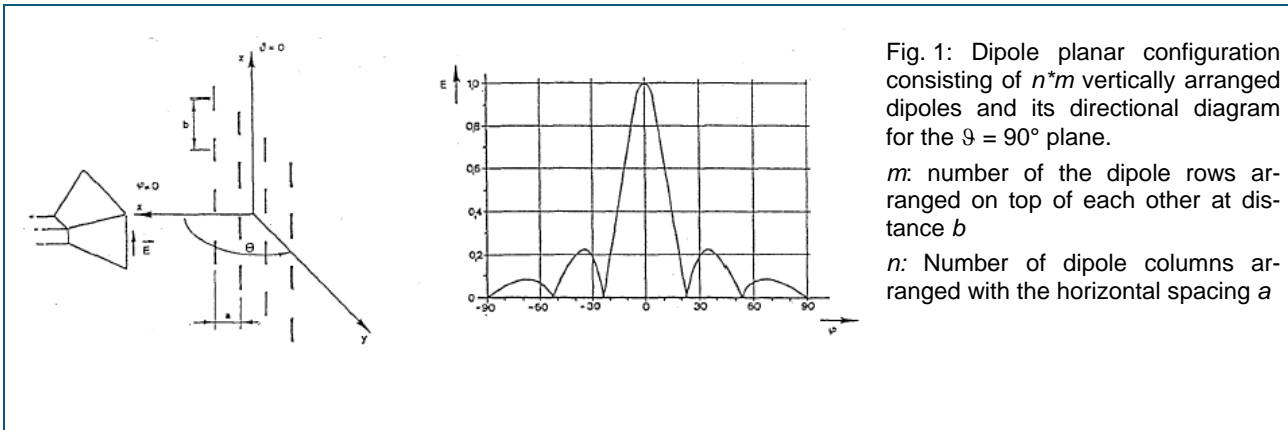


Fig. 1: Dipole planar configuration consisting of  $n \cdot m$  vertically arranged dipoles and its directional diagram for the  $\vartheta = 90^\circ$  plane.

$m$ : number of the dipole rows arranged on top of each other at distance  $b$

$n$ : Number of dipole columns arranged with the horizontal spacing  $a$

### Linear arrays

In practice the slot antenna is very frequently used as a linear array. Due to its fan-formed beam characteristic and high side-lobe attenuation it is preferred in surveillance radar equipment for ship navigation. Slot antennas consist of several coupled single slots. In the next chapter, the beam characteristics of such single slots are investigated. When several slots are arranged in a waveguide, a linear array antenna is born. The slots are fed by a guided wave and radiate a portion of the power supplied into free space. The arrangement, size and alignment of the slots determine the directional characteristic of the complete antenna. Necessary for radiating power out of a slot is that the slot interrupts the surface currents of the wave traveling along the waveguide. If the waveguide is fed with the fundamental mode according to fig. 2, maximum radiation results for slots (2) and (3), while the longitudinal slot 1 running symmetrically and located on the broad side of the waveguide (theoretically) will not radiate. Thus slots in this position are suitable for the assembly of slotted lines, as they are commonly used in waveguide measurement techniques.

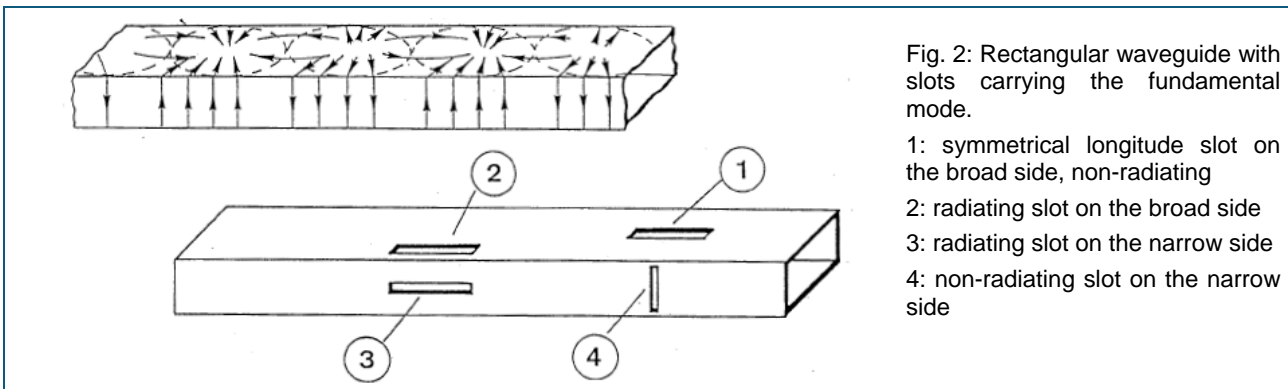
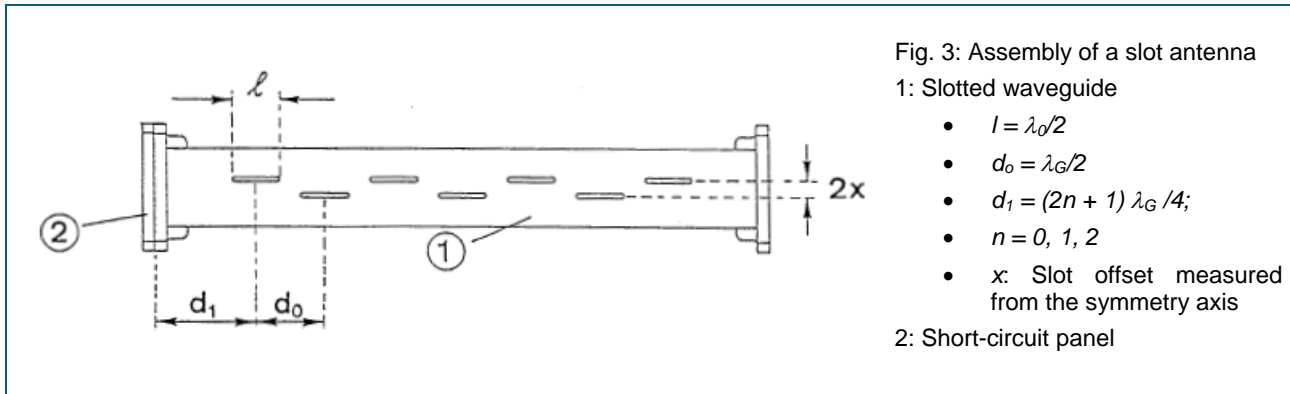


Fig. 2: Rectangular waveguide with slots carrying the fundamental mode.

- 1: symmetrical longitude slot on the broad side, non-radiating
- 2: radiating slot on the broad side
- 3: radiating slot on the narrow side
- 4: non-radiating slot on the narrow side

The construction of the slot antenna for a rectangular waveguide carrying the fundamental mode is depicted in fig. 3.



The slots are alternately arranged around the broad side of the waveguide, showing a slot offset  $x$  from the symmetry axis. The slot distance  $d_0$  amounts to approx.  $\lambda_G/2$ . The alternation from slot to slot around the symmetry axis compensates for the polarity reversal of the wall currents. If the slot length  $l$  amounts to somewhat less than half a free-space wavelength  $\lambda_0/2$  at operating frequency, then the slot is in resonance. The antenna is fed at one end (e.g. by a waveguide). The opposite end is terminated by a short-circuit plate located at a distance  $d_1$  of  $\lambda_G/4$  from the last slot. Thus, the waveguide transforms the short into an open circuit at the location of the last slot. The parallel connection of no-load with the slot impedance leads to no change in impedance. Because the slot spacing  $d_0$  amounts to  $\lambda_G/2$ , the waveguide functions like a  $\lambda/2$  transformer and reproduces the slot impedances unchanged at the location of the adjacent slot. Thus, the sum total of all  $N$  slots has the same effect at the feeding point of the antenna as the parallel connection of  $N$  impedances of equal magnitude! The construction of a slot antenna is carried out in the following steps:

- The operating frequency  $f$  and guided wavelength  $\lambda_G$  determine the length and spacing of the radiating slots  $l = \lambda_0/2$ ,  $d_0 = \lambda_G/2$ .
- The number of slots  $N$  is a consequence of the desired directivity or the mechanical construction requirements.
- The matching requirements at the feeding point give the necessary transverse impedance  $Z_S$  for each slot
- From this the required slot offset  $x$  can be determined.

The feeding of a resonant operating slot antenna is carried out with standing waves resulting in all slots being fed with waves of equal phase. However, if the "output" of the slot antenna is terminated reflection-free with a waveguide termination, then excitation of the slots is carried out with propagating waves. A change in the frequency leads to excitation of the slots with waves of different phase due to a change in the wavelength  $\lambda_G$  of the guided wave. In the directional diagram of the entire antenna array this leads to a squinting effect of the major lobe. If the frequency of the exciting wave is varied periodically, then the direction of the major lobe varies periodically too and beam scanning results. Phase-controlled antennas permit the electronic control of the beam direction and are thus superior to the naturally sluggish mechanical systems in detecting and tracing fast radar targets.

## Planar arrays

A planar antenna array is build up, when several linear arrays are combined in a parallel configuration. Planar arrays in microstrip line technology are of particular interest. Here it is possible to integrate microwave components directly into the antenna structure (PCB-technology). Thus a more economical production of compact systems can be realized.

## Microstrip technology

The construction of a microstrip line is depicted in fig. 4.

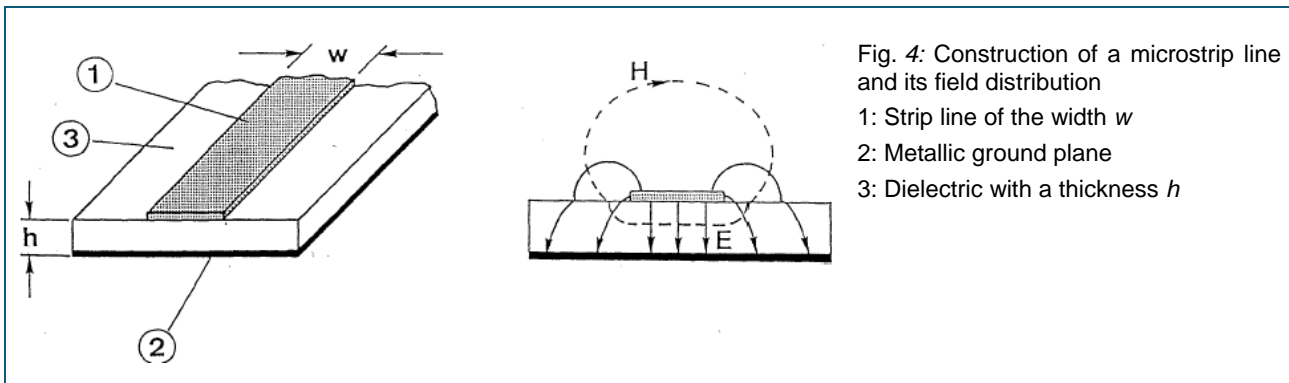


Fig. 4: Construction of a microstrip line and its field distribution

- 1: Strip line of the width  $w$
- 2: Metallic ground plane
- 3: Dielectric with a thickness  $h$

The top of the microstrip line is open. An exact calculation of the field distribution in this kind of system is not possible. Only approximation equations exist for the characteristic impedance  $Z_m$  and wavelength  $\lambda_m$  of microstrip lines. The validity of these equations is dependent on maintaining certain boundary conditions. Thus, a certain experimenting phase still plays a role in the development of circuits in microstrip technology. For  $Z_m$  the literature provides the following equations:

For  $w/h < 1$

$$Z_m = \frac{377\Omega}{\pi\sqrt{2(\epsilon_r + 1)}} \left[ \ln \frac{8h}{w} + \frac{1}{32} \left( \frac{w}{h} \right)^2 - \frac{1}{2} \left( \frac{\epsilon_r - 1}{\epsilon_r + 1} \right) \left( \ln \frac{\pi}{2} + \frac{1}{\epsilon_r} \ln \frac{4}{\pi} \right) \right]$$

And for  $w/h > 1$ :

$$Z_m = \frac{377\Omega}{2\sqrt{\epsilon_r}} \left[ \frac{w}{2h} + 0.441 + 0.082 \left( \frac{\epsilon_r - 1}{\epsilon_r^2} \right) + \left( \frac{\epsilon_r + 1}{2\pi\epsilon_r} \right) \left( 1.451 + \ln \left( \frac{w}{2h} + 0.94 \right) \right) \right]^{-1}$$

Note the thoroughly "bent" exponents and factors as well as the validity range determined by  $w/h$ . The wavelength  $\lambda_m$  on a microstrip line depends on the free space wavelength  $\lambda_0$  and an effective dielectric constant  $\epsilon_{eff}$

$$\lambda_m = \frac{\lambda_0}{\sqrt{\epsilon_{eff}}}$$

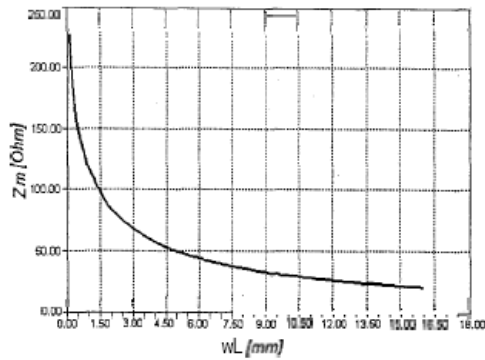


Fig. 5: Characteristic impedance of a microstrip line with:  $h = 1.57 \text{ mm}$ ,  $\epsilon_r = 2.20$ .

The effective dielectric constant  $\epsilon_{eff}$  itself is a function of  $\epsilon_r$ ,  $h$  and  $w$ .

$$\epsilon_{eff} = \frac{1}{2} \left( \epsilon_r + 1 + \frac{\epsilon_r - 1}{\sqrt{1 + \frac{10h}{w}}} \right)$$

### Microstrip antennas

The radiation characteristic of a microstrip antenna consisting of many individual radiators is again determined by array factors. If one array factor was sufficient to discuss linear arrays, two array factors ( $H$  and  $V$ ) have to be taken into account for a plane array. Unfortunately the radiating patches of the array often interact with each other in an uncontrollable manner. This results in deviations to the calculated characteristics of the system which cannot be ignored. This makes predictions a difficult matter. This is especially true for arrays with many radiating patches. The patch radiator of a microstrip antenna can be considered as a stripline resonator operating at no-load at both ends. Frequently, rectangular or disk shaped elements are used as radiators. Fig. 6 shows the cross section of a rectangular resonator and its related field distribution.

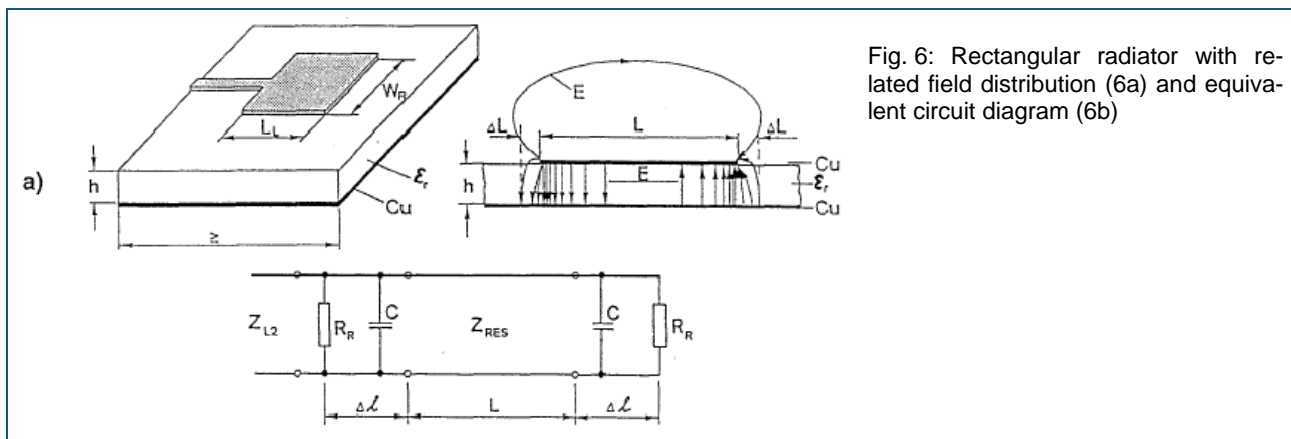


Fig. 6: Rectangular radiator with related field distribution (6a) and equivalent circuit diagram (6b)

The radiation from a single rectangular-shaped patch has almost dipole character. The field distribution at the edges of the resonator demonstrates a "spilling out" of electrical field lines from the resonator. Thus, the electrical length is greater than the mechanical length. This reduction - so-called  $\Delta l$  effect - must be taken into account on both sides when calculating the resonator length  $L$ .



Here, the following holds true:

$$L = \frac{\lambda_m}{2} - 2\Delta l$$

$$\Delta l = 0.412h \left( \frac{\epsilon_{eff} + 0.3}{\epsilon_{eff} - 0.258} \right) \left[ \frac{\frac{w}{h} + 0.264}{\frac{w}{h} + 0.8} \right]$$

The  $\Delta l$  zone of the open circuit patch resonator behaves electrically like a capacitor  $C$ : it stores energy. As can be seen in fig. 6a, a portion of the field lines joins above the resonator. This leads to the radiation of power. Therefore, the  $\Delta l$  zone in the equivalent circuit diagram in fig. 6 can be represented by a complex impedance of  $Z_R = R_R + jX_R$ . The imaginary component  $X_R$  indicates the energy stored in the resonator while the radiation resistance  $R_R$  as the real component describes the radiation through the resonator sides. The radiation resistance is also dependent in a complicated manner on the parameters of the microstrip line ( $w$ ,  $h$ ,  $\lambda_m$ ,  $\epsilon_{eff}$ , etc.). The following applies for radiator widths  $w_R < 0.5 \lambda_m$ :

$$R_R = \frac{180\Omega}{\sqrt{\epsilon_{eff}}} \left( \frac{\lambda_m}{w_R} \right)^2$$

and for  $w_R < 1.5 \lambda_m$ :

$$R_R = \frac{240\Omega}{\sqrt{\epsilon_{eff}}} \left( \frac{\lambda_m}{w_R} \right)^2$$

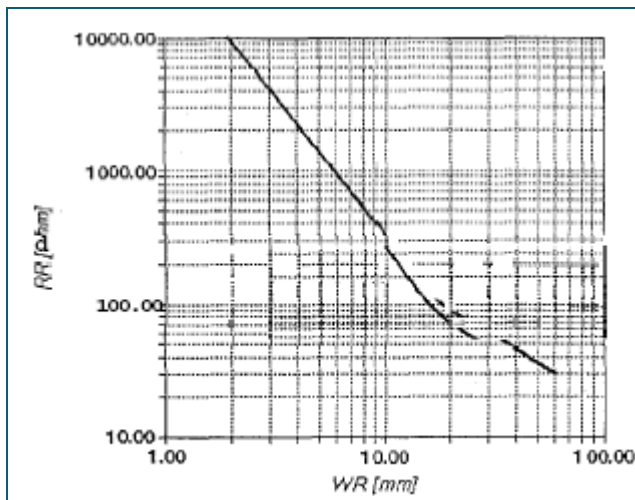


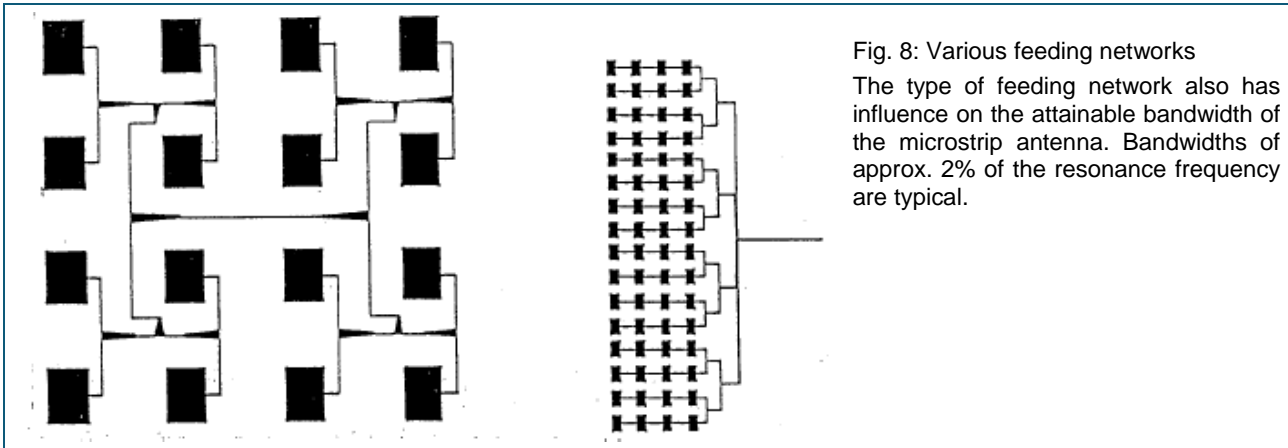
Fig. 7: The radiation resistance  $R_R$  of a rectangular patch as a function of the radiator width  $w_R$

In order to match the patch radiator to the feeding microstrip line, it is necessary to know:

- the complex impedance  $\underline{Z}_R$  of the  $\Delta l$  zone
- the impedance of the patch (length  $L$ ) and
- the characteristic impedance  $\underline{Z}_m$  of the microstrip line.

In the case of resonance only the radiation resistance  $R_R$  has to be matched to the feeding line. The radiation resistance and the total loss resistance determine the efficiency of a microstrip antenna. In this context, the feeding network is of central importance. Feeding networks which have been dimensioned poorly can bear responsibility for up to 50% of the total losses in the antenna. In the design of feeding networks the two main variants illustrated in fig. 8 can be distinguished:

- The series feeding network with the resonators connected in series
- The corporate feeder in which all of the radiators are connected on (electrically) equally long line segments (fig. 8 left)
- A combination of the two (fig. 8 right)



## Questions

1. What is the structure of the feeding network for the microstrip antenna 737 427?
2. Which radiation resistance  $R_R$  is needed in order to assemble an antenna containing 16 elements for 9.40 GHz with the following technical data:
  - Microwave substrate: Duroid RT 5828 with  $h = 1.57$  mm
  - Relative permittivity  $\epsilon_r = 2,20$
  - 4 rows with 4 individual radiators each.
3. What dimensions are required for the radiator patches and the stripline segments of this antenna?
4. Determine the slot offset  $X$  for the Slot antenna 737 424, operating with a frequency of  $f = 9.40$  GHz.

## Material

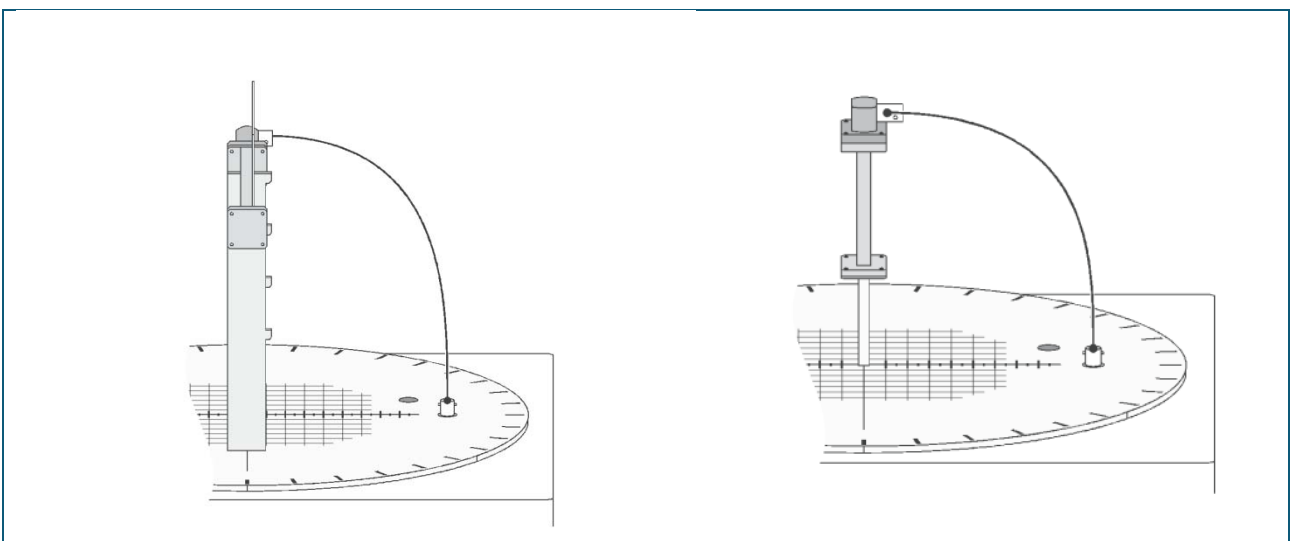
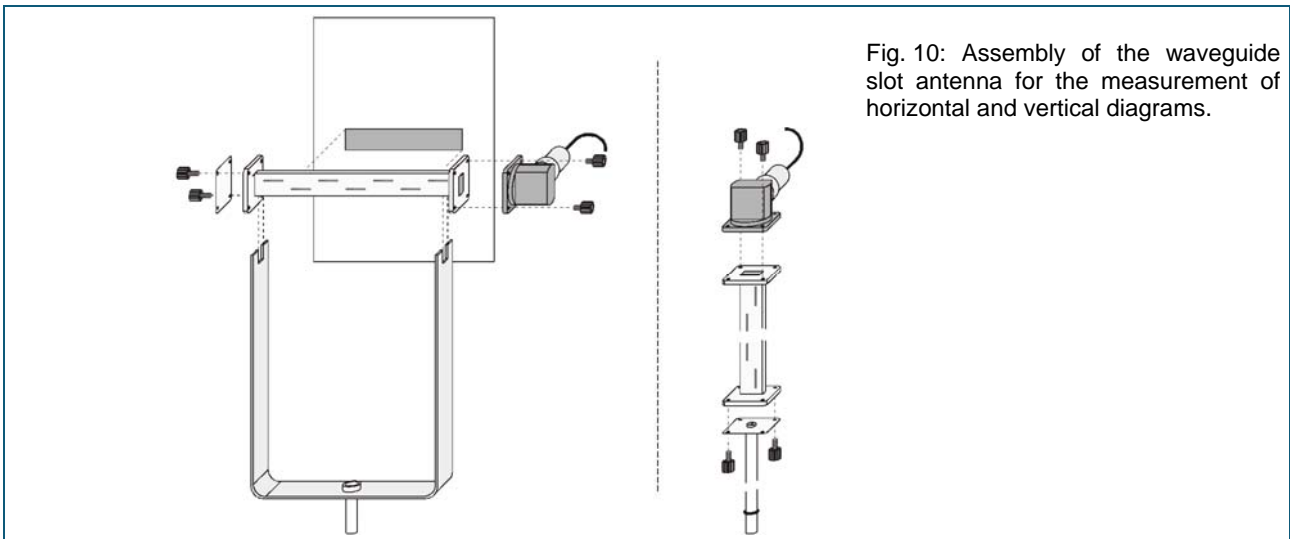
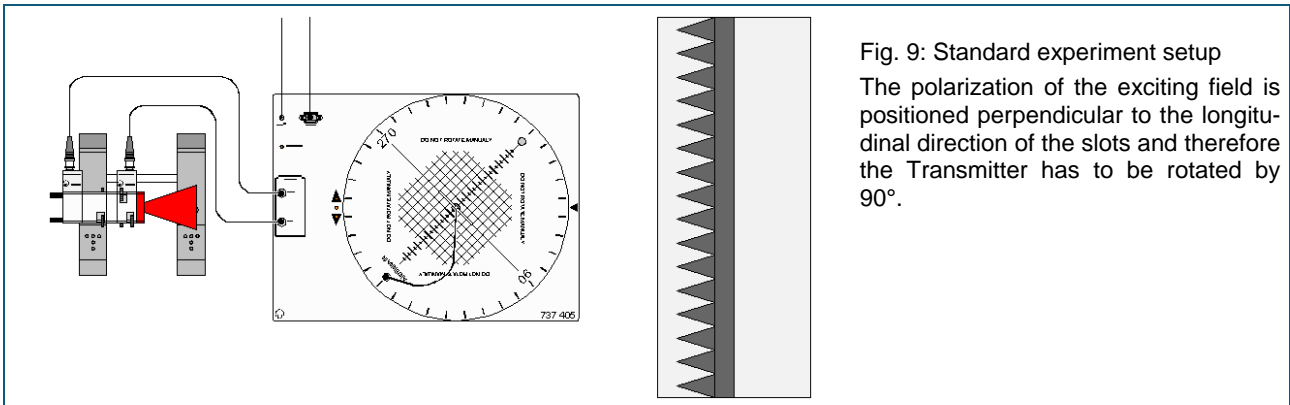
1	737 01	Gunn oscillator
1	737 03	Coax detector
1	737 035	Transition waveguide/coax
1	737 05	PIN modulator
1	737 06	Isolator
1	737 10	Moveable short
1	737 14	Waveguide termination
2	737 15	Support for waveguide components
1	737 21	Large horn antenna
1	737 390	Set of microwave absorbers
1	737 399	Set 10 Thumb screws
1	737 405	Rotating antenna platform
1	737 424	Slot antenna
1	737 427	Microstrip antenna
1	501 02	BNC cable, l = 1 m
1	568 702	Book: Antenna Technology
1	311 77	Steel tape measure
4	301 21	Stand base MF
1		PC with Windows XP or higher version

## Additionally required

1	Roll of aluminium foil
1	Roll of adhesive tape (Scotch tape)

## Experiment set-up

The experiment set-ups are shown in fig. 9 up to fig. 11.



The polarization of the exciting field is positioned perpendicular to the longitudinal direction of the slots.

## Experiment procedure

### 1. Horizontal diagrams of the slot antenna, $N = 7$

- Rotation of the test antenna is carried out in the H-plane of the feeding source antenna.
- Assemble the experiment set-up in accordance with fig. 9 respectively. Fig 10. The source antenna radiates vertically-polarized waves. The broad side of the horn is horizontal.
- Does the distance between the source and test antenna fulfil the far field condition:

$$r_0 \geq \frac{2(d_Q + d_T)^2}{\lambda_0}$$

$d_Q, d_T$ : largest dimensions (in the transverse or longitudinal direction) of the antenna

$r_0$ : distance between the source and test antenna

$\lambda_0$ : wavelength of the radiated wave.

Comment on your results.

- Set up the slot antenna so that the slots are located on the side facing away from the source antenna. Thus you manage to get the major lobe to appear on the screen at  $0^\circ$  and not at  $180^\circ$ . The medium slot should be positioned exactly over the center of the rotating base.
- Record the directional diagram with the following settings:
  - Range from:  $-180^\circ$  to:  $+180^\circ$
  - Angular Increment:  $1^\circ$
  - Bias Current: off
  - Detector Characteristic: Quadratic,  $m = 2$
  - Graphic display:  $A(\vartheta)$  and  $a(\vartheta)$  respectively
- Save your measurement.
- Switch over to the Cartesian coordinate system and determine the 3 dB-Width using the graphics cursor and enter the value into table 1.
- Determine the front-to-back ratio using the cursor. Accordingly determine the minor lobe level in the  $+90^\circ$  range "in the proximity of the major lobe". Enter the values into table 1.

### 2. Horizontal diagrams with reduced number of slots, $N = 5$

- Cover the external slots (left and right) with aluminium foil. Secure it using adhesive tape. Make sure that the foil is as fixed as possible.
- The experiment proceeds as described in point 1.

### 3. Horizontal diagrams with reduced number of slots, $N = 3$

- Cover each of the outer 2 slots with aluminium foil and secure the foil with adhesive tape.
- Proceed with the experiment in accordance with point 1.

4. Vertical diagrams with reduced number of slots,  $N = 3$ 

- The experiment is set up as in fig. 10 and fig. 11. The source antenna radiates horizontally polarized waves, i.e. the E-plane is horizontal.
- Replace the short plate by the short with the holder, in order to set up a vertical assembly. Each of the 2 outer slots of the antenna remain covered with aluminium foil. Insert the slot antenna into the central bore for stand rods in the rotating base.
- Proceed with the experiment in accordance with point 1.

5. Vertical diagrams of the slot antenna,  $N = 7$ 

- Experiment set-up and procedure is described under point 4. Remove the aluminium foil from the slots. Be careful not to accidentally rotate the antenna.

## 6. The formation of grating lobes

- If the slot distance  $d_0$  is considerably more than  $\lambda_G/2$ , then so-called grating lobes are formed, i.e. the energy of the beam field is no longer concentrated on one major lobe alone.
- This effect is simulated here by covering the middle slot with aluminum foil. The directional diagram of the horizontal slot antenna is to be investigated.
- Follow the instructions outlined in point 1. Save the data.

## 7. Beam squinting and scanning by means of phase control

- Experiment set-up as specified in fig. 10 (horizontal mode). Alter the Gunn oscillator as specified in fig. 13 into a mechanically tune able oscillator.
- Remove the coupling diaphragm between the Gunn oscillator and the isolator. Replace the simple short plate with the moveable short. The oscillator frequency can be determined using the frequency meter (737 16). If this device is not available, then the setting of the frequency can be carried out approximately using the following table:

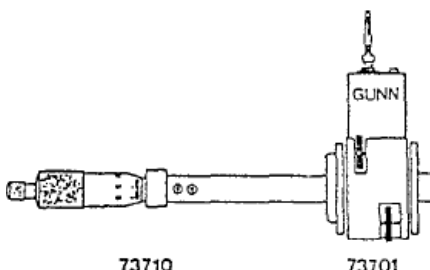


Fig. 13: The mechanically tune able Gunn oscillator. The settings of the moveable short are only coarse search marks. Around these positions look for a detectable microwave power on the level meter **a/dB** and work with your own settings.

Moveable short x/mm	Gunn oscillator f/GHz
21.70	8.9
16.30	9.9
12.50	10.9

- The short plate arranged at one end of the horizontally configured slot antenna is replaced by the reflection-free waveguide termination (737 14). Set the frequency to 8.9 GHz (= setting in the vicinity of 21.70 mm which delivers sufficient microwave power).

- Record the directional diagram. Save the results under SL-89. Repeat the measurements for the frequencies 9.9 GHz and 10.9 GHz, but do not shift the test antenna!
- Jointly display the directional diagrams SL-89, SL-99 and SL109 on the screen. Compare the directional diagrams. Determine the scan angle for the slot antenna. Scan angle = angle difference between the position of the major lobe at minimum and maximum frequency.

#### 8. Horizontal diagrams of the microstrip antenna

- In order to record this directional diagram, a 245 mm long stand rod is screwed into microstrip antenna so that the resonators and the feed lines are aligned horizontally.
- Replace the slot antenna depicted in the experiment set-up in fig. 10 by the microstrip antenna.
- Connect the coax detector to the BNC socket on the rotating antenna platform base using a coaxial cable.
- Re-assemble the Gunn oscillator back into its basic form with a fixed frequency of  $f = 9.40$  GHz.
- Due to the known polarization of the test antenna use the excitation now with a horizontally polarized E-field of the source antenna. The broad side of the horn is vertical.
- In the start position, the rear side of the microstrip antenna should be aligned exactly perpendicularly to the source antenna's main radiation direction.
- Record the directional diagram following the instructions given in point 1.

#### 9. Vertical diagrams of the microstrip antenna

- Turn the microstrip antenna by  $90^\circ$ , so that the resonators and the feed lines are aligned vertically. Now excitation is carried out with a vertically polarized E-field of the source antenna.
- Proceed as described under points 1. Record the vertical directional diagram.

**Table 1: Parameters of slot antennas**

Antenna	3 dB-Width		Sides lobes	F/B-Ratio
	vertical	horizontal		
Slot antenna N=7				
Slot antenna N=5				
Slot antenna N=3				

## Answers

1.

The feeding network is a combination of corporate and series feeder. Four radiators each are connected in a row in series. The four rows are connected with each other at their inputs via a corporate network, which connects all of the rows via microstrip lines all of equal electrical length to the coaxial socket.

2.

The spacing between the individual radiators of a row amounts to  $\lambda_m/2$ . Each row has four radiators. Thus, each row input has an impedance of  $R_R/4$ . All four rows are connected in parallel via a corporate network. In order for the feeding point with 50 Ohm to be properly matched, each radiator element must have a radiation resistance of  $R_R = 16 \cdot 50 \text{ Ohm} = 800 \text{ Ohm}$ .

3.

When  $R_R = 800 \text{ Ohm}$ , we obtain the following parameters for the rectangular patches:

Radiator width  $W_R$ : 6.5 mm

Effective  $DK$ : 1.92 (dielectric constant)

Wavelength  $\lambda_m$ : 23.1 mm

Radiator length: 9.97 mm (including  $\Delta l$  effect)

The characteristic impedance of the feeding network is dependent on the stripline width  $w$ . As the line segments between any two radiators in a row amounts to exactly  $\lambda_m/2$  in length, the characteristic impedance of this line segment can be any value for impedance transformation. For

$Z_m = 100 \text{ Ohm}$  (selected) we obtain:

Line width  $w$ : 1.4 mm

$\epsilon_{\text{eff}}$ : 1.77

Line length  $L$ : 13.25 mm

4.

Slot number:  $N = 7$

From this it follows for the normalized slot impedance of the individual slot:

$$\underline{z} = \frac{\underline{Z}}{\underline{Z}_L} = \frac{1}{N} = \frac{1}{7} \approx 0.14$$



Where:

---

$$a = 10.16 \text{ mm}$$

---

$$b = 22.86 \text{ mm}$$

---

$$\lambda_0 = 31.9 \text{ mm}$$

---

$$\lambda_G = 44.5 \text{ mm}$$

---

$$\text{Thus: } X = 2.5 \text{ mm}$$

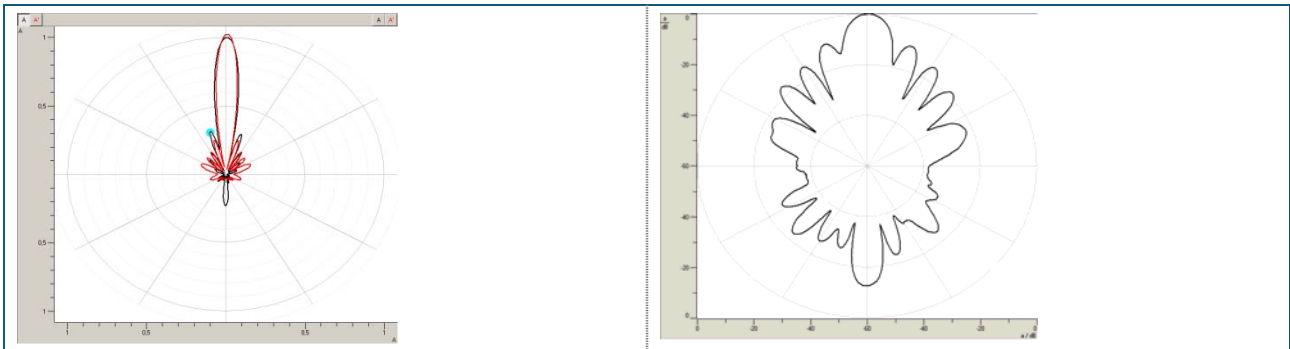
---

## Results

### Far field Condition

Test antenna:	Slot	Remarks
$r_o$ :	1000 mm	Mean distance measured between the source and the test antenna
$\lambda_0$ :	32 mm	Wavelength of the radiated wave
$d_Q$ :	100 mm	Largest transverse measurement of the radiating horn
$d_T$ :	200 mm	Reflector width
$r_o \geq \frac{2(d_Q + d_T)^2}{\lambda_0}$	$r_o > 5625 \text{ mm}$	Far field condition is not fulfilled. The measurements with the slot antenna are conducted in the near field!

#### 1. Horizontal diagrams of the slot antenna, N = 7



H-plane

Polar coordinates

Linear representation:  $A(\vartheta)$

Black: measurement

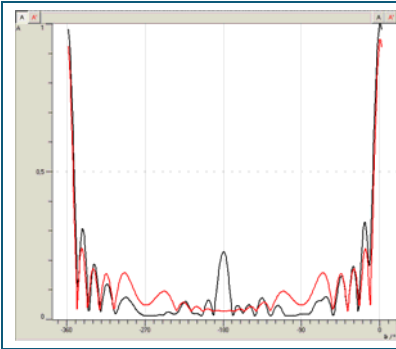
Red: Best fit approximation (with reflector!)

Excitation is carried out with a vertically polarized field

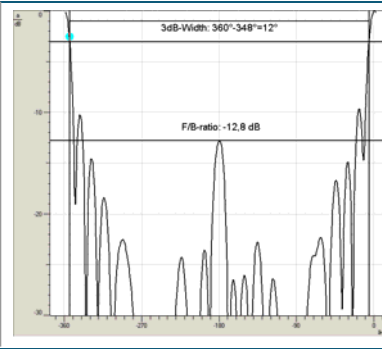
H-plane

Polar coordinates

Logarithmic representation:  $a(\vartheta)$

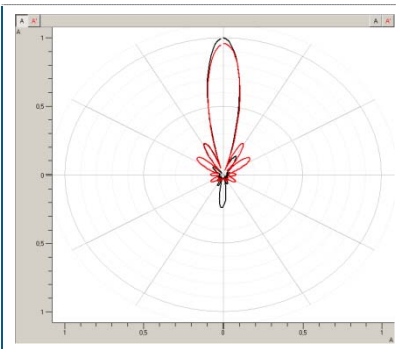


H-plane  
 Cartesian coordinates  
 Linear representation:  $A(\vartheta)$   
 Black: measurement  
 Red: Best fit approximation (with reflector!)

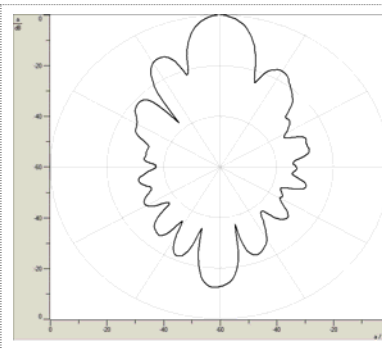


H-plane  
 Cartesian coordinates  
 Logarithmic representation:  $a(\vartheta)$   
 3 dB-Width: 12°  
 Front/back ratio: 13 dB

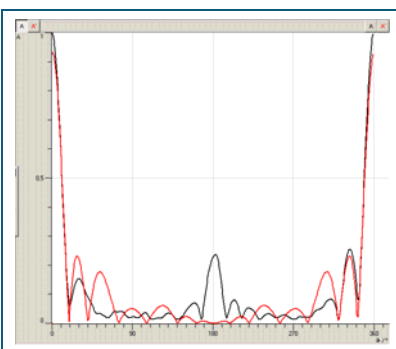
2. Horizontal diagrams with reduced number of slots,  $N = 5$



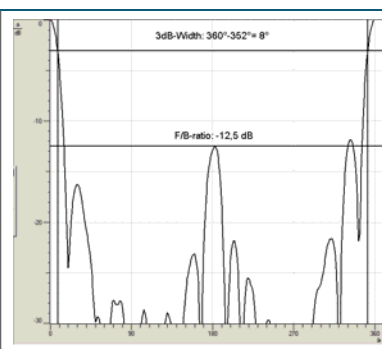
H-plane  
 Polar coordinates  
 Linear representation:  $A(\vartheta)$   
 Black: measurement  
 Red: Best fit approximation (with reflector!)  
 Excitation with vertically polarized field



H-plane  
 Polar coordinates  
 Logarithmic representation:  $a(\vartheta)$

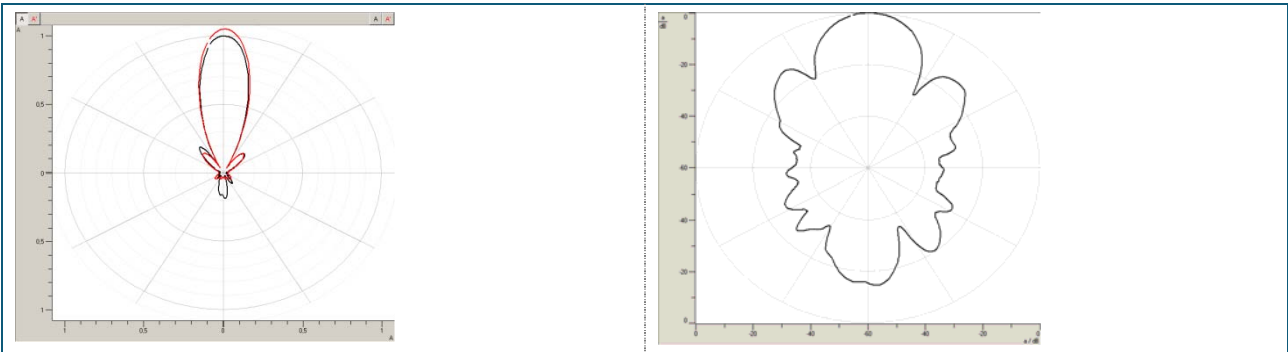


H-plane  
 Cartesian coordinates  
 Linear representation:  $A(\vartheta)$   
 Black: measurement  
 Red: Best fit approximation (with reflector!)



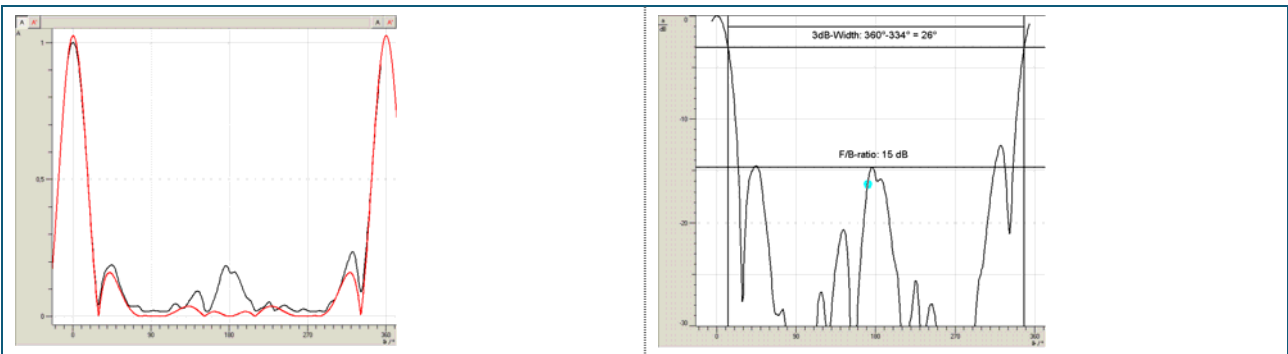
H-plane  
 Cartesian coordinates  
 Logarithmic representation:  $a(\vartheta)$   
 3 dB-Width: 8°  
 Front/back ratio: 13 dB

3. Horizontal diagrams with reduced number of slots,  $N = 3$



H-plane  
 Polar coordinates  
 Linear representation:  $A(\vartheta)$   
 Black: measurement  
 Red: Best fit approximation (with reflector!)  
 Excitation with vertically polarized field

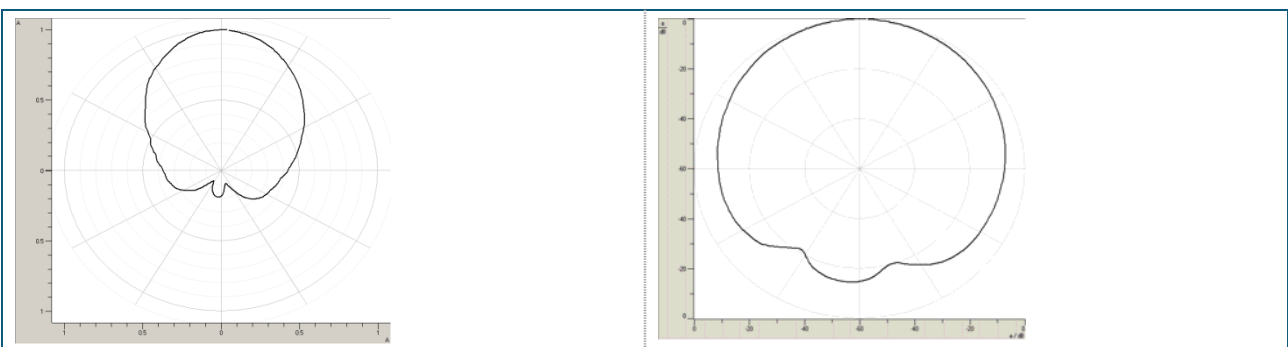
H-plane  
 Polar coordinates  
 Logarithmic representation:  $a(\vartheta)$



H-plane  
 Cartesian coordinates  
 Linear representation:  $A(\vartheta)$   
 Black: measurement  
 Red: Best fit approximation (with reflector!)

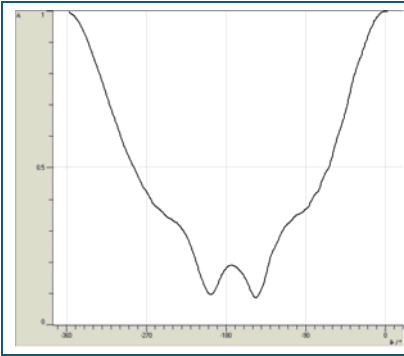
H-plane  
 Cartesian coordinates  
 Logarithmic representation:  $a(\vartheta)$   
 3 dB-Width:  $8^\circ$   
 Front/back ratio: 15 dB

4. Vertical diagrams with reduced number of slots,  $N = 3$

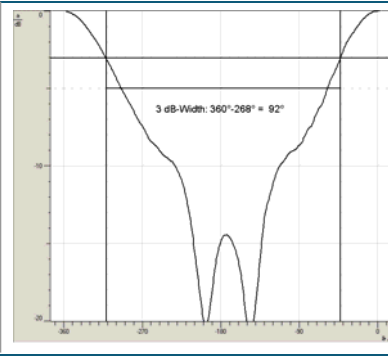


E-plane  
 Polar coordinates  
 Linear representation:  $A(\vartheta)$   
 Black: measurement  
 Excitation with horizontally polarized field

E-plane  
 Polar coordinates  
 Logarithmic representation:  $a(\vartheta)$

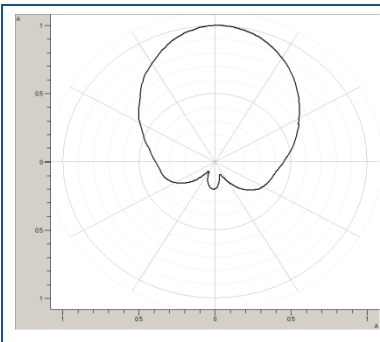


E-plane  
Cartesian coordinates  
Linear representation:  $A(\theta)$

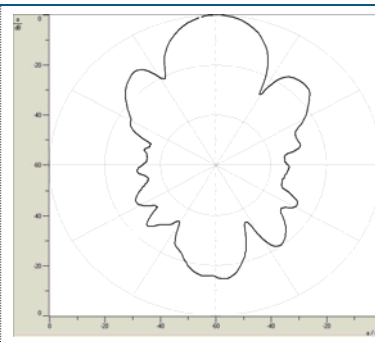


E-plane  
Cartesian coordinates  
Logarithmic representation:  $a(\theta)$   
3 dB-Width:  $92^\circ$   
Front/back ratio: 15 dB

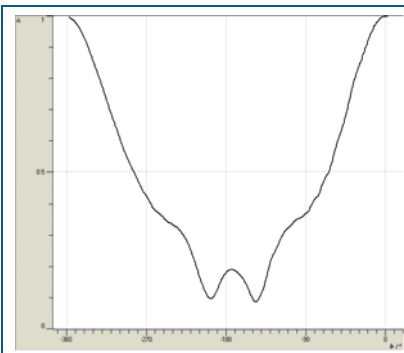
5. Directional diagrams of the vertical slot antenna,  $N = 7$



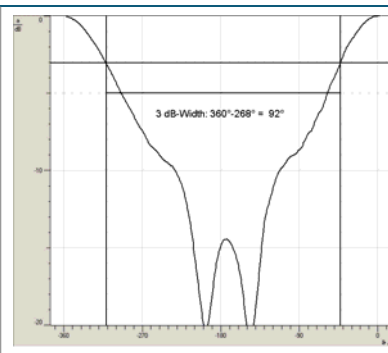
E-plane  
Polar coordinates  
Linear representation:  $A(\theta)$   
Excitation with horizontally polarized field



E-plane  
Polar coordinates  
Logarithmic representation:  $a(\theta)$

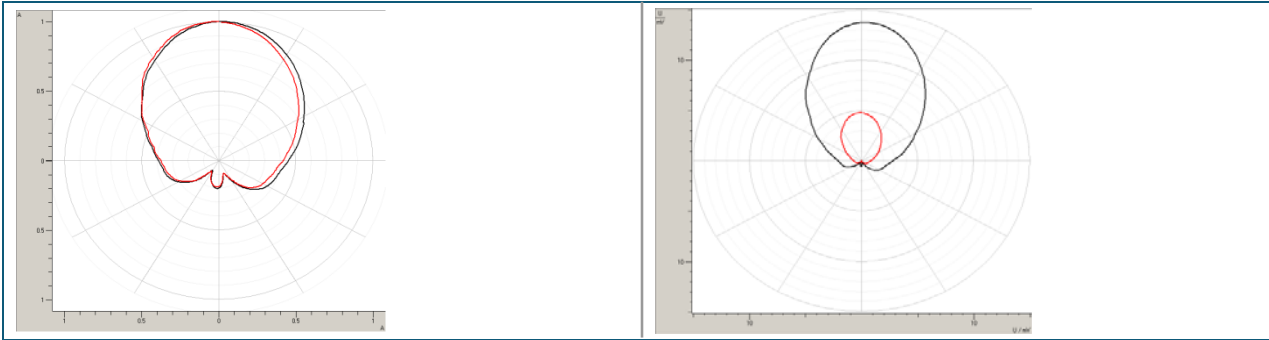


E-plane  
Cartesian coordinates  
Linear representation:  $A(\theta)$   
Black: measurement  
Red: Best fit approximation (with reflector!)



E-plane  
Cartesian coordinates  
Logarithmic representation:  $a(\theta)$   
3 dB-Width:  $92^\circ$   
Front/back ratio: 15 dB

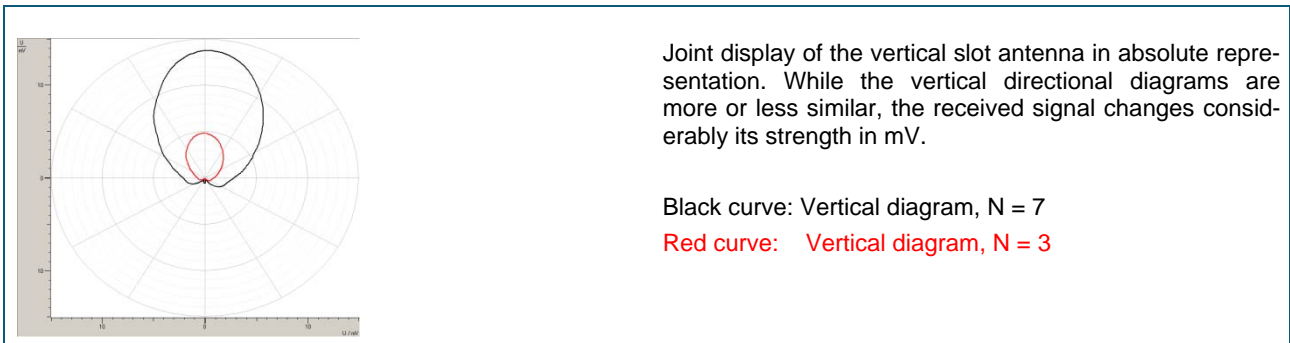
Joint display of the directional diagrams for N = 3 and N = 7 vertical.



E-plane  
 Polar coordinates  
 Linear representation:  $\mathbf{A}(\vartheta)$   
 Black: N = 7  
 Red: N = 3

E-plane  
 Polar coordinates  
 Linear representation:  $\mathbf{U}(\vartheta)$   
 Black: N = 7  
 Red: N = 3

Joint display of vertical slot antennas in absolute quantities



Joint display of the vertical slot antenna in absolute representation. While the vertical directional diagrams are more or less similar, the received signal changes considerably its strength in mV.

Black curve: Vertical diagram, N = 7  
 Red curve: Vertical diagram, N = 3

H-plane  
 Polar coordinates  
 Linear representation:  $\mathbf{U}(\vartheta)$

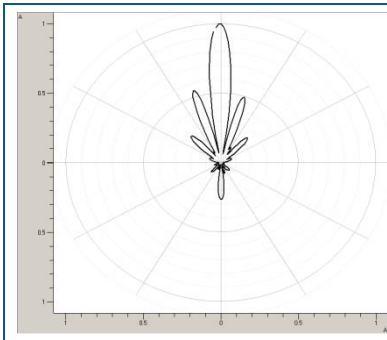
**Observation**

Nearly identical vertical directional diagrams for N = 3 and N = 7. However, in the case of N = 7 higher sensitivity.

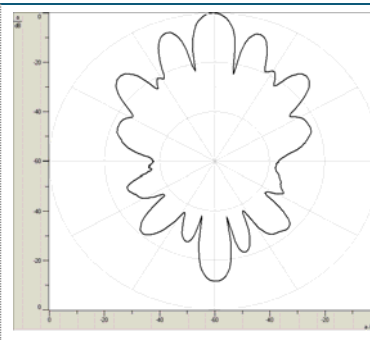
**Conclusion:**

The slot antenna has a pronounced directivity in the H-plane and an excellent fan beam in the E-plane. (This is true for the side with the slots.) This kind of fan-beam characteristic is used particularly for ship navigation.

## 6. The formation of grating lobes

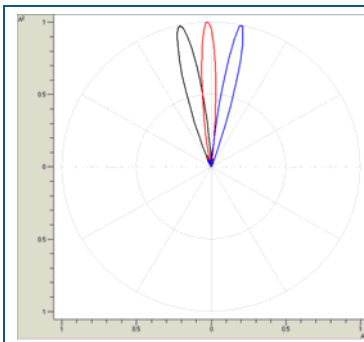


H-plane  
Polar coordinates  
Linear representation:  $\mathbf{A}(\vartheta)$   
Directional diagram of the horizontal slot antenna with the middle slot covered. Excitation with vertically polarized field



H-plane  
Polar coordinates  
Logarithmic representation:  $\mathbf{a}(\vartheta)$

## 7. Beam squinting and scanning by means of phase control



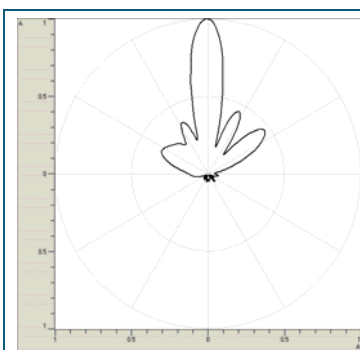
Joint display of the beam scanning and squinting with reflection-free terminated slot antenna.

*Note*

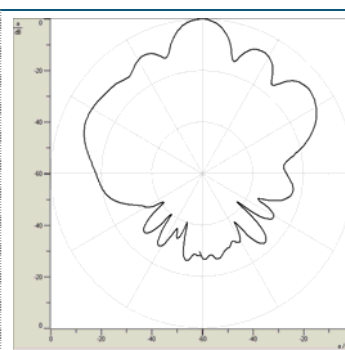
The output power of the Gunn oscillator decreases because of the change in the resonator cavity.

H-plane  
Polar coordinates  
Linear representation:  $\mathbf{A}^2(\vartheta)$

## 8. Horizontal diagrams of the microstrip antenna



E-plane  
Polar coordinates  
Linear representation:  $\mathbf{A}(\vartheta)$   
Excitation with horizontally polarized field

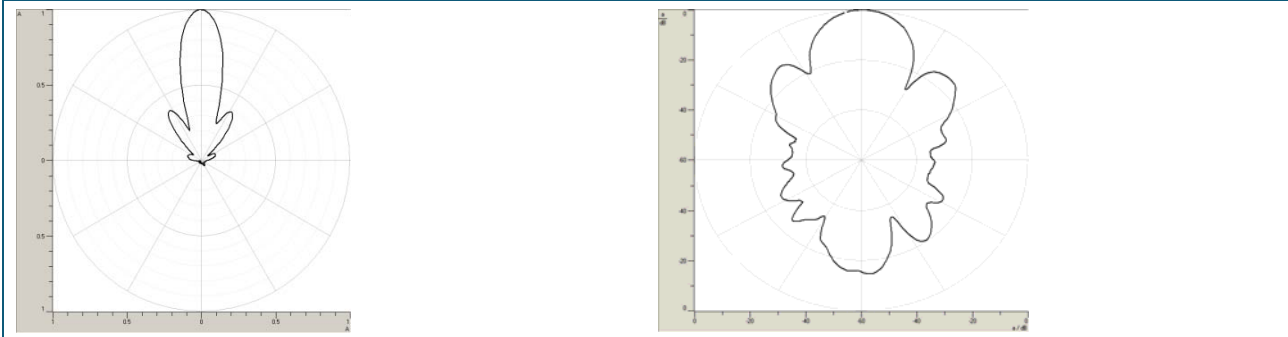


E-plane  
Polar coordinates  
Logarithmic representation:  $\mathbf{a}(\vartheta)$

Observation:

Distortions in the directional diagram in the E-plane are caused by the N-socket and the feeder.

9. Vertical diagrams of the microstrip antenna



H-plane  
Polar coordinates  
Linear representation:  $A(\theta)$

H-plane  
Polar coordinates  
Logarithmic representation:  $a(\theta)$

Observation:

The distortion brought about by the N-socket and the feeding network in the H-plane is considerably smaller than for the horizontal diagram.

**Table 1: Parameters of slot antennas**

Antenna	3 dB-Width		Sides lobes	F/B-Ratio
	vertical	horizontal		
Slot antenna N = 7	94°	12°	-10.3 dB / -18°	13.5 dB
Slot antenna N = 5		14°	-11.4 dB / -23°	13.0 dB
Slot antenna N = 3	90°	27°	-13.5 dB / -41°	14.1 dB



## Gain and matching

### Fundamentals

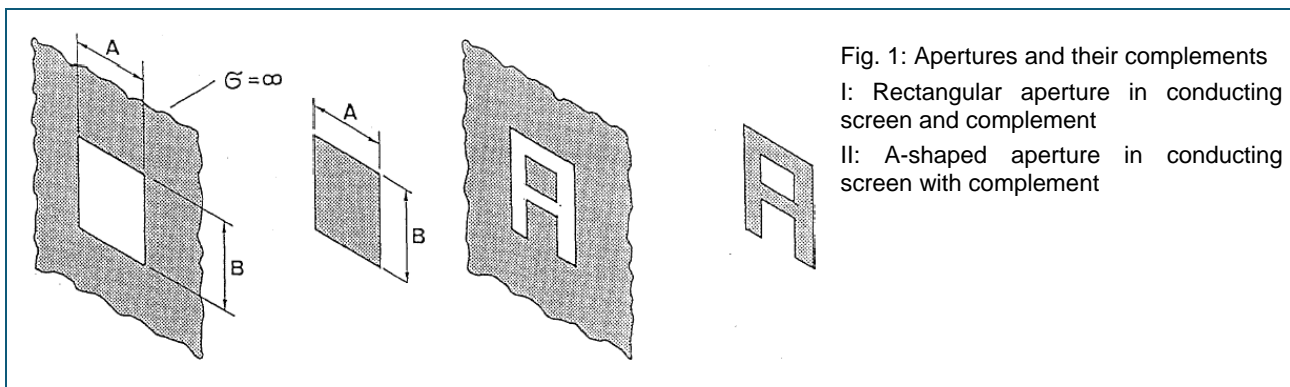
#### Single slots

Radiating slots are normally integrated into arrays. In this manner, beam concentration, gain etc. can be matched to the respective requirements. An array antenna of this kind was examined in the previous chapter. The single slot introduced here, is of interest due to its similarity to the elementary dipole. Regard a radiating slot which extends in an infinite, planar metal plate. Its radiating characteristics are formed by the aperture opening of the length  $w$  and the width  $h$  (see fig. 2). Its function can be described in various ways:

- as a linear aperture (narrow slot for  $L \gg \lambda_0$ )
- as section of a slotted line shorted at the ends (special form of a symmetrical two wire circuit)
- as a complementary dipole antenna after Babinet's principle.

The best results for the slot antennas used in this experiment were obtained using Babinet's duality principle. This is because the complement to a radiating slot is the dipole antenna which is well-known and simple to calculate. Optical laws permit the calculation of directional diagrams for apertures of any given shape, if the directional diagram of the complementary structure is known. By combining the radiating aperture and its complement, an undistorted total screen is achieved, see fig. 1. Important are the following rules:

- Directional diagrams of complementary antennas are identical.
- The directions of the electrical and magnetic field vectors are exchanged.
- The polarization of the antennas is orthogonal with respect to each other.
- In order to achieve identical directional diagrams, the complimentary antenna must be rotated by  $90^\circ$ .



The directional diagram of a short slot thus corresponds to that of a dipole (see fig. 2), up to the fact that the directions of the electrical and magnetic fields have been reversed. The latter also applies for the voltage  $U$ , the current  $I$ , the impedance  $Z$  and the admittance  $Y$  etc. The following applies for the relationship between the slot impedance  $Z_S$  and the impedance of the complementary dipole  $Z_D$ :

$$\sqrt{Z_S Z_D} = \frac{Z_0}{2} = 60\pi$$

Where:

$Z_S, Z_D$ : Impedance of the slot and the complementary dipole

$Z_0 = 120 \pi = 377 \Omega$  Wave impedance of the free space

The fig. 2 shows directional diagram of a dipole as well as the slot ( $L = 15 \text{ mm}$ ;  $w = 2 \text{ mm}$ ) and the corresponding complement. The slot corresponds to the radiator used in the following experiment.

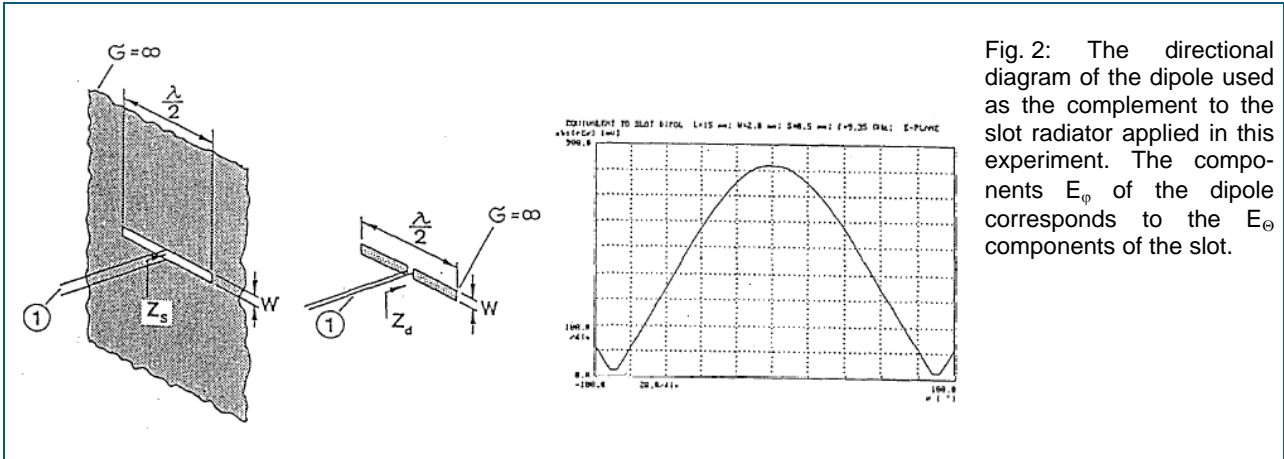


Fig. 2: The directional diagram of the dipole used as the complement to the slot radiator applied in this experiment. The components  $E_{\theta}$  of the dipole corresponds to the  $E_{\theta}$  components of the slot.

The standard premise that the aperture opening of the antenna is located in an infinitely extending, conductive screen (reflector with  $\sigma = \infty$ ), is never fulfilled. Furthermore diffraction at the edges of the reflector alters the directional diagram of the aperture antenna. The influence of the screen dimensions depend on the size of the aperture and the wavelength. Many real aperture antennas (e.g. horns, dishes etc.), operate even without reflectors. Their directional diagrams do not deviate strongly from those with screens, if their apertures are large compared to the wavelength. An example of this kind is the radiating longitudinal slot in the external wall of a round tube. This kind of tube can be perceived as a curved screen. The tube diameter  $D$  then influences the directional diagram of the slot. Tube-shaped slot antennas are frequently used in transmission systems for FM and TV broadcasting. For  $\pi D \gg \lambda_0$ , the slot only radiates on one side, perpendicular to the tube surface. In contrast, when  $\pi D < \lambda_0/2$ , then the directional diagram in the horizontal plane approximates a circle.

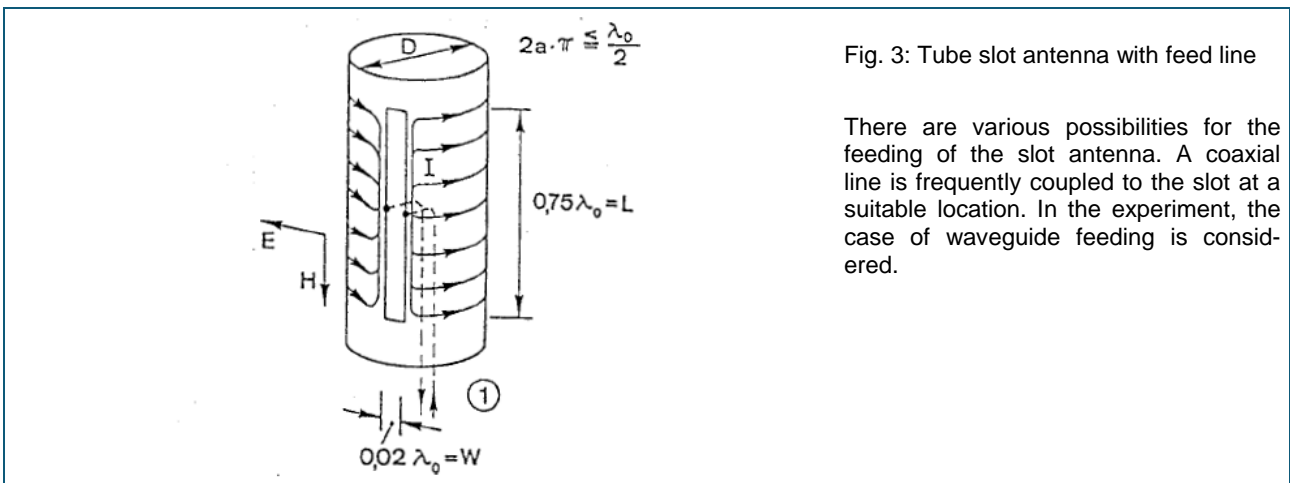


Fig. 3: Tube slot antenna with feed line

There are various possibilities for the feeding of the slot antenna. A coaxial line is frequently coupled to the slot at a suitable location. In the experiment, the case of waveguide feeding is considered.

Let us assume that the fundamental mode  $TE_{10}$  propagates within a rectangular waveguide. Its electrical field is oriented perpendicularly to the broad sides of the waveguide. It is this field distribution which excites the slot. The slot radiates only a portion of the supplied power into the free space. Total power radiation would require a 100% matching of the waveguide mode to the slot impedance. As this prerequisite cannot be fulfilled, a more or less considerable amount of power supplied to the slot is reflected ( $\Gamma > 0$ ). Thus, slot antennas require the use of a matching element for optimum operation. A slot fed via a waveguide only radiates into the hemisphere in front of the base plate (reflector). The directional diagram of the slot in this hemisphere has the identical shape as that of a complementary dipole. The slot's gain is twice as large as that of the dipole, because radiation only occurs in the front direction. (Dipoles radiate in front and back direction). The polarization between dipole and slot is orthogonal.

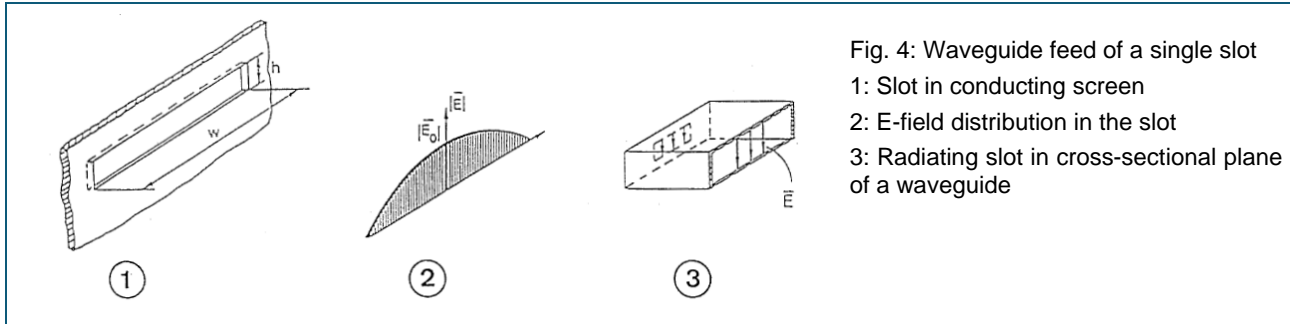


Fig. 4: Waveguide feed of a single slot  
 1: Slot in conducting screen  
 2: E-field distribution in the slot  
 3: Radiating slot in cross-sectional plane of a waveguide

As matching is an important prerequisite for all antennas and especially for slots, in the table 1 reflected and transmitted power in % and dB are given as a function of the various incorrect matching expressed by  $r$  and SWR

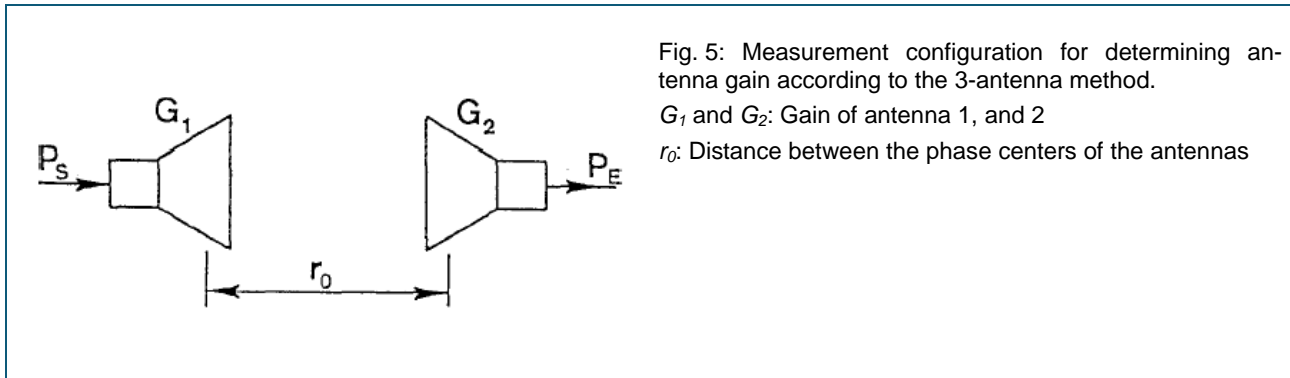
$P_R$  reflected power  
 $P_i$  incident power  
 $P_T$  transmitted power

**Table 1: Reflection losses**

$\rho= \Gamma $	SWR	$P_{\text{refl}}/P_i$ [%]	$P_{\text{refl}}/P_i$ [dB]	$P_T/P_i$ [%]	$P_T/P_i$ [dB]
0.10	1.22	1.0	-20	99	-0.04
0.15	1.35	2.3	-17	98	-0.10
0.20	1.50	4.0	-14	96	-0.20
0.25	1.67	6.3	-12	94	-0.30
0.30	1.85	9.0	-10	91	-0.40
0.35	2.10	12.3	-9	88	-0.60
0.40	2.33	16.0	-8	84	-0.80
0.45	2.64	20.3	-7	80	-1.00
0.50	3.00	25.0	-6	75	-1.25

### The three-antenna method

The 3-antenna method offers permits gain measurements if three unknown, different antennas are available. The method is actually an extension of the 2-antenna method, where two identical antennas are measured.



### Measurement conditions

- The phase centers of all the antennas investigated here are assumed to be located in their aperture planes.
- Both antennas are located in reflection-free space (also without ground reflection!), at a distance from each other which ensures far-field conditions. Then the existence of planar and uniform wave fronts is guaranteed. There is no interaction existing between the antennas.
- The transmitting antenna is matched to the source and the receiving antenna is matched to the receiver (detector). Measurements are to be carried out in a series of 3 gain measurements of two antennas respectively. In the process one antenna is successively replaced for each partial measurement, In this manner a linear equation system with 3 unknown gain values  $G_1, G_2, G_3$  is produced.

First measurement: 1->2

Second measurement: 1->3 (replace 2 with 3)

Third measurement: 2->3 (replace 1 with 2)

- In the measurements the received relative power  $P_i$  with  $i = 1, 2, 3$  and the relative transmitted power  $P_T$  is determined. The distance  $r_0$  must be kept constant, while the wavelength  $\lambda_0$  is a fixed and known value (32 mm). Thus the following equation system with the linear variables  $G_{1,lin}, G_{2,lin}, G_{3,lin}$  can be derived:

$$\frac{P_1}{P_T} = \left( \frac{\lambda_0}{4\pi r_0} \right)^2 G_{1,lin} G_{2,lin}$$

$$\frac{P_2}{P_T} = \left( \frac{\lambda_0}{4\pi r_0} \right)^2 G_{1,lin} G_{3,lin}$$

$$\frac{P_3}{P_T} = \left( \frac{\lambda_0}{4\pi r_0} \right)^2 G_{2,lin} G_{3,lin}$$

With  $a_0$  as the free space attenuation:

$$a_0 = \left( \frac{4\pi r_0}{\lambda_0} \right)^2 \quad \text{solving for } G_{lin} \text{ in logarithmic form } G \text{ gives:}$$

$$G_1 + G_2 = a_0 + 10 \log \frac{P_1}{P_T} = a_0 + a_1 - a_T$$

$$G_1 + G_3 = a_0 + 10 \log \frac{P_2}{P_T} = a_0 + a_2 - a_T$$

$$G_2 + G_3 = a_0 + 10 \log \frac{P_3}{P_T} = a_0 + a_3 - a_T$$

### Notes

This set of linear equations only contains the logarithmic values:

- $G_1/dB$ ,  $G_2/dB$  and  $G_3/dB$ : gain of the 3 antennas under test
- $a_1$ ,  $a_2$ ,  $a_3$ : rel. received power, measured with the level meter **a/dB** of the CASSY-Lab
- $a_T$ : relative transmitted power, measured with the level meter **a/dB** of the CASSY-Lab. This power remains unchanged throughout this experiment.

The variables  $r_0$ ,  $\lambda_0$ , necessary for  $a_0$  are measured or known. Thus the task is to solve a set of three linear equations with the 3 unknown variables  $G_1$ ,  $G_2$ ,  $G_3$ .

## Material

1	737 01	Gunn oscillator
1	737 03	Coax detector
1	737 033	Coax transition male / male N
1	737 035	Transition waveguide/coax
1	737 05	PIN modulator
1	737 06	Isolator
1	737 085	DC-blocker
1	737 09	Variable attenuator
1	737 12	Waveguide 200 mm
1	737 135	3-Screw transformer
1	737 14	Waveguide termination
2	737 15	Support for waveguide components
1	737 18	Cross directional coupler
1	737 197	E-bend
1	737 20	Small horn antenna
1	737 21	Large horn antenna
1	737 22	Set 4 slit diaphragm with holder
1	737 390	Set of microwave absorbers
1	737 399	Set of 10 thumb screws M4
1	737 405	Rotating antenna platform
1	737 424	Slot antenna
1	737 427	Microstrip antenna
1	737 440	Helical antenna kit
1	501 02	BNC Cable, l = 1 m
4	301 21	Stand base MF
1	311 77	Steel tape measure
1	568 702	Book: Antenna Technology
1		PC with Windows XP or higher version

## Experiment procedure

### 1. Horizontal diagrams of single slots

- Assemble the experiment as specified in fig. 6.

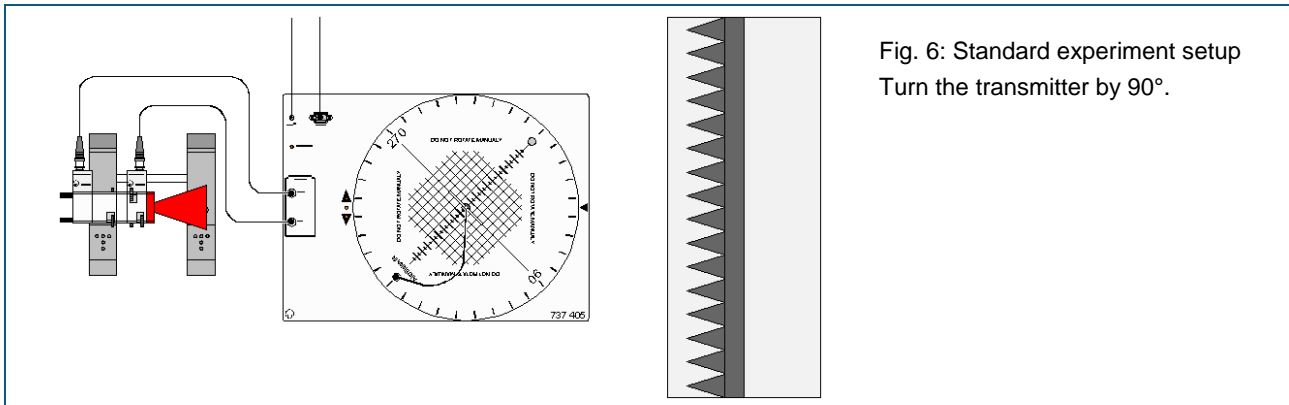


Fig. 6: Standard experiment setup  
Turn the transmitter by 90°.

- The recording of the directional diagrams is carried out in the standard manner.
- The waveguide 200 mm is terminated with the desired diaphragm (type A...D) which is used as the test antenna.
- Use the coax detector to demodulate the microwave signal. Connect its output to the input of the antenna rotating platform.
- Use the special holder with thumb screws to fix the diaphragms.
- Save the measurement under a file name, e.g.:
 

SL-15-0	(Type A)
SL-15-45	(Type B)
SL-10-0	(Type C)
SL-10-90	(Type D).

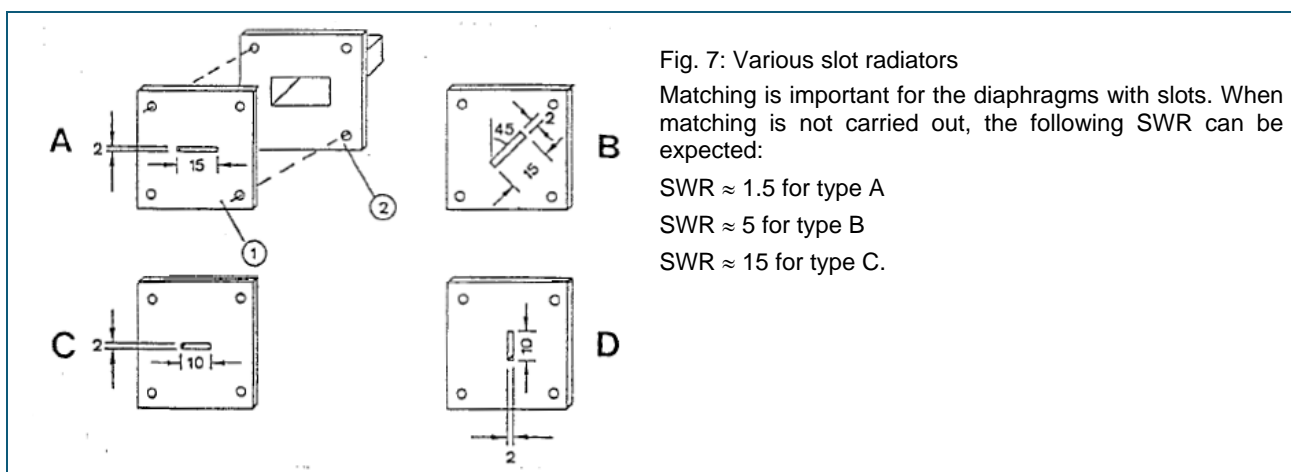


Fig. 7: Various slot radiators

Matching is important for the diaphragms with slots. When matching is not carried out, the following SWR can be expected:

SWR  $\approx$  1.5 for type A

SWR  $\approx$  5 for type B

SWR  $\approx$  15 for type C.

## 2. Matching slot antennas

- Set up the experiment up as specified in fig. 8.

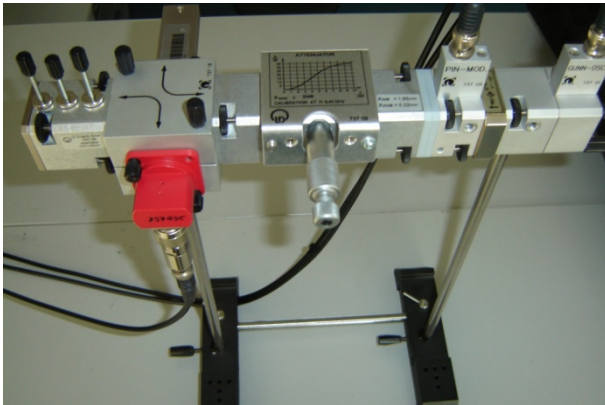


Fig 8: Waveguide part of the experiment setup

- Gunn oscillator 737 01
- Isolator 737 06
- PIN modulator 737 05
- DC-blocker 737 085
- Attenuator 737 09
- Cross directional coupler 737 18
- Waveguide termination 737 14
- Transition waveguide / coax 737 03
- 3-Screw transformer 737 135
- Slit diaphragms & holder 737 22

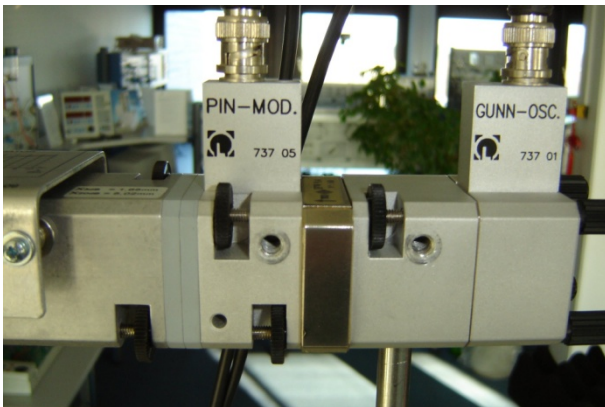


Fig. 8a: Partial view of the microwave source

**Note**

The DC-blocker 737 085 between PIN modulator and attenuator is necessary to avoid an electrical short of the rotation table's supply.

If a short has taken place, restart the table by the power supply. The system is protected.

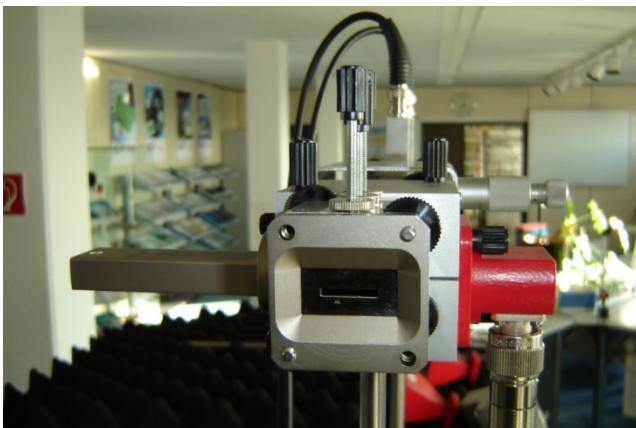


Fig. 8b: Partial view on the radiating slot 15-0°

Use the cross directional coupler 737 18 with 2x cross diaphragm.



- Calibrate the reflected signal to 0 dB. For that replace the slot-15-0 in fig. 8b by a short plate. Mount the coax detector to the transition waveguide / coax. Connect the output of the detector to the input TEST ANTENNA IN of the rotating platform. Turn the micrometer of the attenuator, until the level meter **a/dB** on the screen displays 0 dB. Leave the setting of the attenuator unchanged now.
- Measure the reflected power  $a_{refl}$  for an unmatched diaphragm slot-15-0. For that exchange the short plate to the slot-15-0 (fig. 8b). Note the measured power level  $a_{refl}$  in table 2.
- Move the coax detector to an receiving test antenna, e.g. to the microstrip antenna. Measure the transmitted power  $a_T$  (*distance approx. 1 m*).
- Repeat the experiment after improving the matching via the 3-screw transformer. Enter your measurements into table 2. Comment on the results. How might the matching be improved still more? What can be said about the use of the slotted measuring line? Imagine what the distribution of the standing wave ratio would look like for various mismatches.

**Table 2: Matching the slot-15-0°**

	$a_{refl}/dB$	$a_T/dB$
Calibration with short		
Mismatched		
Matched		

## 3. The three antenna method

- Experiment set-up as specified in fig. 9. The mean distance  $r_0$  between source and test antenna should be around 800 mm.

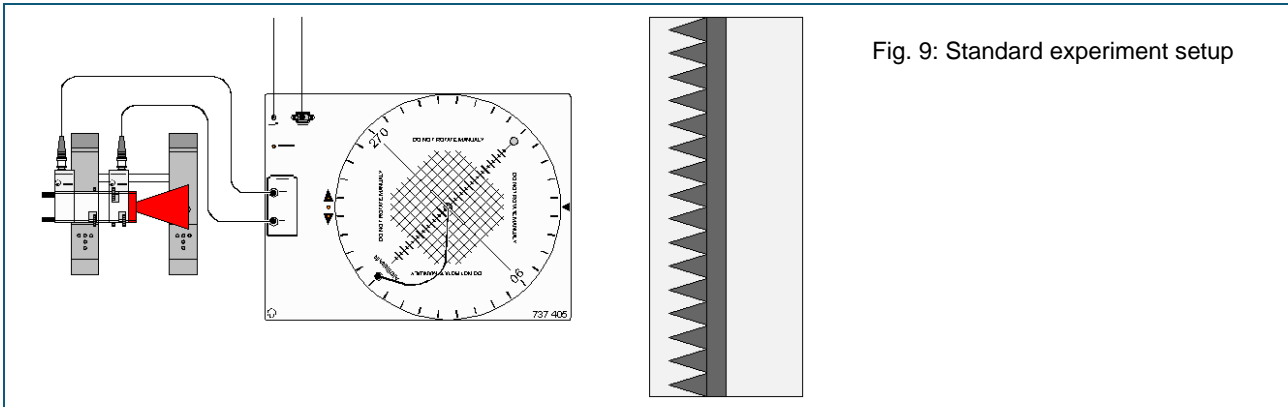


Fig. 9: Standard experiment setup

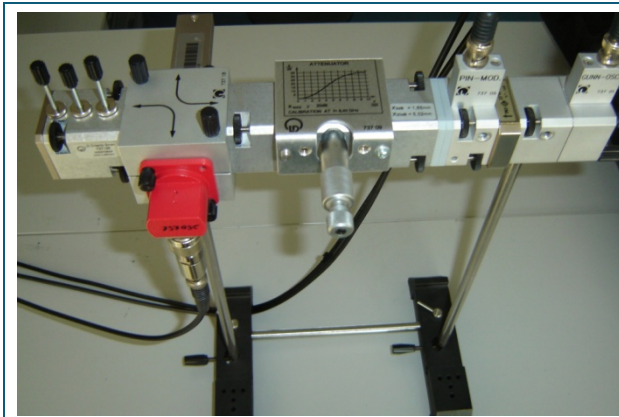


Fig. 10: Waveguide part of the experiment setup

- Gunn oscillator 737 01
- Isolator 737 06
- PIN modulator 737 05
- DC-blocker 737 085
- Attenuator 737 09
- Cross directional coupler 737 18
- Waveguide termination 737 14
- Transition waveguide / coax 737 03
- 3-Screw transformer 737 135
- Slit diaphragms & holder 737 22

- Use a microwave source as described in point 1. Use the DC-blocker to separate the transition waveguide / coax from the rest of the transmitter. Note: without the DC-blocker the antenna rotation platform is short circuited!
- Substitute the diaphragm by the transition waveguide / coax with coax detector and measure the transmitted power  $a_T$ . For that, connect the coax detector output to the input of the rotating antenna platform.
- Using the attenuator calibrate the level meter  $a/dB$  (CASSY-Lab) to exactly  $a_T = 0 \text{ dB}$ . This requires a typical attenuation of about 20 dB and ensures the square law operation of the coax detector.
- Re-establish the following configuration:  
Transmission antenna = antenna 1 (large horn antenna)  
Receiving antenna = antenna 2 (helix antenna). Use the 180 mm stand for the helix antenna.
- Measure the received relative power  $a_1/dB$ . Rotate the receiving antenna by hand until the maximum received signal is measured. Note the value for  $a_1$  in table 2.
- Calculate the wavelength  $\lambda_0$  from the frequency of the Gunn oscillator  $f = 9.40 \text{ GHz}$  and enter this value into table 3 as well.

- The following equation applies for the wavelength:

$$\frac{\lambda_0}{\text{mm}} = \frac{300}{f / \text{GHz}}$$

- Exchange the receiving antenna.  
Transmitting antenna = antenna 1 (large horn antenna)  
Receiving antenna = antenna 3 (microstrip antenna), vertical polarization!
- Determine the receiving power  $a_2$ . Enter the measured values into table 3
- Exchange the transmitting antenna.  
Transmission antenna = antenna 2 (helix antenna with E-bend and transition coax /coax male / male)  
Receiving antenna = antenna 3 (microstrip antenna).
- Determine the receiving power  $a_3$ . Enter the measured values into table 3.
- Calculate the gain for the 3 antennas using the formulas of table 3.

**Table 3: Determining gain**

$$r_0 = 800 \text{ mm}$$

$$\lambda_0 = 32 \text{ mm}$$

$$a_0 = 50 \text{ dB}$$

$$a_T = 0 \text{ dB}$$

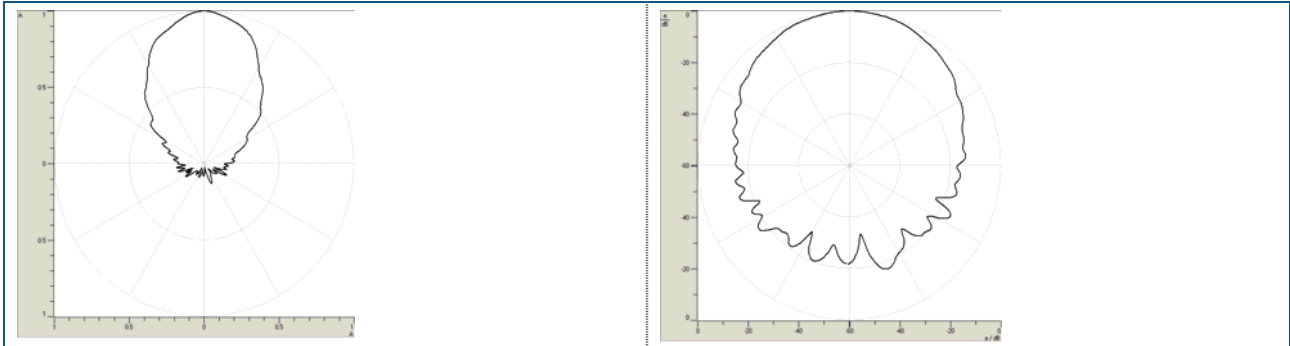
**Measurement**

**Evaluation**

		Level-Meter	Level correction +3 dB	Formula	Gain/dB
<b>TX</b>	<b>RX</b>	<b>a/dB</b>	<b>a<sub>c</sub>/dB</b>		
Horn (G <sub>1</sub> )	Helix (G <sub>2</sub> )	a <sub>1</sub> =	a <sub>1c</sub> =	$G_{1dB} = \frac{1}{2}[a_0 + a_{1c} + a_2 - a_{3c}]$	G <sub>1</sub> =
Horn (G <sub>1</sub> )	μ-Strip (G <sub>3</sub> )	a <sub>2</sub> =	a <sub>2</sub> =	$G_{2dB} = \frac{1}{2}[a_0 + a_{1c} - a_2 + a_{3c}]$	G <sub>2</sub> =
Helix (G <sub>2</sub> )	μ-Strip (G <sub>3</sub> )	a <sub>3</sub> =	a <sub>3c</sub> =	$G_{3dB} = \frac{1}{2}[a_0 - a_{1c} + a_2 + a_{3c}]$	G <sub>3</sub> =

## Results

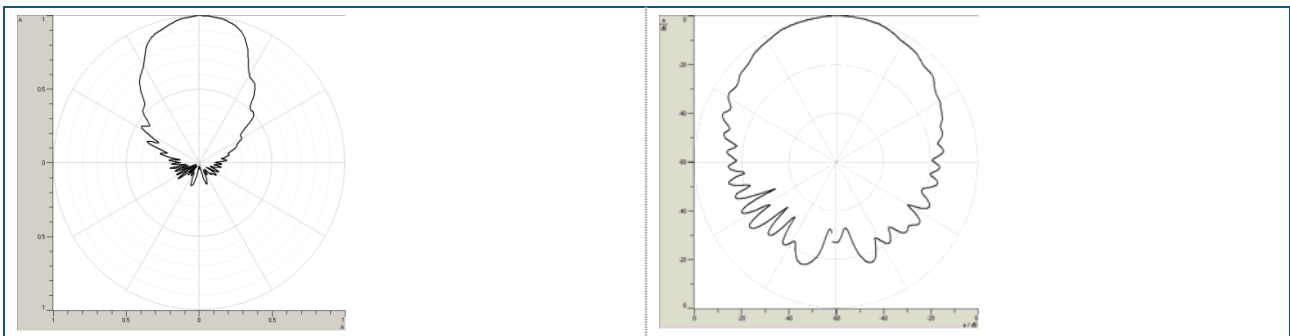
### 1.1 Horizontal diagrams of the single slot, type A



H-plane  
Polar coordinates  
Linear representation:  $A(\vartheta)$   
Excitation with horizontally polarized field

H-plane  
Polar coordinates  
Logarithmic representation:  $a(\vartheta)$

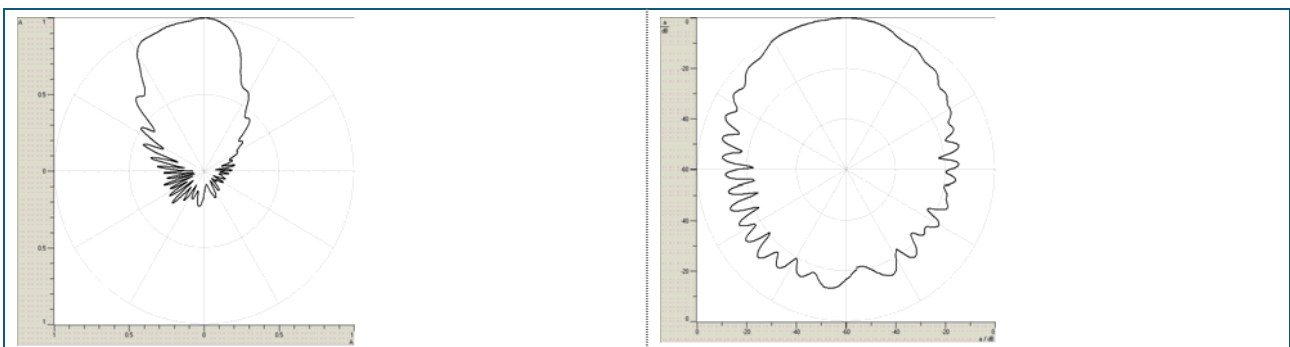
### 1.2 Horizontal diagrams of the single slot, type B



H-plane  
Polar coordinates  
Linear representation:  $A(\vartheta)$

H-plane  
Polar coordinates  
Logarithmic representation:  $a(\vartheta)$

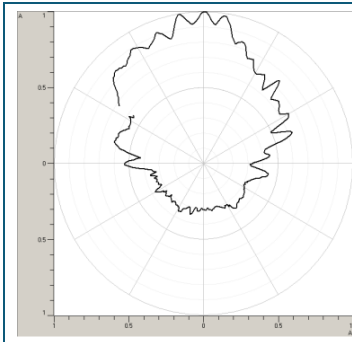
### 1.3 Horizontal diagrams of the single slot, type C



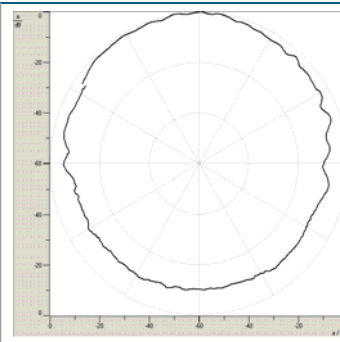
H-plane  
Polar coordinates  
Linear representation:  $A(\vartheta)$

H-plane  
Polar coordinates  
Logarithmic representation:  $a(\vartheta)$

### 1.4 Horizontal diagrams of the single slot, type D

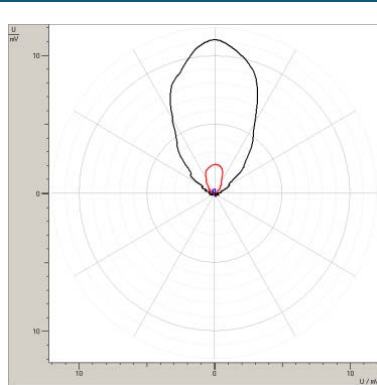


H-plane  
Polar coordinates  
Linear representation:  $A(\vartheta)$



H-plane  
Polar coordinates  
Logarithmic representation:  $a(\vartheta)$

### 1.5 Joint display of all single slots



Joint display of the single slots in absolute representation. While the directional diagrams with the exception of type D are more or less similar, the received signal changes considerably its strength in mV.

Black curve: Type A, slot-15-0°

Red curve: Type B, slot-15-45°

Red curve: Type C, slot-10-0°

Red curve: Type A, slot-10-90°

H-plane  
Polar coordinates  
Linear representation:  $U(\vartheta)$

## 2. Matching slot antennas

**Table 2: Matching the slot 15–0°**

	$a_{refl}/dB$	$a_T/dB$
Calibration with short	0	---
Mismatched	-8.4	-1.4
Matched	-21.5	-1.4

*Observation:*

Improved matching reduces the reflected power considerably, while the transmitted power nearly remains unaffected. The situation is confirmed by the mathematical values from table 1. At a SWR of 3, - 6 dB of the power is reflected. This leads to a reduction in the transmission power by - 1.25 dB. By improving the SWR to 1.22 the reflected power drops by - 14 dB to - 20 dB, while the transmission power increases by exactly +1.2 dB. A graphic representation of the field distribution for various SWRs is provided in fig. 11.

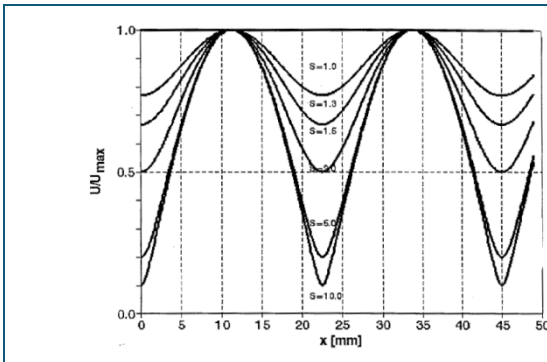


Fig. 11: Field distribution for various values of SWR

*Conclusion:*

- Loads whose SWR are already located in the range 1.5 can have their matching improved only with great difficulty.
- Matching might also be improved using the slide-screw transformer (737 13). Still matching is simplest to control using an arrangement with a reflectometer, as shown in fig. 10.



## Service

Should problems arise with the antenna measuring station, try to determine the source of the disturbances using the following trouble-shooting procedures:

### 1. Is RF power being generated?

RF power can only be generated, when the Gunn oscillator 737 01 is being supplied with DC voltage.

- Measure the supply voltage  $U_G$  and the current  $I_G$  of the Gunn oscillators with external multimeters. Typical values:  $U_G = 9 \text{ V}$   $I_G = -130 \text{ mA}$
- Has the Gunn oscillator been assembled properly? Make sure it has by checking the appropriate instruction sheet. Failure to attach the diaphragm with slot or accidentally exchanging the back wall and the diaphragm definitely prevents the generation of microwave power.
- Are all of the waveguide components connected "flush" with each, i.e. they are not off alignment by  $90^\circ$ ?

### 2. Is the PIN modulator operating?

The amplifier of the antenna rotating platform can only detect AC voltages. Consequently, the microwave signal must be modulated. This occurs in the PIN modulator (5 V approx. 1000 Hz).

### 3. Check the cross-polarization

The source antenna and the test antenna must operate with the same polarization. Otherwise polarization attenuation losses occur.



